

**PRESTRESSED PCBT GIRDERS MADE CONTINUOUS AND COMPOSITE
WITH A CAST-IN-PLACE DECK AND DIAPHRAGM**

by
Stephanie Koch

Thesis submitted to the faculty of the
Virginia Polytechnic Institute and State University
in partial fulfillment of the requirements for the degree of

MASTER OF SCIENCE

in

CIVIL ENGINEERING

Dr. Carin L. Roberts-Wollmann, Chairperson

Dr. Thomas E. Cousins

Dr. Elisa D. Sotelino

April 22, 2008

Blacksburg, Virginia

Keywords: PCBT Girders, Diaphragm, PCA Method, Restraint Moment

**PRESTRESSED PCBT GIRDERS MADE CONTINUOUS AND COMPOSITE
WITH A CAST-IN-PLACE DECK AND DIAPHRAGM**

by
Stephanie Koch

ABSTRACT

This research document focuses on prestressed PCBT girders made composite with a cast-in-place concrete deck and continuous over several spans through the use of continuity diaphragms. The current design procedure in AASHTO states that a continuity diaphragm is considered to be fully effective if a compressive stress develops in the bottom of the diaphragm when the superimposed permanent load, settlement, creep, shrinkage, 50 percent live load, and temperature gradient are summed, or if the girders are stored at least 90 days when continuity is established. It is more economical to store girders for fewer days, so it is important to know the minimum number of days that girders must be stored to satisfy AASHTO requirements.

In 2005, Charles Newhouse developed the positive moment diaphragm reinforcement detail that is currently being adopted by VDOT. This thesis concludes that Newhouse's detail, four No. 6 bars bent 180° and extended into the diaphragm, is adequate for all girders except for the PCBT-77, PCBT-85, and the PCBT-93 when the girders are stored for a minimum of 90 days. It is recommended that two additional bent strands be extended into the continuity diaphragm for these three girder sizes.

It was also concluded that about half of the cases result in a significant reduction in the minimum number of storage days if the designer is willing to perform a detailed analysis. The other half of the cases must be stored for 90 days because the total moment in the diaphragm will never become negative and satisfy the AASHTO requirement. In general, narrower girder spacing and higher concrete compressive strength results in shorter required storage duration. The PCA Method was used in this analysis with the updated AASHTO LRFD creep, shrinkage, and prestress loss models. A recommended quick check is to sum the thermal, composite dead load, and half of the live load restraint moments. The girder must be stored 90 days if that sum is positive, and a more detailed time-dependent analysis would result in a shorter than 90 day storage period if that sum is negative.

ACKNOWLEDGEMENTS

I would like to thank Dr. Carin Roberts-Wollmann, the chair of my research committee, for making the completion of this research possible. Dr. Wollmann has taught me a great deal through her extensive understanding and unwavering patience in communicating it to me. I also genuinely appreciate the time and insight that Dr. Tommy Cousins and Dr. Elisa Sotelino have provided as my committee members.

I am very grateful for the opportunities provided to me by the Charles E. Via, Jr. Department of Civil and Environmental Engineering. I came to Virginia Tech in the pursuit of a Master's degree, but I am leaving with much more than a diploma because of the dedication and hard work of the exceptional faculty and staff.

I also would like to thank the Via family for their generous donations to the fellowship which contributed to my financial support. In addition, I would like to thank the Virginia Transportation Research Council for their continued support of research at Virginia Tech, and in particular for the funding they provided towards the research of PCBT continuity diaphragms.

It has been a pleasure to work with and develop friendships with so many of the students and faculty in the Structural Engineering and Materials program. I am thankful that I have had the opportunity to meet so many talented and kind people while at Virginia Tech.

Also, I also am forever grateful for my family and friends who continue to encourage me to pursue my dreams. I would especially like to thank my future husband, Ray, who has been very supportive and has helped to make the past two challenging years a wonderful experience. I am also thankful for my parents, Ken and Kay, who have always provided me with ample love, encouragement, and guidance. Thanks also to Michelle, Bradley, and Charles who have always been able to balance the right amount of laughter and sincerity. I would not be where I am today without the love and encouragement of my family and friends.

Finally, I would like to thank God for all of the blessings in my life. Only through Him is all of this made possible.

TABLE OF CONTENTS

| | |
|--|------|
| ABSTRACT..... | ii |
| ACKNOWLEDGEMENTS..... | iii |
| LIST OF FIGURES | vii |
| LIST OF TABLES..... | viii |
| CHAPTER 1: INTRODUCTION..... | 1 |
| 1.1 Continuity Diaphragms in Composite Systems..... | 1 |
| 1.2 AASHTO LRFD Bridge Design Specifications..... | 4 |
| 1.3 Research Objectives..... | 5 |
| 1.4 Thesis Organization..... | 8 |
| CHAPTER 2: LITERATURE REVIEW..... | 9 |
| 2.1 Continuous Prestressed Concrete Girder Bridge Systems..... | 9 |
| 2.1.1 History..... | 9 |
| 2.1.2 Continuity Diaphragm Reinforcement..... | 10 |
| 2.2 Time-dependent Effects in Prestressed Concrete..... | 11 |
| 2.2.1 Concrete Shrinkage..... | 12 |
| 2.2.2 Concrete Creep..... | 14 |
| 2.2.3 Relaxation of Prestressing Steel..... | 18 |
| 2.3 Analysis Methods for Creep and Shrinkage..... | 19 |
| 2.3.1 Principle of Superposition..... | 19 |
| 2.3.2 Effective Modulus Method..... | 19 |
| 2.3.3 Rate of Creep Method..... | 21 |
| 2.3.4 Rate of Flow Method..... | 22 |
| 2.3.5 Improved Dischinger Method..... | 22 |
| 2.3.6 Age Adjusted Effective Modulus Method..... | 22 |
| 2.4 Design Procedures for Continuity Diaphragms..... | 23 |
| 2.4.1 PCA Method..... | 23 |
| 2.4.2 NCHRP 322 Method..... | 26 |
| 2.5 Thermal Effects..... | 27 |
| 2.5.1 Background..... | 28 |

| | |
|--|----|
| 2.5.2 AASHTO LRFD Specifications | 29 |
| 2.6 Summary of Need for Research | 30 |
| CHAPTER 3: TESTING THE PCA METHOD | 31 |
| 3.1 Problem Description | 31 |
| 3.2 Separate Sections Method | 32 |
| 3.2.1 Calculation of Change in Stresses Using the Separate Sections Method | 34 |
| 3.2.2 Calculation of Rotation Using the Separate Sections Method | 36 |
| 3.3 PCA Method | 37 |
| 3.3.1 Calculation of Change in Stresses Using the PCA Method | 38 |
| 3.3.2 Calculation of Rotation Using the PCA method | 40 |
| 3.4 Prestress Applied to Composite Cross-Section | 42 |
| 3.5 Set-Up and Results | 43 |
| 3.5.1 Comparison of Stresses | 43 |
| 3.5.2 A Better Creep Coefficient | 44 |
| 3.6 Conclusions | 50 |
| CHAPTER 4: GIRDERS OLDER THAN 90 DAYS | 51 |
| 4.1 Background and Calculations | 51 |
| 4.1.1 Design Variables and Assumptions | 52 |
| 4.1.2 Calculations | 52 |
| 4.1.3 Sample Calculations | 56 |
| 4.2 Results | 56 |
| 4.3 Conclusions | 58 |
| CHAPTER 5: GIRDERS YOUNGER THAN 90 DAYS | 60 |
| 5.1 Introduction | 60 |
| 5.2 Models | 60 |
| 5.2.1 AASHTO Creep Model | 61 |
| 5.2.2 AASHTO Shrinkage Model | 62 |
| 5.2.3 AASHTO Prestress Loss Model | 63 |
| 5.2.4 QConBridge | 63 |
| 5.2.5 Thermal Moment | 64 |
| 5.3 Calculations | 66 |

| | |
|--|-----|
| 5.3.1 Cases Analyzed..... | 66 |
| 5.3.2 MathCAD Spreadsheet | 67 |
| 5.4 Results..... | 68 |
| 5.4.1 Interpreting Results..... | 69 |
| 5.4.2 All Results..... | 70 |
| 5.4.3 General Trends..... | 72 |
| 5.4.3.1 Changes in Length | 72 |
| 5.4.3.2 Changes in Compressive Strength | 72 |
| 5.4.3.3 Changes in Girder Spacing | 72 |
| 5.4.4 Two-Span vs. Three-Span..... | 74 |
| 5.5 Conclusions..... | 75 |
| CHAPTER 6: CONCLUSIONS AND RECOMMENDATIONS..... | 77 |
| 6.1 Conclusions and Recommendations | 77 |
| 6.1.1 Testing the PCA Method | 77 |
| 6.1.2 Girders Older than 90 Days | 77 |
| 6.1.3 Girders Younger than 90 Days | 78 |
| 6.2 Recommendations for Future Work..... | 79 |
| REFERENCES | 81 |
| APPENDIX A: Design of Continuity Diaphragms for Girders Older than 90 Days | 83 |
| APPENDIX B: Strands for PCBT Girder Older than 90 Days..... | 86 |
| APPENDIX C: 2-Span PCBT Girder Systems Younger than 90 Days..... | 91 |
| APPENDIX D: 3-Span PCBT Girder Systems Younger than 90 Days | 128 |
| APPENDIX E: PCBT Details and Section Properties..... | 130 |

LIST OF FIGURES

| | |
|--|----|
| Figure 1.1: Simple Continuity Diaphragm Illustration..... | 1 |
| Figure 1.2: Strains and Stress in a Composite Section | 2 |
| Figure 1.3: Restraint Moment Illustration | 3 |
| Figure 1.4: Charles Newhouse’s Continuity Diaphragm Detail | 7 |
| Figure 2.1: Shrinkage Strain over Time..... | 13 |
| Figure 2.2: Strain Diagram for Creep | 15 |
| Figure 2.3: Superposition of Creep Strains..... | 16 |
| Figure 2.4: Prestress Loss over time | 18 |
| Figure 2.5: Effective Modulus | 20 |
| Figure 2.6: Positive Temperature Gradient through Cross-Section..... | 29 |
| Figure 3.1: Forces, Moments, and Strain Distribution for a Composite Cross-Section | 32 |
| Figure 3.2: Change in Stress Distribution through Cross-Section..... | 35 |
| Figure 3.3: Sample of Change in Curvature along Half of the Span Length..... | 37 |
| Figure 3.4: Stress through Cross-Section if Creep is Zero | 38 |
| Figure 3.5: Stress through Cross-Section if Creep is Infinite | 38 |
| Figure 3.6: Change in Stress through Cross-Section (from Zero to Infinite Creep)..... | 39 |
| Figure 3.7: M/EI Diagram for Straight Strands | 41 |
| Figure 3.8: M/EI Diagram for Harped Strands | 42 |
| Figure 3.9: Percent Difference between PCA Phi and the Best Fit Phi..... | 50 |
| Figure 4.1: Sketch of PCBT Girder with Deck and Haunch..... | 51 |
| Figure 4.2: Length of Prestressing Strand Extended into the Continuity Diaphragm | 54 |
| Figure 4.3: Cracking Moment and Design Strength for PCBT-45 Girder..... | 57 |
| Figure 5.1: Thermal Forces in PCBT Girders..... | 65 |
| Figure 5.2: Restraint Moment..... | 66 |
| Figure 5.3: Continuity Diaphragm Restraint Moments | 69 |

LIST OF TABLES

| | |
|--|----|
| Table 3.1: Sample Given Parameters for Testing the PCA Method..... | 35 |
| Table 3.2: Design Parameters from Newhouse..... | 42 |
| Table 3.3: Sample Stresses (ksi) using the Separate Section Method | 45 |
| Table 3.4: Sample Stresses (ksi) using the PCA Method | 45 |
| Table 3.5: Percent Difference of Stresses for a Girder and Deck Phi of 2.00 | 46 |
| Table 3.6: Percent Difference of Stresses for a Girder and Deck Phi of 1.75 and 2.25 | 48 |
| Table 3.7: Comparison of PCA Phi to Best Fit Phi | 49 |
| Table 4.1: Bent Strands Required and Recommended for PCBT Girders..... | 58 |
| Table 5.1: Experimental Results, PCBT-29 to PCBT 53..... | 70 |
| Table 5.2: Experimental Results, PCBT-61 to PCBT 93..... | 71 |
| Table 5.3: Three-Span Systems vs. Two-Span Systems: Minimum Storage Duration | 75 |

CHAPTER 1: INTRODUCTION

1.1 Continuity Diaphragms in Composite Systems

The amount of pressure on the United States transportation infrastructure continues to increase as our growing population demands new roads and older roadways need to be replaced. Only a portion of the necessary funds are available for building new bridges and replacing deficient ones, so unfortunately there are always additional projects that are not considered a high enough priority. Therefore, research in bridge design is crucial. High quality structures need to be designed and built with increasing efficiency to allow them to better serve society for a longer period of time while leaving finances for other undertakings. This research document focuses on one specific type of bridge system: precast prestressed concrete girders made composite with a cast-in-place concrete deck and made continuous over several spans through the use of continuity diaphragms. This type of bridge system was selected because it has many advantages.

A composite bridge system is one in which the deck and the girders are bonded together so that the system strains and deflects as one unit. Figure 1.1 is a simple illustration of a continuity diaphragm with a cast-in-place deck. Composite construction is generally preferred because there is a substantial increase in strength and stiffness when the deck and girders are tied together. However, it is more difficult to calculate the forces in the system due to time-dependent effects, especially in the case of precast prestressed concrete girders with a cast-in-place deck.

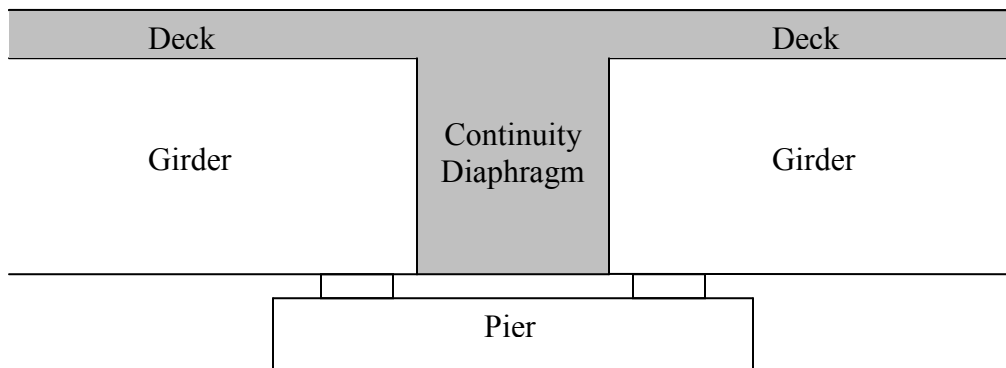


Figure 1.1: Simple Continuity Diaphragm Illustration

The time-dependent effects that occur in the girders and deck include creep, shrinkage, and relaxation of prestressing steel. It is found that the most dominant forces and moments develop from differential shrinkage between the deck and girder, which occurs because each component has a different ultimate value and rate of creep and shrinkage. Nevertheless, the entire cross-section must strain compatibly since the girders and the deck are made composite when the deck is poured. In other words, compression develops in the top of the girder and tension develops in the bottom of the deck since there cannot be discontinuity in the strain through the cross-section of the girder and deck. See Figure 1.2 for illustration. These forces will cause rotation at the end of the girder if it is simply supported, and restraint moments will develop in the continuity diaphragm if the bridge is made continuous.

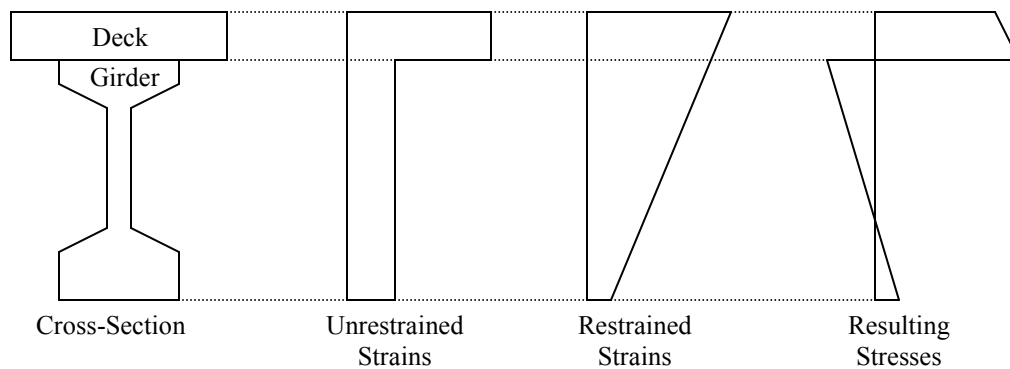


Figure 1.2: Strains and Stress in a Composite Section

A continuous bridge is one in which two or more simple spans are connected end-to-end with continuity diaphragms (see Figure 1.1). To understand the moments that develop in a continuity diaphragm, consider a simply supported system. The ends of the girder are able to rotate freely throughout the service life of the bridge from the effects of creep, shrinkage, prestress loss, live loads, temperature gradients, and other loading conditions. In a continuous system, no further end rotation is allowed after the continuity diaphragm is poured and the ends of the girders are fixed. Restraint moments must then develop in the continuity diaphragm to oppose those moments that would rotate the end of the girder if it were unrestrained. See Figure 1.3

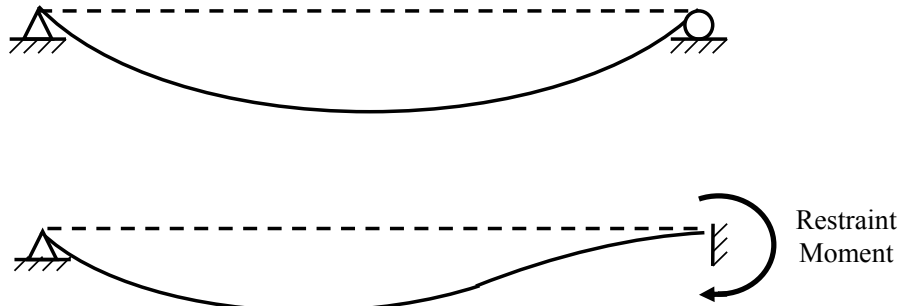


Figure 1.3: Restraint Moment Illustration

A continuous bridge has several advantages over a series of simple span structures. First, there is a reduction in mid-span bending moments and deflections. This is economical because the girder cross-section can be reduced, or fewer prestressing strands can be used in cases where the member size is fixed (Mattock, et al. 1960). Secondly, making a bridge continuous will improve serviceability by eliminating joints in the deck. The removal of joints will improve the riding surface of the bridge, and durability will be increased because the water and salts from the deck will not drain onto the substructure. Many people consider this the most important advantage (Freyermuth 1969). In addition, the exclusion of joints in a design will reduce the initial cost of the bridge and also reduce bridge maintenance. Third, a bridge that has been made continuous will redistribute moments if the load capacity is exceeded for a particular girder in the system (Mattock, et al. 1960). This provides redundancy.

Although the advantages of continuous systems are numerous and many states are using them, there is not much agreement on the best method to calculate the restraint moments that develop in the continuity diaphragms or how to detail the positive moment connection. Note that the negative moment connection is not discussed in this document because it is provided through the deck reinforcement, which is much easier to adjust than the positive moment reinforcement that must enter into the end of the girder. This study uses the current design standards, which are the AASHTO LRFD Bridge Design Specifications, for the analysis of the positive moment connection in continuity diaphragms (AASHTO 2007).

1.2 AASHTO LRFD Bridge Design Specifications

The Virginia Department of Transportation (VDOT) has been designing an increasing number of continuous bridges using the relatively new Precast Concrete Bulb Tee (PCBT) girders. The primary goal of this research is to determine if the continuity diaphragms in bridges using PCBT girders are in compliance with current LRFD Specifications. Section 5.14.1.4.5 in the AASHTO LRFD Bridge Design Specifications states:

“The connection between precast girders at a continuity diaphragm shall be considered fully effective if either of the following are satisfied:

- *The calculated stress at the bottom of the continuity diaphragm for the combination of superimposed permanent load, settlement, creep, shrinkage, 50 percent live load and temperature gradient, if applicable, is compressive.*
- *The contract documents require that the age of the precast girders shall be at least 90 days when continuity is established and the design simplifications of Article 5.14.1.4.4 are used.*

Section 5.14.1.4.4 states:

“ The following simplification may be applied if acceptable to the owner and if the contract documents require a minimum girder age of at least 90 days when continuity is established:

- *Positive restraint moments caused by girder creep and shrinkage and deck slab shrinkage may be taken to be 0.*
- *Computation of restraint moments shall not be required.*
- *A positive moment connection shall be provided with a factored resistance, ΦMn , not less than $1.2 M_{cr}$, as specified in Article 5.12.1.4.9.”*

So, the AASHTO Specifications are straightforward and relatively simple as long as the girders are older than 90 days before they are made composite and continuous. However, since it is less economical to wait until girders are 90 days old, it is preferable to store them for less than

90 days is even though the calculations are more involved. Determining the forces and moments throughout the life of a bridge system can become a fairly in-depth process, especially if both the deck and the girder are creeping and shrinking at different rates. Therefore, a design aid that determines if the continuity diaphragm is fully effective for girders younger than 90 days would be very beneficial.

1.3 Research Objectives

Virginia Department of Transportation (VDOT) has been frequently incorporating the fairly new PCBT girder shape into designs recently. Virginia Tech has been actively performing research on the PCBT bridge girder to assist VDOT in making their designs as efficient as possible. In particular, VDOT is interested in continuity diaphragm details for continuous spans. In 2001, Professors Carin Roberts-Wollmann and Thomas Cousins proposed a research project to study the continuity diaphragm detail for the PCBT girder, called the “Development of an Optimized Continuity Diaphragm for New PCBT Girders.” Ph.D. student Charles Newhouse worked on this project and published his dissertation in 2005 entitled, “Design and Behavior of Precast, Prestressed Girders Made Continuous – An Analytical and Experimental Study” (Newhouse 2005). He determined that the most efficient detail was four No. 6 bars bent 180° and extended into the diaphragm. This detail is shown in Figure 1.4.

Since Newhouse’s work in 2005, the AASHTO LRFD Bridge Design Specifications have been updated. This leads to the two primary objectives of this research:

1. Determine if the continuity diaphragm detail developed by Charles Newhouse (Figure 1.4) for precast concrete girders made continuous and composite with a cast-in-place deck is adequate for all PCBT girders older than 90 days according to the new AASHTO specifications. If the detail is not adequate for particular cases, determine the number of 0.5 in. prestressing strands that should be extended into the diaphragm and bent at a 90° angle to provide sufficient moment capacity.

2. Determine the minimum number of days that a particular PCBT girder in a continuous and composite system must age before being erected so that the new AASHTO specifications are satisfied.

To satisfy the first objective of this research, design parameters were varied to determine if the Newhouse diaphragm detail for PCBT girders is sufficient for all cases. The assumptions include:

- The bridge being analyzed is a two-span continuous structure
- The diaphragm concrete has a compressive strength of 4 ksi
- The deck thickness is 8 in.
- The haunch height is 1 in.
- The yield strength of the reinforcing bars is 60 ksi.

A two-span continuous system is more critical than a three or more span system, and the other assumptions are typical for VDOT designs. The variable parameters include the beam spacing, the span length and the beam size. For each size girder, the design strength (ΦM_n) must be greater than or equal to 1.2 times the cracking moment for multiple combinations of girder spacings and span lengths. If this requirement is not met, additional 0.5 in. prestressing strands are extended into the diaphragm to satisfy the requirement.

To meet the second objective of this research, it is necessary to develop a design aid (in the form of a MathCAD spreadsheet) that will determine when continuity diaphragms for PCBT girder bridges can be assumed to be fully effective according to Article 5.12.1.4.5 of the AASHTO specifications. A variety of different size PCBT girders at different ages, span lengths, compressive concrete strengths, and deck widths were considered in this study. The design aid simplifies the current procedure and allows for continuous bridges to be designed and built more efficiently. This will save time and money in the design and construction processes.

Another component of the second objective is to explore how accurately the PCA Method calculates stresses and strains in composite concrete sections. This is important because the PCA Method is very commonly used and accepted for calculating the restraint moment due to time-dependent effects. Results obtained using the PCA Method are compared to those results

acquired using another method that is considered to be an accurate way to calculate the stress redistribution in composite sections caused by time-dependent effects of creep and shrinkage. Although the PCA Method is frequently used, there are doubts as to how accurate it is, especially when the creep characteristics of the girder and deck are different. Results from this analysis were used to determine if the PCA method can be used in conjunction with the AASHTO LRFD Specifications in the development of the design aid for PCBT continuous spans.

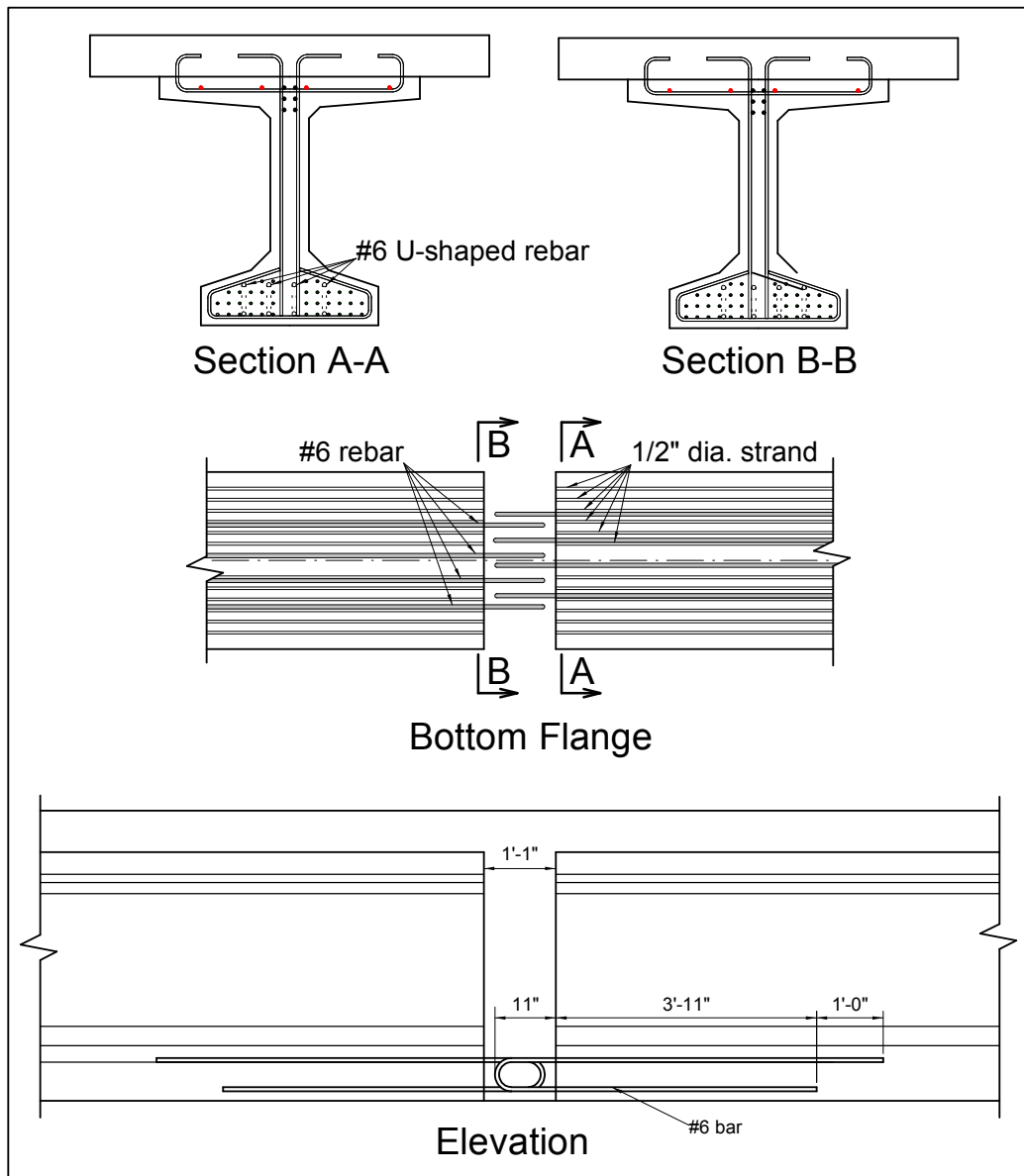


**Figure 1.4: Charles Newhouse's Continuity Diaphragm Detail
(used with kind permission of Charles Newhouse, 2008)**

1.4 Thesis Organization

This document begins with Chapter 1, the Introduction, which includes a brief summary of the current design specifications and the research objectives. The relevant background can be found in the Literature Review in Chapter 2. The analytical investigation and results to determine if the PCA Method is an accurate method of calculating restraint moments in continuity diaphragms due to time-dependent effects are found in Chapter 3, Testing the PCA Method. Chapter 4 presents a discussion, analysis procedure, and conclusions for Girders Older Than 90 Days. Chapter 5, Girders Younger Than 90 Days, determines the minimum number of days that prestressed PCBT girders must be stored before being erected so that the AASHTO LRFD Bridge Design Specifications are met. Finally, the Conclusions and Recommendations can be found in Chapter 6.

CHAPTER 2: LITERATURE REVIEW

2.1 Continuous Prestressed Concrete Girder Bridge Systems

A continuous bridge is one in which two or more simple spans are connected end-to-end with a continuity diaphragm. Some of the earliest long-span continuous highway bridges built in the United States were constructed in the early 1960's and include the Big Sandy River Bridge in Tennessee and the Los Penasquitos Bridge in California (Freyermuth 1969). After a short trial period where these aesthetic bridges displayed excellent performance, many states began to research and design their own continuous bridge systems. Since then, continuous prestressed concrete girder systems have become a popular choice around the country because of their numerous advantages. Although people agree on their advantages, there is still much discrepancy on methods used for design of these systems and the associated reinforcement details.

2.1.1 History

One of the early methods of making a bridge continuous over two or more spans was to place the ends of the girders close to each other and post-tension them together. However, this method was not efficient because the anchorages and tensioning were relatively expensive and there was considerable friction loss due to the severe curves necessary to make the post-tensioning effective (Mattock, et al. 1960). Because of these disadvantages, an alternative method began to develop. The improved method called for leaving a small space between the ends of the girders and extending positive moment reinforcing steel, instead of post-tensioning strands, into that region from the beams. Concrete would be added to this section at the time when the deck was poured to provide continuity over the joint. This area is known as a continuity diaphragm.

It is important that the continuity diaphragm be fully effective for positive bending moments. Positive moment occurs in the continuity diaphragm because of creep due to the prestressing force and thermal effects. The 2005 NCHRP Project 12-53 concluded that cracking of the diaphragm due to positive bending does not necessarily affect the continuity of the system.

It was estimated that continuity was only reduced by 30% when the connection was near failure (Dimmerling, et al. 2005). However, it is still recommended that full continuity be achieved. Negative moment occurs in the continuity diaphragm because of differential shrinkage, dead load creep, loss in prestress, live loads, and superimposed dead load. The negative moment reinforcement is placed in the deck, and does not need to enter into the end of the girder.

Cracking that develops due to diaphragm moments can present maintenance and aesthetic problems. Also, it is important to limit cracking over the pier because cracking reduces the stiffness of the system, which will cause the bridge to behave like a series of simple spans under large loading events. The resulting increased moment at mid-span could cause failure at a smaller than expected loading or could reduce the service life of the structure.

2.1.2 Continuity Diaphragm Reinforcement

NCHRP Project 12-53 examined methods of making a positive moment connection for the portion of a continuous bridge over an interior support (Dimmerling, et al. 2005). Cracking of the diaphragm reduces the effectiveness of continuity for service loads and also reduces the ductility of the structure. Positive moment reinforcement will help moderate or eliminate this cracking. Therefore, it is important to design for the appropriate amount of positive moment so that the cracking of the diaphragm can be controlled and a significant loss of continuity can be avoided.

Two basic details that are used for positive moment reinforcement in continuous spans are compared in NCHRP Project 12-53. Variations of these two details represent the majority of positive moment reinforcement in continuity diaphragms commonly used in design today. The first detail consists of prestressing strands that are extended from the end of the girder into the diaphragm and bent at a 90° angle. The second detail uses mild reinforcing steel that is embedded into the ends of the girder to be extended into the diaphragm. Experimental testing in this NCHRP Project concluded that positive moment connections could be made using either of these methods, although embedding mild reinforcement provided slightly improved connection capacity over using extended prestressing strands. However, bent bar connections are more difficult to construct than bent strand connections (Dimmerling, et al. 2005).

Charles Newhouse published a study on continuity diaphragms in 2005, part of which analyzed the performance of various positive moment connections for continuous Precast Concrete Bulb-Tee (PCBT) girders. The reinforcement details selected for analysis in Charles' study were similar to those used in the NCHRP Project 12-53. The test specimens included ½ in. prestressing strands extended from the bottom of the girders and bent at a 90° angle, No. 6 mild reinforcing bars extended from the bottom of the girders and bent at a 180° angle, and no reinforcement in the diaphragm. Newhouse concluded that the best design feature was the 180° hooks of mild reinforcement that extended from the end of the girder into the diaphragm. He stated that this detail “remained stiffer during the testing and is expected to provide for better long term connections” (Newhouse 2005).

The Virginia Department of Transportation (VDOT) is in the process of adopting Newhouse's recommended continuity diaphragm detail as a design standard. Since the objective of this research is to develop a design aid for the Virginia Transportation Research Council (VTRC), this study will only examine Newhouse's continuity diaphragm standard detail of four No. 6 “U” shaped pieces of mild reinforcing steel.

2.2 Time-dependent Effects in Prestressed Concrete

Creep and shrinkage of concrete members and relaxation of prestressing strands cause time-dependent changes in strains in a prestressed bridge system, which result in changes in stress throughout the cross-section. These stresses can have a large impact, and must be considered when calculating deformations and the redistribution of forces that occurs (Menn, 1986). Time-dependent effects are defined as those that develop after the hardening of the deck and continuity diaphragm concrete. There are several causes of time-dependent changes in strain. These include the creep from girder weight and initial prestressing force, the creep due to the slab weight, and the differential shrinkage between the girder and the deck (ACI 209R-92).

Nearly all concrete structures are built in stages, and all have time-dependent effects from creep, shrinkage, and other factors. In many cases, the primary reason to accurately predict time-dependent losses in prestressed concrete members is to determine prestress loss and the deflection of the member. In these situations, an elastic analysis of the structure as a whole is sufficient to approximately determine the forces present. A simple lump sum of losses or a

simplified approach may then be used to determine the time-dependent effects at various stages of construction. It is recommended that losses should be assumed to be between 15 and 20% for pre-tensioned structures and between 10 and 15% for post-tensioned structures (ACI 209R-92).

However, pronounced time-dependent effects would require analysis at multiple stages of construction. A more in-depth analysis is needed in continuous and composite construction where the internal forces at a certain stage of construction are substantially different from those at another stage. This requires a more accurate estimation of the forces and moments in the system at multiple times during the construction and service life of the structure.

The time-dependent restraint moments that occur in the continuity diaphragm can become difficult to compute, especially if prestressed concrete girders are used with a cast-in-place deck. In general, the negative moments will be caused predominately by differential shrinkage between the deck and the girder and by the creep of the deck. There will also be positive moments that will develop due to the creep of the prestressed girders, among others. The dead load and live load that act on adjacent and remote spans will also have an effect on the restraint moments that will develop in the continuity diaphragms.

2.2.1 Concrete Shrinkage

Shrinkage is defined as the decrease in the volume of concrete over time. Similarly to creep, shrinkage occurs rapidly at first, but then at a slower rate as it approaches an asymptote after a large amount of time (Nilson 1987). Unlike creep, shrinkage is independent of the loading of the concrete. This makes computation simpler because shrinkage of individual concrete members will not be affected by different construction sequences. Figure 2.1 illustrates how shrinkage strain changes over time from an initial time, t_0 , to a final time, t .

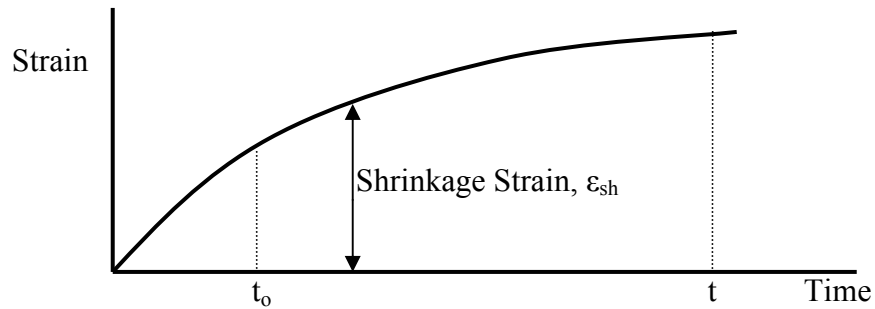


Figure 2.1: Shrinkage Strain over Time

The three main types of shrinkage are autogenous shrinkage, carbonation shrinkage, and drying shrinkage. First to be discussed is autogenous shrinkage, which occurs because the physical materials in concrete take up less space after hydration (MacGregor, et al. 2005). It does not include any type of moisture exchange between the member and the environment, and is also known as basic shrinkage or chemical shrinkage (ACI 209R-05). Second is carbonation shrinkage, which is when water and carbon dioxide mix with the calcium hydroxide in the cement paste to produce calcium carbonate and additional water. This process of reducing the volume of the cement only occurs if the humidity is not too high or too low, because moisture is needed for the reaction but too much will restrict the reaction. Finally, drying shrinkage occurs when moisture is allowed to enter and leave the member, and is the focus of most research at this time. It occurs because water slowly moves to the surface of the concrete and is lost due to evaporation, so the other particles become more compact (MacGregor, et al. 2005). For the duration of this study, the term “shrinkage” will refer solely to “drying shrinkage.” This is because researchers commonly assume that all of the shrinkage strain is due to drying shrinkage for normal weight concrete, while the contributions from autogenous and carbonation shrinkage can be neglected (ACI 209R-05).

Differential shrinkage occurs between two pieces of concrete if they must strain together but have different rates of shrinkage. An example of this is a prestressed girder with cast-in-place deck, because shrinkage occurs at different rates if both are allowed to shrink separately (Mattock, et al. 1961). They have different shrinkage rates because they are cast with different types of concrete and the concrete in the deck is younger. In this case where the deck is made composite with the girder, new forces and moments are introduced since there still must be a constant change in strain throughout the entire cross-section. Since the girder with a composite

deck would deflect downward if a simple span were being analyzed, the corresponding rotations at the end of the girder would result in a negative restraint moment in a continuity diaphragm.

There are several factors in the mix design that influence shrinkage rates and the ultimate value of shrinkage strain. Aggregates restrain shrinkage, so the volume of aggregates in the concrete is often considered to be the most important factor limiting shrinkage (ACI 209R-05). Likewise, stiffer and larger aggregate results in less shrinkage because the concrete is better restrained (MacGregor, et al. 2005). Increasing water content will cause more shrinkage because the total volume of the aggregates must be reduced (ACI 209R-05). For similar reasons, shrinkage will increase when there is a greater ratio of the volume of cement to the volume of concrete (MacGregor, et al. 2005). The type of cement will also influence shrinkage, with those having more finely ground cement or low quantities of sulfate exhibiting more shrinkage (ACI 209R-05).

The ambient environment during the life of the member also influences shrinkage, so the curing process and the duration of the drying period will have an effect. For example, steam curing can significantly reduce shrinkage by as much as 30%, and extended periods of moist curing can reduce shrinkage by 10 to 20% (ACI 209R-05). Humidity at the construction site will also affect shrinkage, with low humidity causing increased shrinkage. Temperature also affects shrinkage, but the effects are minimal when compared to humidity (MacGregor, et al. 2005).

Finally, the size and shape of a member will also influence shrinkage. This is because shrinkage will occur more slowly when moisture has to travel through more material to reach the air (ACI 209R-05). In other words, a very long and slender member would shrink more than a short compact one, if all other factors were the same. A volume-to-surface-area ratio is often computed to measure this geometric property, and assists in calculations of shrinkage. The relationship that is defined by the ACI 209 committee states that shrinkage is considered to be inversely proportional to the square of the volume-to-surface-area ratio (MacGregor, et al. 2005).

2.2.2 Concrete Creep

Creep is defined as the deformation of concrete under sustained loading, or an increase of strain under constant stress. In other words, constant stress in a member will not result in

constant strain because creep will cause the member to increasingly deform throughout time. Creep causes strain to increase quickly at first, but then it will increase at a slower rate as it approaches an asymptote (Nilson 1987).

Consider a sustained load that is applied to a member. Instantaneous elastic strains occur in the member at the time the load is applied, t_0 , and then creep strains develop slowly over time as the load is sustained. Figure 2.2 illustrates this example.

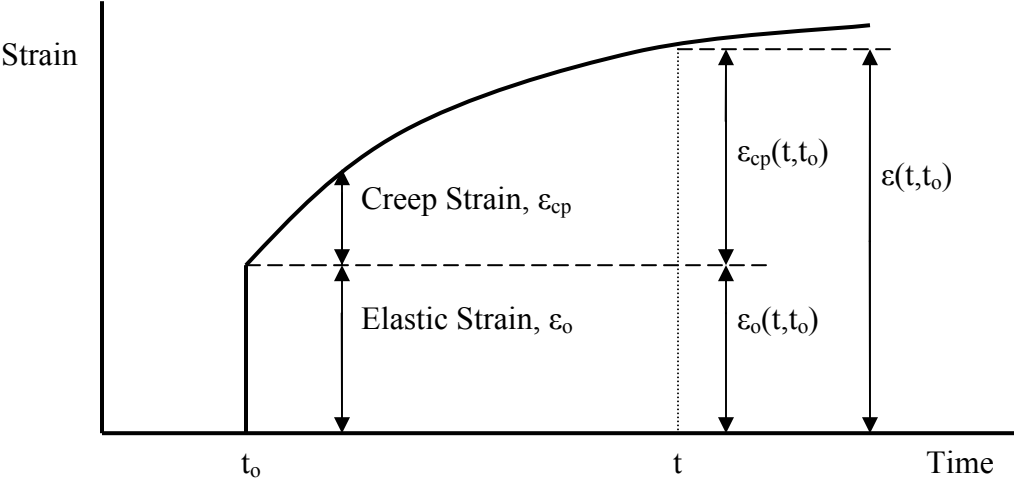


Figure 2.2: Strain Diagram for Creep

The process of calculating the strain due to creep becomes more complicated if there is more than one applied load. This is because concrete becomes increasingly stiff as it ages; in other words, the modulus of elasticity increases over time. Figure 2.3 depicts multiple loadings on a specimen.

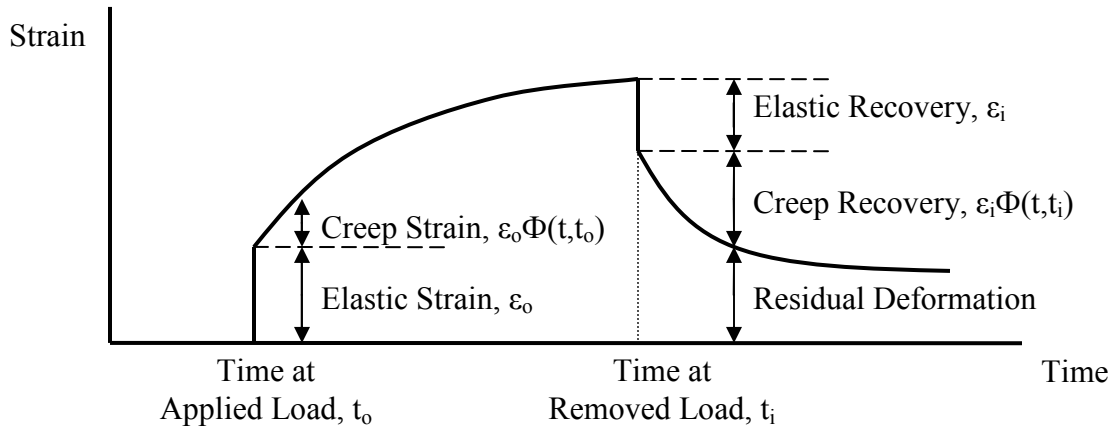


Figure 2.3: Superposition of Creep Strains

Notice in Figure 2.3 that the elastic recovery when the load is removed is less than the elastic strain when the load is applied. The elastic change in strain associated with a particular stress decreases with time because the modulus of elasticity increases with time. The result of this effect is residual deformation that will remain throughout the life of the structure.

The time that the load was applied and the duration of the load must be known to thoroughly express creep. In Figure 2.2, $\epsilon_{cp}(t, t_0)$ refers to the creep strain at a certain time, t , due to the loading at the initial time of the applied load, t_0 . Likewise, $\epsilon_0(t, t_0)$ refers to the initial elastic strain at a certain time, t , due to the load at the initial time of the applied load, t_0 . The total strain is therefore $\epsilon(t, t_0)$, and it is the sum of the elastic strain and the creep strain. Generally, the creep strains are about one to three times the elastic strains at the end of service life (MacGregor, et al. 2005). Therefore, they are very important to consider in calculations because they can result in greater deflections, as well as a decrease in prestressing forces and the redistribution of stresses within cross sections.

Creep can be divided into two main types. Basic creep is the change in strain due to a sustained load when moisture loss is prevented, so it is independent of the size of the member (ACI 209R-05). Although basic creep increases quickly at first and then more slowly over time, it has not yet been proven that basic creep will approach an asymptote (Bazant 1975). Drying creep is the additional creep that occurs when the movement of moisture is allowed, so it depends on the size of the member. The ratio of creep strain per unit of load is defined as specific creep (ACI 209R-05).

Some of the factors that influence the creep of concrete include the mix design, curing process, humidity, temperature, and age of concrete when loaded (MacGregor, et al. 2005). One of the most important is the mix design, which includes the quantity of aggregate, size of aggregate, elastic properties of the aggregate, water content, air content, and cement content. Creep will generally be greater when the aggregate volume is smaller, the aggregate has lower elastic properties, the water content is higher, and the air content is higher. The cement content and the size of the aggregate do cause variations in creep, but it is difficult to determine their definitive effects. Another important factor is the surrounding environment, which affects the drying creep of a concrete member. The ambient relative humidity and temperature will cause greater creep if they encourage the evaporation of moisture from the specimen (ACI 209R-05).

A common way to express creep is by using the creep coefficient, $\Phi(t, t_0)$. The creep coefficient can be described as a ratio of the creep strain at a time, t , for a stress applied at an initial time, t_0 , to the initial elastic strain at age t_0 . This equation is written as:

$$\phi(t, t_0) = \frac{\varepsilon_{cp}(t, t_0)}{\varepsilon_o} = \frac{\varepsilon(t, t_0) - \varepsilon_o}{\varepsilon_o} \quad (2.1)$$

Another way to express creep is by using the creep compliance function, $J(t, t_0)$. ACI states that the creep compliance function is a ratio of the total strain minus the drying shrinkage and autogenous shrinkage strain to applied stress. This assumes that creep strains are proportional to the applied stress, if linear creep is assumed (ACI 209R-92). In other words, a stress applied to a member at a specific time, σ_o , times a creep function, $J(t, t_0)$, is equal to a resulting strain at a later time, $\varepsilon(t)$. The equation is written as:

$$\varepsilon(t) = \sigma_o J(t, t_0) \quad (2.2)$$

It is also known that there is a direct relationship between the creep coefficient and the creep function, which can be related by the modulus of elasticity at the initial time. The following equation shows this relationship (ACI 209R-92):

$$\phi(t, t_0) = E(t_0) \cdot J(t, t_0) - 1 \quad (2.3)$$

2.2.3 Relaxation of Prestressing Steel

A concrete member is put into compression when the prestressing tendons are cut or when the post-tensioning strands are stressed. This tensile force keeps the member uncracked for a longer period of time, which results in additional stiffness. However, there are both instantaneous and time-dependent losses that cause a reduction in the prestressing force.

The immediate loss that occurs in a pre-tensioned member is due to the elastic shortening of the concrete, although it is assumed that the change in length of the member is negligible for computational purposes. If a member is post-tensioned, the instantaneous losses would also include the friction between the tendons and the duct and the anchorage slip when the jacking force is transferred to the member (Nilson 1987). Since these elastic losses occur immediately after the transfer of compression to the member, they will not have long term effects on the system. However, there is creep that will occur in the girder because of this prestressing force.

One of the time-dependent losses is due to the relaxation of the prestressing steel. This loss is gradual, and the amount of the relaxation depends on the stress in the stand and the length of time that the stress has been applied. Like shrinkage, prestress loss occurs rapidly at first, but slows as it approaches an asymptote after a large amount of time (Nilson 1987). See Figure 2.4 for illustration.

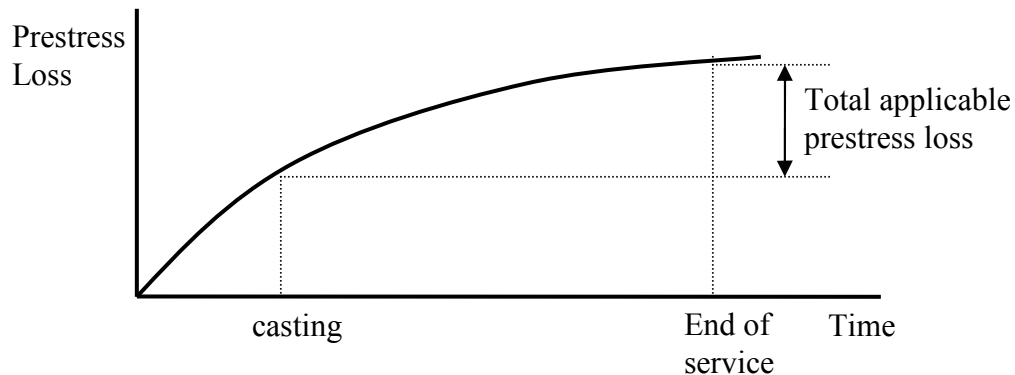


Figure 2.4: Prestress Loss over time

To find the time-dependent effects of steel relaxation in a pre-tensioned member, it is important to calculate the losses that occur from the time that the concrete is cast to the end of

service life. This is found by subtracting the losses that occur from the initial time of prestressing to the time when the concrete is cast from the losses that occur from the initial time of prestressing to the end of service life.

2.3 Analysis Methods for Creep and Shrinkage

Although the individual properties of creep and shrinkage are fairly well understood, several different methods have been developed to analyze their behavior over time.

2.3.1 Principle of Superposition

The principle of superposition is an analysis method used to determine the change in strain from multiple loading and unloading conditions through time. This method determines the value of creep strain at a particular time due to a load applied at an earlier time. If more than one load has been applied through the life of the member, all of the creep strain components are then summed to determine the final creep curve due to all of the loading and unloading cases that occur at various times. Therefore, this method is fairly straightforward if it is assumed that the modulus of elasticity of the concrete is constant and if the stress history is well known. A problem is that this method predicts complete creep recovery, because the modulus of elasticity is considered to be constant, which is not true.

2.3.2 Effective Modulus Method

The effective modulus method was developed by McMillan (1916) and Farber (1927), and it is one of the oldest methods to predict the effects of creep (ACI 209R-92). In this method, the initial modulus of elasticity is adjusted by a factor to account for creep. Figure 2.5 illustrates this relationship.

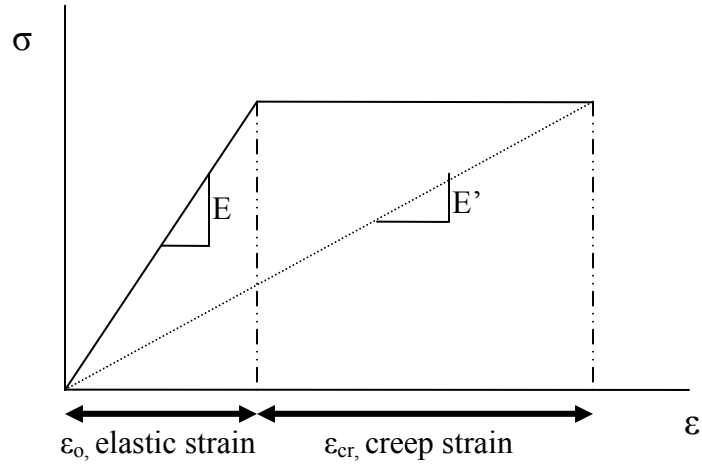


Figure 2.5: Effective Modulus

In Figure 2.5, the left portion of the x-axis is elastic strain, ε_0 , which occurs at the initial application of the load. The right portion of the graph is the creep strain, ε_{cr} , which occurs under sustained loading.

As shown in Figure 2.5, the modulus of elasticity, E , must change over time since the strain increases due to creep but stress remains constant. It is known that:

$$E = \frac{\sigma}{\varepsilon_0} \quad (2.4)$$

$$E' = \frac{\sigma}{\varepsilon_{cr} + \varepsilon_0} \quad (2.5)$$

$$\phi = \frac{\varepsilon_{cr}}{\varepsilon_0} \quad (2.6)$$

The variable Φ is known as the creep coefficient, and is simply a ratio of the creep strain to the elastic strain. Setting stress in equations (2.4) and (2.5) equal to each other yields:

$$E \cdot \varepsilon_0 = E' \cdot (\varepsilon_0 + \varepsilon_{cr}) \quad (2.7)$$

$$E' = E \cdot \frac{\varepsilon_0}{\varepsilon_0 + \varepsilon_{cr}} = \frac{E}{1 + \phi} \quad (2.8)$$

The effective modulus, E' , is therefore a reduced modulus, which can be used in an elastic analysis to take into account the effects of creep. This method is simple, but is incorrect for cases of varying stress. Since the creep strain at a particular time only depends on the current stress, the stress history is excluded. Also, complete recovery of strain is predicted if the stress is removed, which is fundamentally incorrect (Mattock, et al. 1961). Therefore, the stress in the concrete must be fairly constant over the analysis period and the concrete must be older so that there is not a significant change in the modulus of elasticity in order for this method to be used (ACI 209R-92).

2.3.3 Rate of Creep Method

Glanville (1930) developed another method to calculate creep, which is known as the rate of creep method. The basic equation for calculating creep under variable stress using the rate of creep method is:

$$creep = \int_0^T f \frac{d\varepsilon_c}{dT} dT \quad (2.9)$$

where:

T = time

$d\varepsilon_c/dT$ = rate of creep

f = stress

The rate of creep method is based on Glanville's findings that show that the rate of creep is independent of the age of the concrete for young members. The method assumes that concrete will creep at a rate of $f*d\varepsilon_c/dT$ regardless of the stress conditions that occurred in its earlier history, and therefore the creep coefficient is assumed to be independent of the time of loading (Mattock, et al. 1961). In other words, all of the forces that are building up with time are assumed to creep at the same rates as the initially applied load. Since this is not true, this method is generally considered to be outdated. However, newer methods were developed from the basic

principles of the rate of creep method that accounted for the underestimation of creep and creep recovery in older members.

2.3.4 Rate of Flow Method

The rate of flow method was developed by England and Illston (1965) to improve the rate of creep method. They suggested that the creep compliance functions should be the sum of the elastic strain, the delayed elastic strain, and the irrecoverable flow. The delayed elastic strain developed much faster than the irrecoverable flow component, so they needed to be separate components in the formulation of the creep function (ACI 209R-92). The rate of flow method provided a much needed improvement to the rate of creep method, but it still underestimated the value of creep under increasing stress.

2.3.5 Improved Dischinger Method

The improved Dischinger method was formulated when Nielsen (1970) tried to further advance the development of the creep function by combining the rate of creep and the rate of flow methods. He proposed that the irrecoverable flow should be treated similarly as the total creep in the rate of creep method. This method was presented in the CEB-FIP Model Code in 1978 after Rusch, Jungwirth, and Hilsdorf (1973) provided additional modifications.

2.3.6 Age Adjusted Effective Modulus Method

Another method was developed by Trost (1967) and later modified by Bazant (1972) which is today known as the Age Adjusted Effective Modulus method. This method improves upon the previously discussed effective modulus method by making use of an aging coefficient (ACI 209R-92). When a load is applied at a time after the initial loading, an adjustment to the ultimate value of creep is needed because the concrete ages. So, the effective modulus, E' , must be further modified to the age-adjusted effective modulus, E'' . It can be found by:

$$E'' = \frac{E}{1 + \chi\phi} \quad (2.10)$$

In equation (2.10), χ is the age-adjusted factor or the aging coefficient which accounts for changes with time because creep occurs at a slower rate as a member continues to age. The aging coefficient can only be used if the support conditions change instantaneously or if the support conditions change at approximately the same rate as creep, which is the case for shrinkage (ACI 209R-92). In other words, the aging coefficient can be used as long as support conditions do not change considerably faster or slower than creep.

The aging coefficient has a value between 0.5 and 1.0. If the concrete does not age, as in the case of an old member loaded for a short amount of time, the aging coefficient is almost 1.0. On the other hand, if a young member is loaded for a very long period of time, the aging coefficient is nearly 0.5 (Jirsasek 2002). It is recommended that an aging coefficient of 0.8 be used for most analyses (Dilger 1983, Bazant 2002). The Age Adjusted Effective Modulus method is a method that is commonly used in analysis and design of concrete structures today.

In 1982, Dilger published his work on creep-transformed section properties to help analyze members with steel reinforcement. Previously, all of the steel would be combined into one layer for calculations, which would produce inaccurate results. This was a widespread problem since many prestressed structures have more than one layer of steel. This method states that unrestrained creep, free shrinkage, and reduced inherent relaxation should be applied to the creep-transformed cross-section (ACI 209R-92). This study ignores the steel reinforcement, since it is minimal in comparison to the amount of concrete present.

2.4 Design Procedures for Continuity Diaphragms

There currently are several design procedures that calculate the restraint moment in a continuity diaphragm. These include the PCA Method (Freyermuth 1969) and the National Cooperative Highway Research Program (NCHRP) 322 Method (Oesterle, et al. 1989).

2.4.1 PCA Method

In the 1950's the Portland Cement Association (PCA) undertook several projects that focused on composite construction so that an analysis method could be developed (Hongstad, et al. 1960). The findings of a well-known researcher, Mattock, were also included in the

development of the PCA Method which states, “the effects of creep under prestress and dead load can be evaluated by an elastic analysis assuming that the girder and slab were cast and prestressed as a monolithic continuous girder” (Mattock, et al. 1961). The result was the “Design of Continuous Highway Bridges with Precast Prestressed Girders” bulletin (Freyermuth 1969), which laid out the PCA Method that is still used in the calculation of restraint moments in continuity diaphragms today.

The article published by Freyermuth (1969) stated that the effects of the prestressing force and dead load can be modified to account for creep by multiplying by a factor of:

$$1 - e^{-\phi} \quad (2.11)$$

The negative restraint moment due to shrinkage can be modified by a factor of:

$$\frac{1 - e^{-\phi}}{\phi} \quad (2.12)$$

The PCA Method also outlined a method to calculate the creep coefficient. The specific creep strain for a loading that occurs at a girder age of 28 days is based on the modulus of elasticity at the time of the loading. This modulus is obtained from a 20-year loading curve, assuming that the ultimate creep occurs at 20 years. Another figure is then used to adjust the creep strain for the actual age of the concrete at loading, which occurs when the girder is prestressed. A size coefficient is used to adjust the creep strain for a particular volume to surface-area ratio that is being analyzed. Since this method is used to analyze composite and continuous systems, another figure is used to determine the coefficient that represents the percent of the ultimate creep that will have occurred at the time the connection is made. The creep strain that must be developed by the continuity diaphragm must therefore be adjusted by a factor of 100 percent minus the percent of creep strain that has occurred up to the time of continuity. The creep coefficient, Φ , for the creep strain that is remaining can be found by the following:

$$\phi = \frac{\varepsilon_{creep}}{\varepsilon_{elastic}} \quad (2.13)$$

$$E = \frac{1}{\varepsilon_{elastic}} \quad (2.14)$$

$$\phi = \varepsilon_{creep} \cdot E \quad (2.15)$$

where:

ε_{creep} = creep strain

$\varepsilon_{elastic}$ = elastic strain

E = initial modulus of elasticity

The PCA Method also defined the differential shrinkage moment due to the different shrinkage rates of the girder and the deck. It can be applied to the girder along its entire length:

$$M_s = \varepsilon_{diff} \cdot E_b \cdot A_b \cdot \left(e'_2 + \frac{t}{2} \right) \quad (2.16)$$

$$\varepsilon_s = \frac{\varepsilon_{su} \cdot T}{N_s + T} \quad (2.17)$$

$$N_s = 26.0 \cdot e^{0.36 \cdot V/S} \quad (2.18)$$

where:

ε_{diff} = differential shrinkage strain

E_b = elastic modulus for the deck slab concrete

A_b = cross-sectional area of deck slab

e'_2 = centroid of the composite section

t = thickness of the slab

ε_s = shrinkage strain at any time, T

ε_{su} = ultimate shrinkage strain

V/S = volume to surface-area ratio

The 1969 PCA bulletin contained an equation to calculate the time-dependent restraint moment over the pier. It is:

$$M_r = (Y_c - Y_{DL}) \cdot (1 - e^{-\phi}) - Y_s \cdot \left(\frac{1 - e^{-\phi}}{\phi} \right) + Y_{LL} \quad (2.19)$$

where:

M_r = final restraint moment

Y_c = restraint moment at a pier due to creep under prestress force

Y_{DL} = restraint moment at a pier due to creep under dead load

Y_s = restraint moment at a pier due to differential shrinkage between the slab and girder

Y_{LL} = positive live load plus impact moment

PCA bulletin also recommended positive and negative moment reinforcement. It was decided that a viable option for the positive moment continuity reinforcement was reinforcing bars at right angles that were extended into the diaphragm. This detail was tested, and it is recommended that 60% of the yield stress should be used in design of the diaphragm so that the live load plus impact stress range is reduced and there is more assurance against the possibility of diaphragm cracking. It was also suggested that the negative moment continuity reinforcement be designed using the compressive strength of the girder concrete. This bulletin notes that the shear provisions in the AASHTO Specifications of Highway Bridges provide a conservative estimate of the shear capacity of the beams in a continuous system, but the formulas must be applied over the full length instead of only over the middle half of the spans.

The second part of the article published by Freyermuth in 1969 included design examples. The first was for a bridge with four continuous spans with an arbitrary length. The next model expanded on the details of the first example, and spans of 130 ft were selected for the Type IV AASHTO girders.

2.4.2 NCHRP 322 Method

By the early 1980's, continuous bridge design had changed considerably since the PCA Method was developed and implemented. Bridges could span larger distances and have a girder spacing that was greater. Also, the material properties of concrete were changing along with the methods of analysis to model the behavior of these structures. Therefore, although the bridges

that were designed using the PCA Method seemed to be performing fairly well, a new method was sought that would predict the behavior of these structures more accurately.

In the 1980's the National Cooperative Highway Research Program (NCHRP) performed a study to develop procedures for the computation of design moments in the continuity diaphragms of prestressed bridge girders. It was known as NCHRP Project 12-29, and the objectives were to investigate the positive and negative moments to be used in the design of the connections in precast prestressed bridge girders made continuous. The work completed included several experimental investigations involving creep and shrinkage that were performed in Skokie, Illinois, and several analytical investigations of typical continuous bridges.

The NCHRP 322 report summarized and explained the findings of NCHRP Project 12-29. The report noted that the time-dependent effects and the construction sequences must be considered for design. Suggested combinations of girder age at time of deck and diaphragm placement, and age of girder at live load moments, were also included. In addition, computer programs that calculate the service moments using the NCHRP 322 method were developed to aid designers.

2.5 Thermal Effects

Temperature is an important factor influencing creep and shrinkage of a concrete structure. For example, tests have shown that creep strains are approximately two to three times greater for specimens at 122°F, compared to those at 68 to 75°F (Manual of Concrete Practice). Changes in the average temperature of the structure can occur throughout the entire cross-section of the bridge. This will result in translational distortions if the bridge is free to expand and contract, while stresses are introduced if the superstructure is restrained. Also, temperature variations can exist through the cross-section of the bridge. Temperature gradients will cause rotational distortions if the bridge is unrestrained, and bending moments in bridges that are continuous. It is important to be able to model and analyze the effects of temperature gradients on a continuous concrete structure because the bending moments that are introduced must be included in the restraint moment that develops in the continuity diaphragm.

2.5.1 Background

Heat can be transferred by radiation, convection, and conduction. Usually the contributions from convection and conduction are so small that a single coefficient will consider these effects (Imbsen, et al. 1985). Heat transfer by radiation occurs when the structure is exposed to sunlight, and often results in noticeable thermal changes.

Temperature gradients occur because the top and bottom of a member are exposed to a change in temperature and absorb heat rapidly, while the middle portion is predominately insulated from these effects due to the relatively non-conductive nature of concrete. A positive thermal gradient is one in which the deck is warmer than the girder, and a negative thermal gradient is one in which the deck is cooler than the girder. A maximum positive thermal gradient would occur on a sunny and warm day after a few days of cool overcast weather. Likewise, a negative temperature gradient may be applicable on a cool day following warm weather.

Thermal gradients in structures were often not considered before 1980. Then, even after the importance of accounting for temperature changes was universally recognized, there were many different opinions on how to quantify them to predict the best responses. Although thermal effects were known to introduce some additional strain in the cross-section of a bridge, there were not many reported cases where temperature caused significant damage (Imbsen, et al. 1985). Researchers now attribute this to the slightly conservative nature of the design process. Also, the effects of temperature were often largely overlooked, even in situations where temperature was cited as being a likely reason for cracking, because it was known that creep and shrinkage also contributed to the problem.

Engineers realized that bridge design in the United States could be slightly simplified if a standard temperature gradient could be agreed upon and modified to account for geographically specific thermal conditions. In 1978, the British Standard BS 5400 published results defining a negative thermal gradient. This gradient was adopted by the 1985 NCHRP Report 276 as the standard negative thermal gradient for use in the United States. In 1983, a study was published by Potgieter and Gamble that outlined a positive thermal gradient to be used in the design of typical US bridges (Potgieter, et al. 1983). This gradient was based on data gathered from weather stations around the country. This was the positive thermal gradient that was adopted by the 1985 NCHRP Report 276 (Imbsen, et al. 1985) as the standard for use.

The NCHRP Report 276 was very important because at that time states considered the effects of axial length changes to be the most severe, and no state included temperature gradient effects in its typical design codes. In this report, field tests and meteorological data were compiled to divide the United States into four zones for solar radiation (Imbsen, et al. 1985). This temperature gradient was later modified and introduced into the AASHTO LRFD Bridge Design Specifications and is further discussed in Section 2.5.2.

Although a standard temperature gradient is used in continuity diaphragm calculations today, thermal effects are still being researched. A series of experimental tests were completed in 2005 as part of the NCHRP Project 12-53 to examine the performance of diaphragm reinforcement common in the United States. It was concluded that daily temperature changes affect the end reactions in a continuous system by as much as 25%, which reinforced the importance of including thermal effects in the design of continuity diaphragms (Dimmerling, et al. 2005).

2.5.2 AASHTO LRFD Specifications

The AASHTO LRFD Bridge Design Specifications Section 3.12.3 outlines the current temperature gradient that should be used to calculate thermal effects that occur through a cross-section of a bridge system. The standard temperature gradient is from Figure 3.12.3-2 in the AASHTO Specifications and is shown in Figure 2.6.

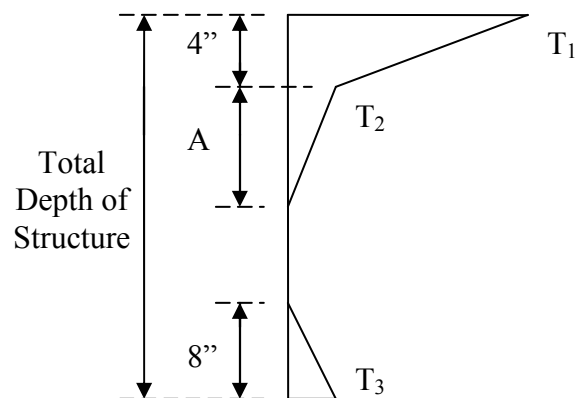


Figure 2.6: Positive Temperature Gradient through Cross-Section

As stated in Section 2.5.1, the United States is divided into 4 zones based on climate. From Figure 3.12.3-1 in the AASHTO Specifications, it is obtained that Virginia is in Zone 3. Table 3.12.3-1 in AASHTO Specification shows that the temperatures associated with Zone 3 are:

$$T_1 = 41^{\circ}\text{F}$$

$$T_2 = 11^{\circ}\text{F}$$

Section 3.12.3 in AASHTO states that T_3 should be taken as 0°F unless a site study indicates otherwise, and the maximum value that can be used for T_3 is 5°F . For the analysis in this project, T_3 will be taken to be 0°F since no other data is available. Section 3.12.3 also defines the value of the dimension A in Figure 2.6 as 12.0 in. for concrete superstructures that have a depth of 16 in. or more. All of the PCBT girders, which are the types that will be considered in this study, fall into this category.

2.6 Summary of Need for Research

First, the PCA Method is often considered to be fairly accurate and conservative in the calculation of time-dependent restraint moments that develop in continuity diaphragms. Since the basis of this method was developed by Mattock in the early 1960's, it would be beneficial to confirm that the PCA Method is still accurate for bridges with modern properties.

Secondly, it is important to further analyze the continuity diaphragm detail developed by Charles Newhouse. It must be checked that the detail is adequate for all PCBT girders that are stored for 90 days according to the new AASHTO specifications.

Finally, it would be advantageous to develop a design aid that assists in the calculation of time-dependent restraint moments for girders that are stored for less than 90 day according the new AASHTO specifications. Although previous research studies discuss the time-dependent moments that develop in continuity diaphragms of concrete bridge systems, one does not exist that calculates the restraint moments for PCBT girders according to new code requirements.

CHAPTER 3: TESTING THE PCA METHOD

3.1 Problem Description

The time-dependent restraint moment that develops in a continuity diaphragm includes the differential shrinkage restraint moment, the prestress losses restraint moment, the moment to restrain prestress creep rotations, and the moment to restrain dead load creep rotations. The PCA Method (Equation 2.19) is a widely accepted method used to calculate the restraint moment due to time-dependent effects. It is often preferred because it is relatively simple and considered to be conservative.

The work of Alan Mattock is the basis for what is known as the PCA Method today (Mattock, et al. 1961). He states that moments develop to restrain the end rotation that would have occurred if the girders in continuous spans were not rigidly connected. Mattock concluded from his research that these moments, “are similar in character and distribution to the secondary moments which are set up in monolithic prestressed continuous girders, prestressed by a non-concordant prestressing tendon”. He also concluded that, “for design purposes, and assuming usual construction procedures, it may be assumed that the distribution of moments and forces will change toward that which would have occurred if the loads applied to the individual elements before continuity was established had instead been applied to the structure after continuity was established” (Mattock, et al. 1961). Mattock assumes that the creep coefficients of the girder and deck are the same, but problems arise because that is not the case for most real bridge structures. Also, it has been debated if the prestress force should be applied to the girder alone instead of the composite cross-section as Mattock suggests. Therefore, there are two questions that needed to be answered before the PCA Method was used in the calculation of prestress restraint moments for this research:

1. Should the prestress moment be applied only to the girder or to the composite cross-section?
2. Does the PCA Method accurately predict the restraint moment in continuity diaphragms if the creep coefficients for the girder and the deck are different?

3.2 Separate Sections Method

To answer the above questions, results from the PCA Method were compared to an alternative method to determine if the PCA Method accurately calculates the diaphragm restraint moment due to the prestress force. A method was developed by Trost and updated by Menn to calculate the final stresses in a composite cross-section (Menn 1986). This method is referred to as the Trost-Menn Method or the Separate Sections Method in this thesis, and is considered to be an accurate method for calculating the stress redistribution in composite sections caused by time-dependent effects of creep and shrinkage. The stresses from the PCA Method were compared to the stresses from the Separate Sections Method to determine the accuracy of the PCA Method.

Figure 3.1 shows the initial creep producing forces and moments, the changes in forces and moments, and the change in strain that occur in a composite system over time due to creep and shrinkage.

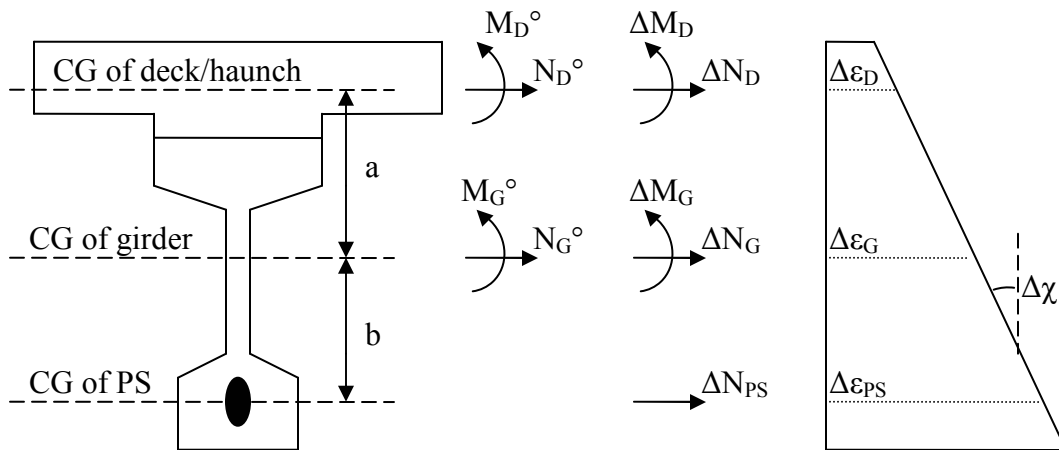


Figure 3.1: Forces, Moments, and Strain Distribution for a Composite Cross-Section

where:

M_D^0 = Initial moment in the deck

N_D^0 = Initial force in the deck

M_G^0 = Initial moment in the girder

N_G^0 = Initial force in the girder

- ΔM_D = Change in the moment in the deck
 ΔN_D = Change in the force in the deck
 ΔM_G = Change in the moment in the girder
 ΔN_G = Change in the force in the girder
 ΔN_{PS} = Change in the force in the deck
 $\Delta \varepsilon_D$ = Change in strain in the deck
 $\Delta \varepsilon_G$ = Change in strain in the girder
 $\Delta \varepsilon_{PS}$ = Change in strain in the prestress
 $\Delta \chi$ = Change in curvature of the system
 a = Distance from centroid of the deck and haunch to the centroid of the girder
 b = Distance from the centroid of the girder to centroid of prestress

The separate sections method is based on the equations of internal equilibrium, the equations relating forces to deformations in the girder and the deck (constitutive equations), and compatibility of deformations through the depth of the cross-sections using the above listed variables. It is assumed that all changes in moments and forces are positive, so a negative change in force resulting from the solution of the simultaneous equations denotes a more compressive force. The equations are shown below:

Equilibrium:

$$\Delta N_D + \Delta N_G + \Delta N_{PS} = 0 \quad (3.1)$$

$$a \cdot \Delta N_D + b \cdot \Delta N_{PS} + \Delta M_D + \Delta M_G = 0 \quad (3.2)$$

Constitutive:

$$\Delta \varepsilon_D = \frac{N_D^o}{E_D A_D} \phi_D + \frac{\Delta N_D}{E_D A_D} (1 + \mu \cdot \phi_D) \quad (3.3)$$

$$\Delta \varepsilon_G = \frac{N_G^o}{E_G A_G} \phi_G + \frac{\Delta N_G}{E_G A_G} (1 + \mu \cdot \phi_G) \quad (3.4)$$

$$\Delta \varepsilon_{ps} = \frac{\Delta N_{ps}}{A_{ps} \cdot E_{ps}} \quad (3.5)$$

$$\Delta \chi = \frac{M_D^o}{E_D I_D} \phi_D + \frac{\Delta M_D}{E_D I_D} (1 + \mu \cdot \phi_D) \quad (3.6)$$

$$\Delta \chi = \frac{M_G^o}{E_G I_G} \phi_G + \frac{\Delta M_G}{E_G I_G} (1 + \mu \cdot \phi_G) \quad (3.7)$$

Compatibility:

$$\Delta \varepsilon_D = \Delta \varepsilon_G - \Delta \chi \cdot a \quad (3.8)$$

$$\Delta \varepsilon_{ps} = \Delta \varepsilon_G + \Delta \chi \cdot b \quad (3.9)$$

After the equations are derived, they can be solved simultaneously. Tensile stresses and elongating strains are considered to be positive, while moments and curvatures with compression at the top and tension at the bottom are positive. The initial forces and moments are considered to be known parameters because they are found from the initial loads on the section. Solving the system of equations gives the changes in the forces, moments, and strains in the system. Note that shrinkage was ignored for this study. Also notice that the prestress relaxation is not included in this analysis because it is considered to be negligible compared to the other forces.

3.2.1 Calculation of Change in Stresses Using the Separate Sections Method

Equations (3.1) through (3.9) are solved simultaneously so the stress distribution changes can be determined for the cross-section. Consider an example of a PCBT 77 girder with a span length of 130 ft, girder spacing of 6 ft, 38 prestressing strands, and a creep coefficient of 2.0 for the girder and deck. The given parameters at mid-span are found in Table 3.1. The stress distribution for this example at mid-span, found using the Separate Sections Method, is shown in Figure 3.2. Note that tension is considered to be positive. The first term in Equation 2.19 calculates the creep due to the quantity of the prestressing minus dead load times the reduction

factor $(1 - e^{-\phi})$. This is the portion of the PCA Method equation that is being analyzed in this study. So, the initial moments and forces, inserted into Equations 3.1 to 3.9, are computed due to the prestress force and the composite dead load.

Table 3.1: Sample Given Parameters for Testing the PCA Method

| | |
|----------|-------------------------|
| A_D | 576 in. ² |
| E_D | 3605 ksi |
| N_D^0 | 0 kips |
| Φ_D | 2.0 |
| I_D | 3072 in. ⁴ |
| M_D^0 | 0 in.-kips |
| μ | 0.8 |
| A_G | 970.7 in. ² |
| E_G | 5098 ksi |
| N_G^0 | -942 kips |
| Φ_G | 2.0 |
| I_G | 788700 in. ⁴ |
| M_G^0 | 9167 in.-kip |
| A_{PS} | 5.814 in. ² |
| E_{PS} | 28000 ksi |
| a | 43 in. |
| b | 29.7 in. |

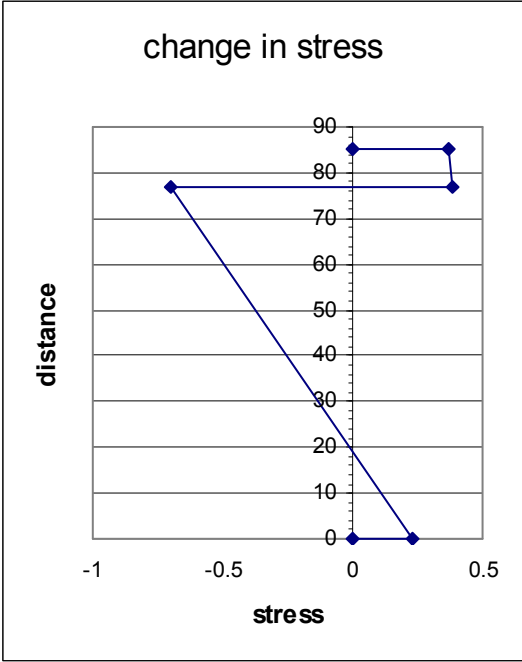


Figure 3.2: Change in Stress Distribution through Cross-Section

3.2.2 Calculation of Rotation Using the Separate Sections Method

The goal of this analysis is to determine if the PCA Method accurately predicts the restraint moments in continuity diaphragms due to prestressing forces when compared to the Separate Sections Method. Therefore, it is important to determine if the two methods give similar rotations at the end of the girder, since the rotation at the ends of the beams is needed to compute the restraint moments that develop in continuity diaphragms. Note that change in curvature is defined as the rate of strain change through the depth of a section, while change in rotation is considered to be the amount that the section rotates (in radians) throughout a given time. For example, the rotation at an end of a simply supported uniformly loaded beam is found by summing the area under the curvature diagram over half of the beam.

To estimate the change in rotation, the change in curvature should be obtained for several critical points. These include the end of the beam, the end of the transfer length, half the distance to the harping point, the harping point, and mid-span. It is necessary to calculate the change in rotation at these points, if not more, because the location of the center of gravity of the strands will cause a variable prestressed moment along the length of the beam and a variable dead load moment will also be present. The Moment Area Method is used to compute the change in rotation.

See Figure 3.3 for a general plot of how the change in curvature varies from the support to mid-span. Note that, for simplicity, it is assumed that there is a linear relationship between each of these points so that the area under a portion of the curve (and therefore the change in rotation) can be found by averaging the changes in curvature between points and multiplying by the distance between them. The total change in rotation at a support is then the total area under half of the change in curvature diagram, if the beam is symmetric about mid-span. This change in curvature is then modified by multiplying by $(1 - e^{-\phi})$ because the moment will “relax” due to creep as time progresses.

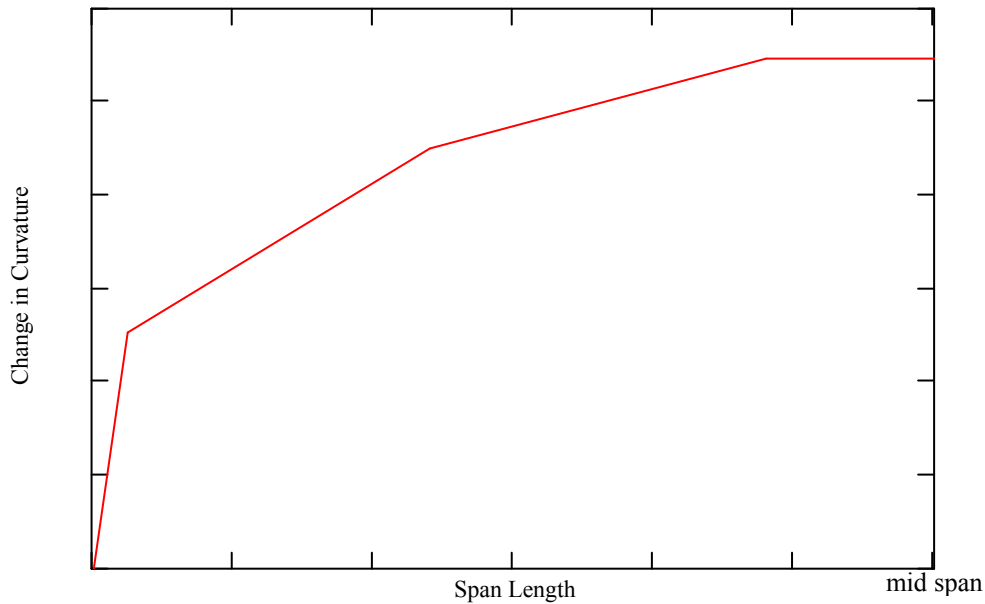


Figure 3.3: Sample of Change in Curvature along Half of the Span Length

Also, note that a certain distance is needed to develop the prestressing force, which is known as the transfer length. AASHTO states that testing indicates that the transfer length is about 50 times the strand diameter. Therefore, the prestressing force, and consequently the moment caused by the prestressing force, is zero at the end of the beam. It is assumed in our example, which uses 0.5 in. diameter prestressing strands, that the full prestressing force is transferred at 25 in. from the end of the beam.

3.3 PCA Method

As previously mentioned, the PCA Method only considers the creep coefficient of the girder. This allows stresses and strains to be computed directly, which avoids the complicated simultaneous equations necessary in the Separate Sections Method. Stresses and strains are computed and compared to the results from the Separate Sections Method. This example is again for a PCBT 77 girder with a span of 130 ft, girder spacing of 6 ft, 38 strands, and creep coefficient of 2.0 for the girder and deck that was discussed in Section 3.2.1.

3.3.1 Calculation of Change in Stresses Using the PCA Method

First, the stress must be calculated due to the prestress assuming that there is no creep, which uses the section properties of the bare girder. This is because there would be no transfer of force or moment from the prestress in the girder to the deck or haunch at the time the deck is placed. The stress distribution uses the moments and forces from the prestressing and dead load. Figure 3.4 shows the initial stress distribution on the bare girder at mid-span.

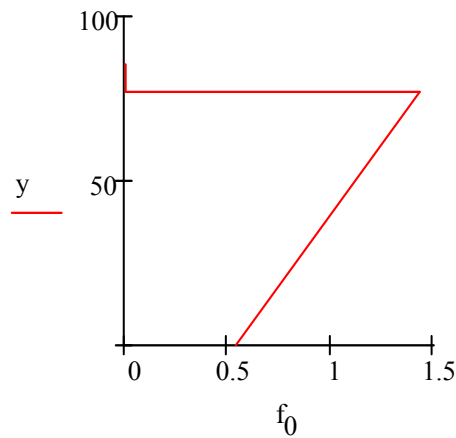


Figure 3.4: Stress through Cross-Section if Creep is Zero

Then, the stress is computed if the creep is infinite. In this case, the forces are applied to the composite cross-sectional properties of the girder and deck. This is because an infinite amount of creep would make the sections essentially behave as one. The stress distribution is shown in Figure 3.5. Note the sudden change in stress at the deck-girder interface (at the girder height, 77 in.). This is due to the difference in the moduli of elasticity at this point.

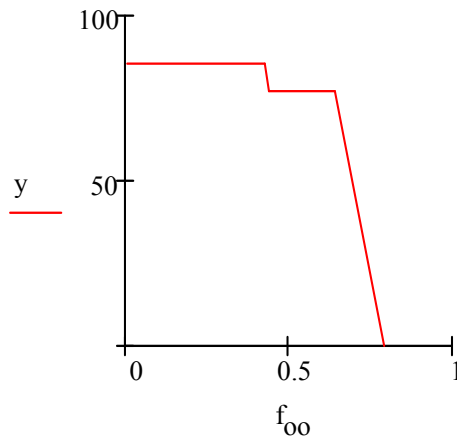


Figure 3.5: Stress through Cross-Section if Creep is Infinite

Subtracting the stress when creep is infinite from the stress when there is no creep will yield the change in stress due to creep. This is shown in Figure 3.6.

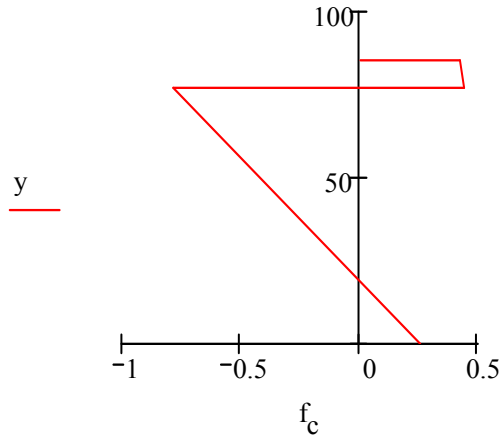


Figure 3.6: Change in Stress through Cross-Section (from Zero to Infinite Creep)

Then, the final stress for the top of the deck, bottom of the deck, top of the girder, and bottom of the girder can be found using the relationships defined in the PCA Method. They are:

$$f_{td,f} = f_{td,o} + f_{td,c} \cdot (1 - e^{-\phi g}) \quad (3.10)$$

$$f_{bd,f} = f_{bd,o} + f_{bd,c} \cdot (1 - e^{-\phi g}) \quad (3.11)$$

$$f_{tg,f} = f_{tg,o} + f_{tg,c} \cdot (1 - e^{-\phi g}) \quad (3.12)$$

$$f_{bg,f} = f_{bg,o} + f_{bg,c} \cdot (1 - e^{-\phi g}) \quad (3.13)$$

where:

$f_{tg,f}$ = stress in the top of the girder at final time

$f_{tg,o}$ = stress in the top of the girder at no creep

$f_{tg,c}$ = change in stress in the top of the girder from no creep to infinite creep

Φg = creep coefficient of the girder

The other variables in Equations (3.11) to (3.13) are defined similarly to those in Equation (3.10) for the bottom of the deck, the top of the girder, and the bottom of the girder. Note that differential shrinkage is ignored.

3.3.2 Calculation of Rotation Using the PCA Method

Using the initial stresses and the change in stresses, the following equations were used to compute the change in curvature:

$$\Delta \varepsilon_{gt} = \frac{\phi_g}{E_g} (f_{tg,o} + f_{tg,c}) \quad (3.14)$$

$$\Delta \varepsilon_{bt} = \frac{\phi_g}{E_g} (f_{bg,o} + f_{bg,c}) \quad (3.15)$$

$$\Delta \chi = \frac{\Delta \varepsilon_{tg} - \Delta \varepsilon_{bg}}{h} \quad (3.16)$$

where:

$\Delta \varepsilon_{gt}$ = change in strain at the top of the girder

Φ_g = creep coefficient of the girder

E_g = modulus of elasticity of the girder

$f_{tg,o}$ = initial stress at the top of the girder

$f_{tg,c}$ = change in stress at the top of the girder

$\Delta \varepsilon_{bt}$ = change in strain in the bottom of the girder

$f_{bg,o}$ = initial stress at the bottom of the girder

$f_{bg,c}$ = change in stress at the bottom of the girder

$\Delta \chi$ = change in curvature

h = height of the girder

Equations (3.13) through (3.15) were computed at mid-span, and were compared to the change in curvature at mid-span using the Separate Sections Method. As mentioned previously, it is important to compare the unrestrained rotation at the end of the beams since that will cause diaphragm restraint moments to develop in continuous spans. The PCA Method states that the rotation at the end of the beam can be computed using the following equations:

$$\theta_{pca_s} = \frac{S_s \cdot P_{eff} \cdot (y_{comp} - e_s) \cdot L}{2 \cdot E_g \cdot I_{comp}} \quad (3.17)$$

$$\theta_{pca_h} = \frac{S_h \cdot P_{eff} \cdot [0.1(y_{comp} - eh_{ms}) - 0.2(eh_{end} - y_{comp})] \cdot L}{E_g \cdot I_{comp}} \quad (3.18)$$

$$\theta_{pca} = \theta_{pca_s} + \theta_{pca_h} \quad (3.19)$$

where:

θ_{pca_s} = rotation due to straight strands

θ_{pca_h} = rotation due to harped strands

θ_{pca} = total rotation

S_s = number of straight strands

S_h = number of harped strands

P_{eff} = effective prestressing force per strand

y_{comp} = composite centroid measured from the bottom of the girder

e_s = centroid of straight prestressing strands measured from the bottom of the girder

eh_{ms} = centroid of harped prestressing strands from the bottom of the girder at mid-span

eh_{end} = centroid of harped prestressing strands from the bottom of the girder at end of beam

L = span length

E_g = modulus of elasticity of the girder

I_{comp} = composite moment of inertia

Note that one of the objectives of Chapter 3 is to determine if θ_{pca} should involve the centroid of the bare beam instead of the composite centroid. See Section 3.4 for this discussion. Also, notice that Equations (3.17) and (3.18) are derived using the Moment Area Method, so the M/EI diagrams for straight and harped strands are shown in Figure 3.7 and Figure 3.8.

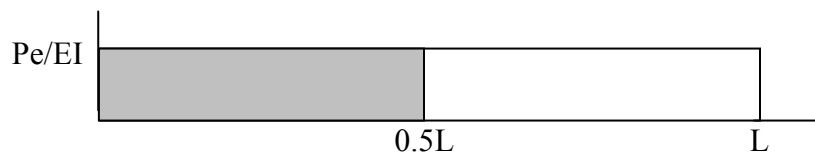


Figure 3.7: M/EI Diagram for Straight Strands

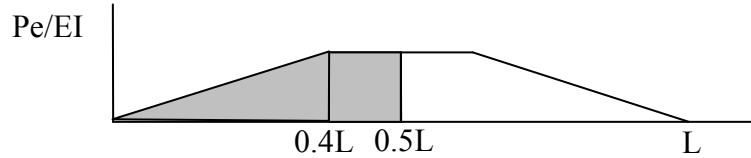


Figure 3.8: M/EI Diagram for Harped Strands

3.4 Prestress Applied to Composite Cross-Section

A brief study is needed to show if the prestress force should be applied to the composite cross-section as recommended by the PCA Method. The prestress was the only loading condition considered in this study, and shrinkage was ignored. The work of Charles Newhouse (Newhouse 2005) contains a design example which can be used to compare the PCA Method and the Separate Sections Method. The parameters are found in Table 3.2.

Table 3.2: Design Parameters from Newhouse

| | |
|---|--------------------------|
| Girder Size | PCBT-45 |
| Girder compressive strength | 8 ksi |
| Span length | 100 ft |
| Modulus of the girder | 4578 ksi |
| Moment of inertia of the girder | 207,300 in. ⁴ |
| Distance from girder centroid to the bottom | 22.23 in. |
| Area of the girder | 746.7 in. ² |
| Deck width | 6 ft |
| Thickness of the deck | 7.5 in. |
| Haunch thickness | 1.5 in. |
| Composite moment of inertia | 432700 in. ⁴ |
| Creep Coefficients (Girder and Deck) | 2.0 |

The updated AASHTO LRFD models for creep, shrinkage, and prestress loss are used in the time-dependent calculations. The Separate Sections Method gives a rotation of 16,705,478/EI. The rotation using the PCA Method when the prestressing force is applied to the bare beam is 9,921,428/EI, while the rotation when the PCA Method is used applying the prestressing force to the composite beam gives a rotation of 16,943,831/EI. See the document published by Newhouse in 2005 for a more in-depth discussion of the calculations using the Separate Sections Method.

Notice that there is substantially more error when the prestress is applied only to the girder cross-section. No extensive study was needed because limited results showed very clearly that applying the prestress to the composite section is more accurate.

3.5 Set-Up and Results

Several trials with a variety of parameters were run to determine if the PCA Method and the Separate Sections Method gave similar results. It was out of the scope of this document to analyze all combinations of parameters that could be associated with this problem, so a few were selected that would provide an overall representation of results. The parameters that were used include three types of PCBT girders (45, 61, and 77), a deck width of 6 ft and 9 ft, and a long and medium span length for each case. The suggested number of prestressing strands for each trial was obtained from the VDOT design guide (see Appendix E).

3.5.1 Comparison of Stresses

The prestressing force was applied to the composite cross-section. The calculated stress results showed that there was less than 5% error in the calculation of stress at the bottom and top of the deck and at the bottom and top of the girder for all cases where the creep coefficient of the girder and the deck were equal. However, there was error introduced when the creep coefficients were not equal. In general, the greatest percent error occurred in the top of the deck (about 20% to 25%), and the smallest error occurred in the bottom of the girder (5% or less). The PCA Method conservatively over-predicted the stress in the bottom of the girder and deck in nearly all cases, but was not always conservative when predicting the stress in the top of the girder and deck.

As mentioned in the beginning of section 3.1, the PCA Method is a simplified approach that assumes the creep coefficients of the girder and the deck are the same and equal to the creep coefficient of the girder. The results from this study provide reassurance that using the creep coefficient of the girder was sufficient if the creep coefficients of the girder and the deck were the same. However, although the PCA Method was almost always conservative, results did vary if the creep coefficients were different. Since it seems that the creep coefficient of the girder did

not provide highly accurate results, an investigation was undertaken to determine if a creep coefficient can be used in the PCA Method that will more accurately model stresses.

3.5.2 A Better Creep Coefficient

This set of parametric studies addresses if the girder creep coefficient can be modified so that use in the PCA Method would provide more accurate results in composite systems. It was quickly determined that an average or a weighted average of the girder and deck creep coefficients was not the best solution. Using one of these methods increases the creep coefficient used in the PCA Method because the deck creep coefficient is always greater than or equal to the girder creep coefficient because the deck concrete is younger than girder concrete. The creep coefficients that give results closest to those found using the superposition method were less than the girder creep coefficients.

A parametric study was completed to determine the best creep coefficient to compute stresses through a cross-section using the cases discussed in Section 3.5, including girder and deck creep coefficients of 2.00 and 2.00, 1.75 and 2.25, 1.50 and 2.50, 1.25 and 2.75, and 1.00 and 3.00 respectively. Once again, the effects of shrinkage were not included. First, the more exact stresses were found at several locations through the depth of the composite cross-section using the Separate Sections Method and the specified creep coefficients. Then, the stresses were found using the PCA Method and a creep coefficient varying from 2.00 to 0.30 with 0.05 increments. The “best fit” PCA creep coefficient, Φ , was the one that minimized the percent error for the stresses along the depth of the composite cross-section when compared to those obtained using the Separate Sections Method.

For example, consider a PCBT 45 girder, with 6 ft girder spacing, a span length of 60 ft, and 16 prestressing strands. Stresses were calculated using the Separate Sections Method with numerous values of the girder and deck creep coefficients, and are presented in Table 3.3. The stresses were then calculated using the PCA Method with varying creep coefficients. For the above example, the PCA stresses are shown in Table 3.4.

Table 3.3: Sample Stresses (ksi) using the Separate Section Method

| Φ_g | Φ_d | top deck | bottom deck | top girder | bottom girder |
|----------|----------|----------|-------------|------------|---------------|
| 2.0 | 2.0 | 0.072 | 0.119 | -0.256 | 0.655 |
| 1.75 | 2.25 | 0.067 | 0.103 | -0.281 | 0.647 |
| 1.5 | 2.5 | 0.061 | 0.089 | -0.306 | 0.638 |
| 1.25 | 2.75 | 0.053 | 0.074 | -0.333 | 0.628 |
| 1.0 | 3.0 | 0.045 | 0.060 | -0.362 | 0.618 |

Table 3.4: Sample Stresses (ksi) using the PCA Method

| PCA Φ | top deck | bottom deck | top girder | bottom girder |
|------------|----------|-------------|------------|---------------|
| 2.00 | 0.075 | 0.123 | -0.247 | 0.658 |
| 1.95 | 0.074 | 0.122 | -0.249 | 0.657 |
| 1.90 | 0.074 | 0.121 | -0.251 | 0.656 |
| 1.85 | 0.073 | 0.120 | -0.253 | 0.655 |
| 1.80 | 0.072 | 0.119 | -0.256 | 0.655 |
| 1.75 | 0.071 | 0.117 | -0.258 | 0.654 |
| 1.70 | 0.071 | 0.116 | -0.261 | 0.653 |
| 1.65 | 0.070 | 0.115 | -0.263 | 0.652 |
| 1.60 | 0.069 | 0.113 | -0.266 | 0.651 |
| 1.55 | 0.068 | 0.112 | -0.269 | 0.650 |
| 1.50 | 0.067 | 0.110 | -0.272 | 0.649 |
| 1.45 | 0.066 | 0.109 | -0.275 | 0.648 |
| 1.40 | 0.065 | 0.107 | -0.278 | 0.647 |
| 1.35 | 0.064 | 0.105 | -0.282 | 0.645 |
| 1.30 | 0.063 | 0.103 | -0.286 | 0.644 |
| 1.25 | 0.062 | 0.101 | -0.290 | 0.643 |
| 1.20 | 0.060 | 0.099 | -0.294 | 0.641 |
| 1.15 | 0.059 | 0.097 | -0.298 | 0.640 |
| 1.10 | 0.058 | 0.095 | -0.302 | 0.638 |
| 1.05 | 0.056 | 0.092 | -0.307 | 0.636 |
| 1.00 | 0.055 | 0.090 | -0.312 | 0.635 |
| 0.95 | 0.053 | 0.087 | -0.318 | 0.633 |
| 0.90 | 0.051 | 0.084 | -0.323 | 0.631 |
| 0.85 | 0.050 | 0.081 | -0.329 | 0.629 |
| 0.80 | 0.048 | 0.078 | -0.335 | 0.627 |
| 0.75 | 0.046 | 0.075 | -0.341 | 0.624 |
| 0.70 | 0.044 | 0.072 | -0.348 | 0.622 |
| 0.65 | 0.041 | 0.068 | -0.355 | 0.619 |
| 0.60 | 0.039 | 0.064 | -0.363 | 0.617 |
| 0.55 | 0.037 | 0.060 | -0.371 | 0.614 |
| 0.50 | 0.034 | 0.056 | -0.379 | 0.611 |
| 0.45 | 0.031 | 0.052 | -0.388 | 0.608 |
| 0.40 | 0.029 | 0.047 | -0.397 | 0.605 |
| 0.35 | 0.026 | 0.042 | -0.406 | 0.601 |
| 0.30 | 0.022 | 0.037 | -0.416 | 0.598 |

After the stresses are computed using the Separate Sections Method and PCA Method, they can be compared. See Table 3.5 for percent difference of stresses with the girder and deck creep coefficients of 2.00.

Table 3.5: Percent Difference of Stresses for a Girder and Deck Phi of 2.00

| Φg | top deck | bottom deck | top girder | bottom girder |
|----------|----------|-------------|------------|---------------|
| 2.00 | -4 | -3 | 4 | 0 |
| 1.95 | -3 | -3 | 3 | 0 |
| 1.90 | -3 | -2 | 2 | 0 |
| 1.85 | -1 | -1 | 1 | 0 |
| 1.80 | 0 | 0 | 0 | 0 |
| 1.75 | 1 | 2 | -1 | 0 |
| 1.70 | 1 | 3 | -2 | 0 |
| 1.65 | 3 | 3 | -3 | 0 |
| 1.60 | 4 | 5 | -4 | 1 |
| 1.55 | 6 | 6 | -5 | 1 |
| 1.50 | 7 | 8 | -6 | 1 |
| 1.45 | 8 | 8 | -7 | 1 |
| 1.40 | 10 | 10 | -9 | 1 |
| 1.35 | 11 | 12 | -10 | 2 |
| 1.30 | 13 | 13 | -12 | 2 |
| 1.25 | 14 | 15 | -13 | 2 |
| 1.20 | 17 | 17 | -15 | 2 |
| 1.15 | 18 | 18 | -16 | 2 |
| 1.10 | 19 | 20 | -18 | 3 |
| 1.05 | 22 | 23 | -20 | 3 |
| 1.00 | 24 | 24 | -22 | 3 |
| 0.95 | 26 | 27 | -24 | 3 |
| 0.90 | 29 | 29 | -26 | 4 |
| 0.85 | 31 | 32 | -29 | 4 |
| 0.80 | 33 | 34 | -31 | 4 |
| 0.75 | 36 | 37 | -33 | 5 |
| 0.70 | 39 | 39 | -36 | 5 |
| 0.65 | 43 | 43 | -39 | 5 |
| 0.60 | 46 | 46 | -42 | 6 |
| 0.55 | 49 | 50 | -45 | 6 |
| 0.50 | 53 | 53 | -48 | 7 |
| 0.45 | 57 | 56 | -52 | 7 |
| 0.40 | 60 | 61 | -55 | 8 |
| 0.35 | 64 | 65 | -59 | 8 |
| 0.30 | 69 | 69 | -63 | 9 |

The percent difference that is shown in Table 3.5 is the difference in stresses calculated using the PCA and Separate Sections Methods. As shown in Table 3.5 by the highlighted region, the creep coefficient recommended for use by the PCA Method is 2.00 because the creep coefficient of the girder is 2.00. However, it is observed in Table 3.5 that a creep coefficient of about 1.80 should be used in the PCA Method to produce results closest to those obtained using the more accurate Separate Sections Method. Note that the difference may be due to the aging coefficient that must be assumed in the Separate Sections Method. A typical value of 0.8 for the aging coefficient is used in this example.

Likewise, consider girder and deck creep coefficients of 1.75 and 2.25, respectively. Table 3.6 illustrates the associated percent difference. The creep coefficient used for the PCA Method is 1.75 because the PCA Method specifies that the creep coefficient of the girder be used in calculations. However, 1.35 is a more accurate estimation of a creep coefficient that would give similar results in stress to those obtained using the Separate Sections Method. This more accurate creep coefficient, Φ , will be regarded as the “best fit Φ ” for the remainder of this document.

This process of determining a creep coefficient that can be used in the PCA Method to produce stresses closest to those from the Separate Sections Method was repeated for creep coefficients of the girder and deck of 1.50 and 2.50, 1.25 and 2.75, and 1.00 and 3.00, respectively. Then, this process was repeated for different girder sizes, span lengths, and girder spacings, and the results are shown in Table 3.7.

Table 3.6: Percent Difference of Stresses for a Girder and Deck Phi of 1.75 and 2.25

| PCA Φ | top deck | bottom deck | top girder | bottom girder |
|------------------------------|-----------------|--------------------|-------------------|----------------------|
| 2.00 | -12 | -19 | 12 | -2 |
| 1.95 | -10 | -18 | 11 | -2 |
| 1.90 | -10 | -17 | 11 | -1 |
| 1.85 | -9 | -17 | 10 | -1 |
| 1.80 | -7 | -16 | 9 | -1 |
| 1.75 | -6 | -14 | 8 | -1 |
| 1.70 | -6 | -13 | 7 | -1 |
| 1.65 | -4 | -12 | 6 | -1 |
| 1.60 | -3 | -10 | 5 | -1 |
| 1.55 | -1 | -9 | 4 | 0 |
| 1.50 | 0 | -7 | 3 | 0 |
| 1.45 | 1 | -6 | 2 | 0 |
| 1.40 | 3 | -4 | 1 | 0 |
| 1.35 | 4 | -2 | 0 | 0 |
| 1.30 | 6 | 0 | -2 | 0 |
| 1.25 | 7 | 2 | -3 | 1 |
| 1.20 | 10 | 4 | -5 | 1 |
| 1.15 | 12 | 6 | -6 | 1 |
| 1.10 | 13 | 8 | -7 | 1 |
| 1.05 | 16 | 11 | -9 | 2 |
| 1.00 | 18 | 13 | -11 | 2 |
| 0.95 | 21 | 16 | -13 | 2 |
| 0.90 | 24 | 18 | -15 | 2 |
| 0.85 | 25 | 21 | -17 | 3 |
| 0.80 | 28 | 24 | -19 | 3 |
| 0.75 | 31 | 27 | -21 | 4 |
| 0.70 | 34 | 30 | -24 | 4 |
| 0.65 | 39 | 34 | -26 | 4 |
| 0.60 | 42 | 38 | -29 | 5 |
| 0.55 | 45 | 42 | -32 | 5 |
| 0.50 | 49 | 46 | -35 | 6 |
| 0.45 | 54 | 50 | -38 | 6 |
| 0.40 | 57 | 54 | -41 | 6 |
| 0.35 | 61 | 59 | -44 | 7 |
| 0.30 | 67 | 64 | -48 | 8 |

Table 3.7: Comparison of PCA Phi to Best Fit Phi

| Girder, span, length | Φ_g, Φ_d | Difference of Φ_g & Φ_d | PCA Φ | BestFit Φ | Difference in Φ, PCA & Best Fit | % Difference of Φ, PCA & Best Fit |
|-----------------------------|------------------------------------|--|------------------------------|----------------------------------|--|--|
| PCBT45,S6,L90 | 2.00,2.00 | 0.0 | 2.00 | 1.80 | 0.200 | 11 |
| | 1.75,2.25 | 0.5 | 1.75 | 1.40 | 0.350 | 25 |
| | 1.50,2.50 | 1.0 | 1.50 | 1.05 | 0.450 | 43 |
| | 1.25,2.75 | 1.5 | 1.25 | 0.83 | 0.420 | 51 |
| | 1.00,3.00 | 2.0 | 1.00 | 0.60 | 0.400 | 67 |
| PCBT45,S6,L60 | 2.00,2.00 | 0.0 | 2.00 | 1.80 | 0.200 | 11 |
| | 1.75,2.25 | 0.5 | 1.75 | 1.35 | 0.400 | 30 |
| | 1.50,2.50 | 1.0 | 1.50 | 1.05 | 0.450 | 43 |
| | 1.25,2.75 | 1.5 | 1.25 | 0.80 | 0.450 | 56 |
| | 1.00,3.00 | 2.0 | 1.00 | 0.60 | 0.400 | 67 |
| PCBT45,S9,L60 | 2.00,2.00 | 0.0 | 2.00 | 1.80 | 0.200 | 11 |
| | 1.75,2.25 | 0.5 | 1.75 | 1.43 | 0.320 | 22 |
| | 1.50,2.50 | 1.0 | 1.50 | 1.10 | 0.400 | 36 |
| | 1.25,2.75 | 1.5 | 1.25 | 0.85 | 0.400 | 47 |
| | 1.00,3.00 | 2.0 | 1.00 | 0.62 | 0.380 | 61 |
| PCBT61,S6,L120 | 2.00,2.00 | 0.0 | 2.00 | 1.80 | 0.200 | 11 |
| | 1.75,2.25 | 0.5 | 1.75 | 1.35 | 0.400 | 30 |
| | 1.50,2.50 | 1.0 | 1.50 | 1.03 | 0.470 | 46 |
| | 1.25,2.75 | 1.5 | 1.25 | 0.80 | 0.450 | 56 |
| | 1.00,3.00 | 2.0 | 1.00 | 0.60 | 0.400 | 67 |
| PCBT77,S6,L130 | 2.00,2.00 | 0.0 | 2.00 | 1.80 | 0.200 | 11 |
| | 1.75,2.25 | 0.5 | 1.75 | 1.35 | 0.400 | 30 |
| | 1.50,2.50 | 1.0 | 1.50 | 1.00 | 0.500 | 50 |
| | 1.25,2.75 | 1.5 | 1.25 | 0.75 | 0.500 | 67 |
| | 1.00,3.00 | 2.0 | 1.00 | 0.55 | 0.450 | 82 |
| Average | 2.00,2.00 | 0.0 | 2.00 | 1.80 | 0.200 | 11 |
| | 1.75,2.25 | 0.5 | 1.75 | 1.38 | 0.374 | 27 |
| | 1.50,2.50 | 1.0 | 1.50 | 1.05 | 0.454 | 44 |
| | 1.25,2.75 | 1.5 | 1.25 | 0.81 | 0.444 | 55 |
| | 1.00,1.00 | 2.0 | 1.00 | 0.59 | 0.406 | 69 |

It can be seen that there is similarity in the percent difference between the PCA Φ and the Best Fit Φ among the cases analyzed in Table 3.7. Graphically, the results are represented in Figure 3.9. This figure shows that the percent error increases as the creep coefficients of the girder and the deck become more different. This suggests that the PCA Method would accurately predict the stresses in a cross-section as long as the creep coefficients are similar. More research in this area should be done to determine if an appropriate adjustment factor could increase the accuracy of the PCA Method.

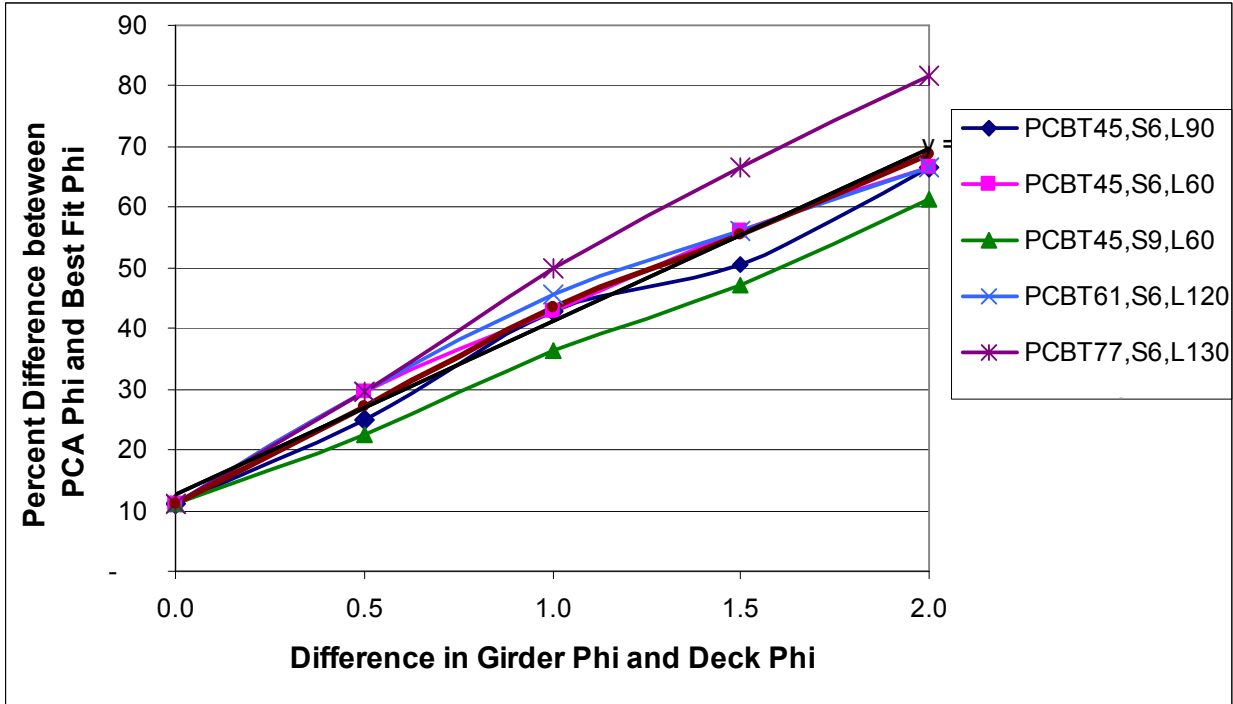


Figure 3.9: Percent Difference between PCA Phi and the Best Fit Phi

3.6 Conclusions

It is important to notice that the PCA Method is conservative. In all cases, the girder creep coefficient used in the PCA Method was larger than the best fit coefficient. For a particular case, the best fit creep coefficient is the one that can be used in the PCA Method to predict stresses closest to those obtained from the Separate Sections Method. This means that the PCA Method predicts a greater redistribution of stresses and moments than what is actually occurring in the cross-section. However, as discussed previously, the PCA Method does not always overestimate the stresses everywhere in the cross-section. The PCA Method generally underestimates the compressive stress that occurs in the top of the girder, but this is not critical because concrete is much stronger in compression than in tension. It can therefore be concluded that the PCA Method can be used in the calculations of time-dependent moments for the remainder of this document.

CHAPTER 4: GIRDERS OLDER THAN 90 DAYS

4.1 Background and Calculations

This portion of this document analyzes prestressed concrete girders that are a minimum age of 90 days when continuity is established. See Appendix E for exact dimensions of the PCBT girders that are analyzed in this study and Figure 4.1 for an approximate sketch.

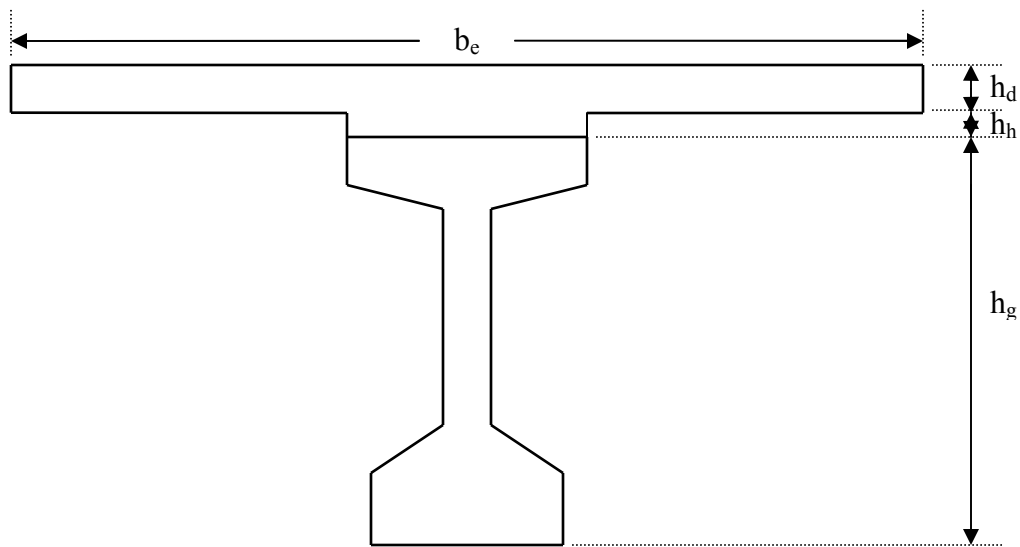


Figure 4.1: Sketch of PCBT Girder with Deck and Haunch

The objective of this section is to determine if the standard continuity diaphragm detail proposed by Charles Newhouse (See Figure 1.4) will provide sufficient moment capacity for all Prestressed Concrete Bulb “T” beams older than 90 days. The applicable AASHTO LRFD article requires that the factored nominal moment of the diaphragm be greater than or equal to 1.2 times the cracking moment, as long as the beams are stored 90 days before establishing continuity. Newhouse’s detail consists of four No. 6 bars bent at a 180° angle, with a total area of 3.52 in^2 . If the detail, with mild reinforcing bars only, does not provide adequate strength, it is necessary to determine how many 0.5 in. diameter prestressing strands or additional No. 6 bars must be extended into the section to provide the sufficient moment capacity.

4.1.1 Design Variables and Assumptions

Not all combinations of possible design parameters can be tested. So, some basic assumptions were made to analyze PCBT continuity diaphragm details. Two-span cases are considered in the analysis because they are the most critical. The deck and diaphragm concrete compressive strength is assumed to be 4 ksi, the deck thickness is 8 in., and the haunch height is 1 in. The area of steel in one No. 6 bar is 0.44 in.², and the yield strength of the bars is 60 ksi. Therefore, the design parameters that are varied are the beam spacing, span length, and beam size.

4.1.2 Calculations

The diaphragm details are evaluated based on the AASHTO LRFD Bridge Design Specifications for diaphragms connecting girders older than 90 days. In particular, the applicable equation is from Article 5.14.1.4.9 in the 2007 AASHTO LRFD Specifications. The article requires, for girders that are older than 90 days at the time continuity is established, that the factored nominal moment of the diaphragm be greater than or equal to 1.2 times the cracking moment. The equation is shown below:

$$\phi M_n \geq 1.2 M_{cr} \quad (4.1)$$

It is very important to assure that the appropriate capacity past cracking is obtained in the diaphragm. This ensures that if a crack opens, the steel will not immediately yield and the cracks should remain well controlled. This strength requirement is necessary because additional capacity past cracking will allow for a warning before larger problems occur. Article 5.5.4.2 defines the appropriate resistance factor, Φ , as 0.9.

The nominal moment resistance, M_n , is the total strength of the continuity diaphragm, and it is defined in Article 5.7.3.2.2 of AASHTO. The following equation results after the appropriate terms are eliminated for the particular cases being analyzed:

$$M_n = A_{ps} f_{ps} \left(d_p - \frac{a}{2} \right) + A_s f_s \left(d_s - \frac{a}{2} \right) \quad (4.2)$$

where:

A_{ps} = area of prestressing steel

f_{ps} = average stress in prestressing steel at nominal flexural resistance

d_p = distance from extreme compression fiber to the centroid of prestressing tendons

a = depth of the compression block

A_s = area of non-prestressed tension reinforcement

f_s = stress in the mild steel tension reinforcement at nominal flexural resistance

d_s = distance from extreme compression fiber to the centroid of non-prestressed tensile reinforcement

The area of prestressed and non-prestressed steel, the average stress in the mild steel, and the distance from the extreme compression fiber of the member to the centroid of the prestressing tendons and to the centroid of the non-prestressed steel can be easily determined. The area of mild steel is based on the detail developed by Charles Newhouse, and is held constant. The area of the prestressing steel is variable, so it is necessary to adjust the number of strands extended into the continuity diaphragm until the factored nominal moment is greater than 1.2 times the cracking moment for all of the cases that are tested.

Assuming that the strains are within the elastic range, the stress in one strand at general slip can be taken as (Salmons 1975):

$$f_{ps} = \frac{L_e - 8.25}{.163} \quad (4.3)$$

where:

L_e = length of the strand

The strand length, L_e , is calculated as the summation of “ a ” and “ b ” in the Figure 4.2. According to the research done by the Missouri Department of Transportation and considering the minimum lengths specified by AASHTO, the detail considered for this analysis has a value a of 10 in. and a value b of 20 in. So, the total strand length is 30 in.

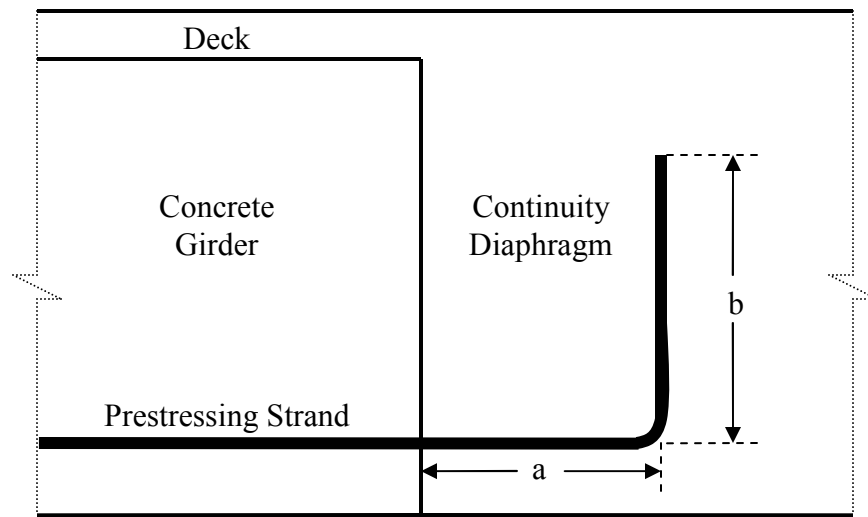


Figure 4.2: Length of Prestressing Strand Extended into the Continuity Diaphragm

Due to the very broad top flange width (see Figure 4.1), the depth of the compression block, a , can be assumed to be less than the depth of the deck. The equation to determine this value is:

$$a = \frac{A_s f_s + A_{ps} f_{ps}}{0.85 f'_c b_{eff}} \quad (4.4)$$

where:

b_{eff} = the effective flange width

f'_c = the specified compression strength

Note that it is important to confirm that the depth of the compression block is indeed less than the depth of the deck after it has been calculated.

The effective flange width, or b_{eff} , is defined in Article 4.6.2.6.1 of AASHTO, and must be calculated to determine the depth of the compression block, a . So, b_{eff} is the least of:

- $\frac{1}{4}$ the effective span length
- 12 times the average depth of the deck, plus the greater of the web thickness or $\frac{1}{2}$ the width of the top flange of the girder
- Average adjacent spacing of the girders

Also, article 4.6.2.6 defines the effective span length for a continuous span as being “the distance between the points of permanent load inflection”. So, for a two-span bridge, the distance between points of permanent load inflection is half the span length.

The cracking moment must be found to determine if the diaphragm reinforcement is adequate for girders older than 90 days. Article 5.7.3.3.2 of AASHTO defines the cracking moment, M_{cr} , as being:

$$M_{cr} = S_c(f_r + f_{cpe}) - M_{dnc} \left(\frac{S_c}{S_{nc}} - 1 \right) \leq S_c f_r \quad (4.5)$$

where:

f_{cpe} = compressive stress in concrete due to effective prestress forces only (after allowance for all prestress losses) at extreme fiber of section where tensile stress is caused by externally applied loads

M_{dnc} = total unfactored dead load moment acting on the monolithic or noncomposite section

S_c = section modulus for the extreme fiber of the composite section when tensile stress is caused by externally applied loads.

S_{nc} = section modulus for the extreme fiber of the monolithic or noncomposite section where tensile stress is caused by externally applied loads

f_r = modulus of rupture

It is important to note that f_{cpe} and M_{dnc} in the previous equation are equal to 0 for the purpose of calculating the diaphragm cracking moment. Therefore, the above equation can be reduced to (see Figure 4.1 for sketch of cross-section):

$$M_{cr} = S_c f_r = \frac{I_{composite}}{y_{composite}} \cdot f_r \quad (4.6)$$

where:

$I_{composite}$ = the moment of inertia for the composite section

$y_{composite}$ = the distance from the bottom of the girder to the centroid of the composite section

Article 5.4.2.6 in the AASHTO LRFD Specifications defines the modulus of rupture, f_r , for normal weight concrete as:

$$f_r = 0.24\sqrt{f'_c} \quad (4.7)$$

Note that f'_c , for the calculations in this section, refers to the compressive strength of the diaphragm concrete, not the compressive strength of the girder.

4.1.3 Sample Calculations

Consider a PCBT-77 girder with a girder spacing of 8 ft and a span length of 130 ft. For this study, the following parameters are considered to be constant:

- Diaphragm compressive strength of 4 ksi
- Slab thickness of 8 in.
- Haunch height of 1 in.
- Area of steel bars of 3.52 in.² (Newhouse standard detail of four No. 6 bars bent 180°)

For this particular girder size, the following parameters can be found:

- Beam moment of inertia of 788,700 in.⁴
- Beam area of 970.7 in.²
- Beam height of 77 in.
- Distance from bottom of beam to centroid of 37.67 in.

See Appendix A for the calculations.

- 1.2 M_{cr} = 16,490 in.-k
- ΦM_n = 16,930 in.-k
- No additional strands are needed

4.2 Results

As previously mentioned, it is important to determine how many prestressing strands or additional mild reinforcing bars must be extended into diaphragms so that the total strength is greater than 1.2 times the cracking moment for girders older than 90 days. A certain amount of strength is obtained from the detail developed by Charles Newhouse, so the remaining strength must come from the prestressing strands or the additional steel.

Consider, for example, the PCBT-45 shown in Figure 4.3. Notice that the design strength is greater than 1.2 times the cracking moment for all cases. So, for this beam size, no additional reinforcement is required.

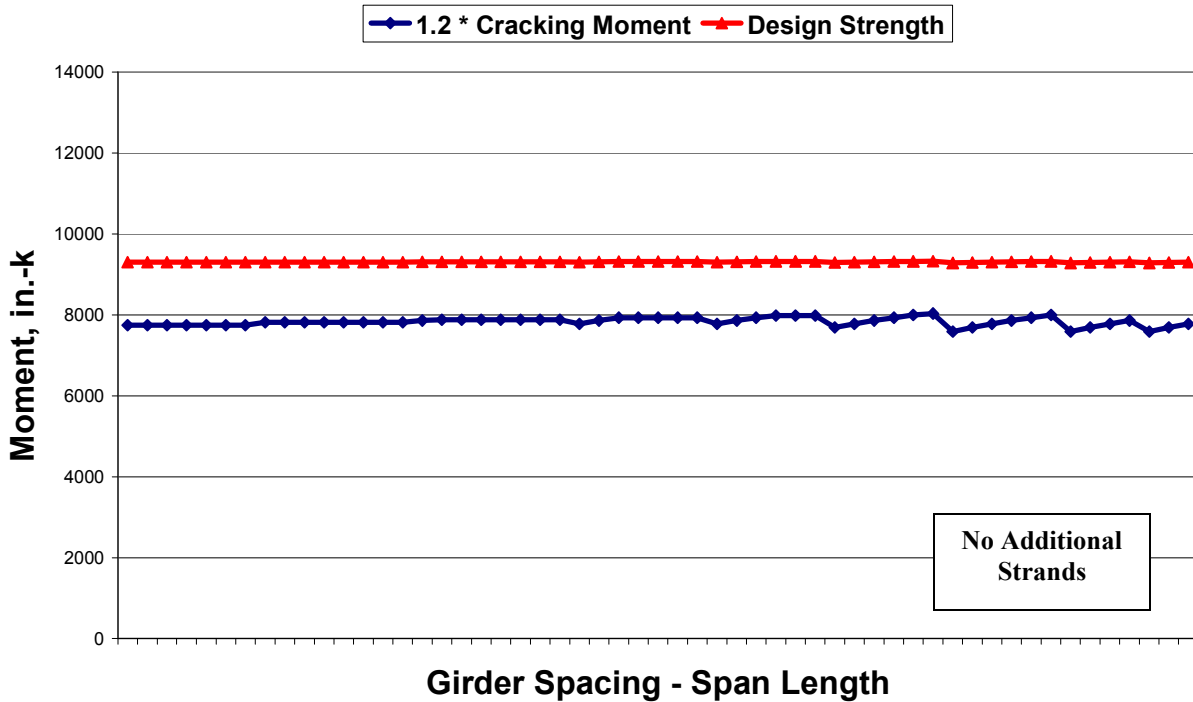


Figure 4.3: Cracking Moment and Design Strength for PCBT-45 Girder

It is also important to note the slight variations in the nominal moment and cracking moment for the PCBT-45 girder in Figure 4.3. The span length and the girder spacing affect the effective width of the deck (“ b_e ” in Figure 4.1). Therefore, the effective deck width is the only variable that changes in the calculation of the nominal moment and cracking moment of the continuity diaphragm. Figures similar to Figure 4.3, which present results for other girders, can be found in Appendix B.

This process was repeated for each PCBT girder for a variety of span lengths and girder spacings. The following cases were investigated:

- For the PCBT-29: 10 cases with a beam spacing varying from 6 ft to 8 ft and a span length varying from 40 ft to 60 ft
- For the PCBT-37: 29 cases with a beam spacing varying from 6 ft to 10 ft and a span length varying from 40 ft to 80 ft

- For the PCBT-45: 55 cases with a beam spacing varying from 6 ft to 10 ft and a span length varying from 40 ft to 100 ft
- For the PCBT-53: 68 cases with a beam spacing varying from 6 ft to 10 ft and a span length varying from 40 ft to 115 ft
- For the PCBT-61: 70 cases with a beam spacing varying from 6 ft to 10 ft and a span length varying from 50 ft to 125 ft
- For the PCBT-69: 66 cases with a beam spacing varying from 6 ft to 10 ft and a span length varying from 60 ft to 135 ft
- For the PCBT-77: 60 cases with a beam spacing varying from 6 ft to 10 ft and a span length varying from 80 ft to 145 ft
- For the PCBT-85: 60 cases with a beam spacing varying from 6 ft to 10 ft and a span length varying from 95 ft to 150 ft
- For the PCBT-93: 59 cases with a beam spacing varying from 6 ft to 10 ft and a span length varying from 100 ft to 160 ft

4.3 Conclusions

For cases for which bars alone were not adequate, the numbers of strands were adjusted until the design strength was at least 1.2 times the cracking moment for all cases. Table 4.1 presents the results.

Table 4.1: Bent Strands Required and Recommended for PCBT Girders

| Girder | # Bent Strands Required | # Bent Strands Recommended |
|---------------|--------------------------------|-----------------------------------|
| PCBT-29 | 0 | 0 |
| PCBT-37 | 0 | 0 |
| PCBT-45 | 0 | 0 |
| PCBT-53 | 0 | 0 |
| PCBT-61 | 0 | 0 |
| PCBT-69 | 1 | 0 |
| PCBT-77 | 1 | 2 |
| PCBT-85 | 2 | 2 |
| PCBT-93 | 2 | 2 |

Note that the PCBT-69 girder almost has sufficient moment capacity beyond the cracking moment without any bent strands. In fact, the design strength was 1.17 times the cracking moment, instead of the needed 1.2, for the worst case analyzed for this girder without bent strands. Therefore, it is recommended that no additional strands be used because it is highly likely that this detail is adequate without extended strands, but the decision to add strands should be left to the discretion of the designer.

There is another option if extending prestressing strands into the diaphragm is not preferable. If the designer would rather not extend prestressing strands, additional mild steel could be used for the continuity diaphragm reinforcement. Using six, rather than four, No. 6 bars bent at a 180° angle would provide adequate capacity for the diaphragm for all cases.

CHAPTER 5: GIRDERS YOUNGER THAN 90 DAYS

5.1 Introduction

Section 5.14.1.4.5 of the AASHTO LRFD Bridge Design Specifications gives two conditions that can be used to determine if a bridge can be considered fully continuous for live loads. Either a negative moment must develop over time in the diaphragm or the girders must be at least 90 days old. It is important to determine when, if ever, the diaphragm moment will become negative because it is not profitable to store girders longer than necessary. However, one must be able to predict long-term effects in order to determine if the AASHTO requirement is met for girders that are stored less than 90 days before continuity.

This chapter presents the method of calculating continuity diaphragm restraint moments for girders younger than 90 days. The PCA Method was used in the analysis with the updated creep and shrinkage models presented in the AASHTO LRFD Bridge Design Specifications. The discussion of the models is followed by the presentation of calculations for time-dependent effects in continuity diaphragms. Finally, an overview of the results and conclusions for PCBT girders is presented towards the end of this chapter.

5.2 Models

Although time-dependent effects in prestressed concrete are fairly well understood, many different models exist to calculate their influences. The two widely used models to determine creep and shrinkage values for design today are the AASHTO LRFD Bridge Design Specifications and the CEB-FIP Model Code 1990. This study was conducted to develop a design aid for continuous concrete bridges with a cast-in-place deck for the Virginia Department of Transportation (VDOT).

VDOT uses the AASHTO LRFD Specifications for design. Therefore, this study uses the AASHTO creep, shrinkage, and prestress loss models with the PCA Method to determine the time-dependent moments in the diaphragm, except $\Phi/(1+\Phi\chi)$ is used instead of $(1-e^{-\Phi})$. These two factors are generally equivalent, but $\Phi/(1+\Phi\chi)$ is consistent with the prestress loss method. To show that these two factors are equivalent, consider typical values of 2.0 for Φ and 0.7 for χ :

$$1 - e^{-2} = 0.865$$

$$2 / (1 + 0.7 * 2) = 0.833$$

Also, some additional consideration of the time-dependent moment that is applied to the continuity diaphragm is in order. AASHTO states that the time-dependent moment must be considered if it is positive because it produces a more critical result, but it should be ignored if it is negative. This illustrates that there is much uncertainty in modeling the time-dependent effects in concrete, so AASHTO chooses the conservative option of ignoring beneficial effects but considering harmful ones.

The moments that must be calculated include the time-dependent, thermal, composite dead load, and live load. This section presents the models used in the calculation of these moments. A MathCAD spreadsheet was developed, using the AASHTO specifications, to determine the restraint moment that will develop in the continuity diaphragm.

5.2.1 AASHTO Creep Model

According to AASHTO LRFD 2007 Bridge Design Specifications Section 5.4.2.3.2, the creep coefficient can be calculated by using the following equations:

$$\psi(t, t_i) = 1.9 k_{vs} k_{hc} k_f k_{td} t_i^{-0.118} \quad (5.1)$$

$$k_{vs} = 1.45 - 0.13(V/S) \geq 0 \quad (5.2)$$

$$k_{hc} = 1.56 - 0.008H \quad (5.3)$$

$$k_f = \frac{5}{1 + f'_{ci}} \quad (5.4)$$

$$k_{td} = \frac{t}{61 - 4f'_{ci} + t} \quad (5.5)$$

where:

$\psi(t, t_i)$ = creep of a member at a given time, t , due to a load applied at an initial time, t_i

H = relative humidity (%)

- k_{vs} = factor for the effect of the volume-to-surface ratio of the component
 k_f = factor for the effect of the concrete strength
 k_{hc} = humidity factor for creep
 k_{td} = time development factor
 t = maturity of concrete (days)
 t_i = age of concrete when the initial load is applied (days)
 V/S = volume-to-surface area ratio (in.)
 f'_{ci} = specified compressive strength of concrete at time of prestressing (ksi)

Note that it can be observed that one day of accelerated steam curing is equal to 7 days of regular curing. The above calculated factors can be used to predict the creep that will occur from any time to any other time.

5.2.2 AASHTO Shrinkage Model

Section 5.4.2.3.3 of the AASHTO LRFD Interim 2005 Bridge Design Specifications defines shrinkage as follows:

$$\varepsilon_{sh} = -k_{vs}k_{hs}k_fk_{td}0.48 \times 10^{-3} \quad (5.6)$$

$$k_{hs} = 2.00 - 0.014H \quad (5.7)$$

where:

- ε_{sh} = shrinkage of a member
 k_{hs} = humidity factor for shrinkage

All other factors correspond to those defined in section 5.1.1.

5.2.3 AASHTO Prestress Loss Model

The AASHTO LRFD 2007 Bridge Design Specifications Section 5.9.5.4.1 defines the loss in prestress due to time-dependent changes by the following equation:

$$\Delta f_{pLT} = (\Delta f_{pSR} + \Delta f_{pCR} + \Delta f_{pR1})_{id} + (\Delta f_{pSD} + \Delta f_{pCD} + \Delta f_{pR2} - \Delta f_{pSS})_{df} \quad (5.8)$$

where:

Δf_{pLT} = change in prestressing steel stress due to time-dependent loss

Δf_{pSR} = prestress loss due to shrinkage of girder from transfer to deck placement

Δf_{pCR} = prestress loss due to creep of girder from transfer to deck placement

Δf_{pR1} = prestress loss due to relaxation of strands from transfer to deck placement

Δf_{pSD} = prestress loss due to shrinkage of girder from deck placement to final time

Δf_{pCD} = prestress loss due to creep of girder from deck placement to final time

Δf_{pR2} = prestress loss due to relaxation of strands from deck placement to final time

Δf_{pSS} = prestress loss due to shrinkage of deck from deck placement to final time

5.2.4 QConBridge

QConBridge is a Windows-based software program that was developed by the Washington State DOT to perform live load analyses. It is used in this document to compute the maximum negative moments in continuity diaphragms for two-span and three-span continuous bridges under live load events. For simplification, only systems with equal span lengths are analyzed.

QConBidge uses the AASHTO LRFD HL93 live load model. In particular, this document uses the dual tandem truck train and the lane load to determine the maximum negative moment for each case, which will occur over the interior support. For use in the comprehensive spreadsheet, the greatest negative moments in equal span systems will be determined for span lengths from 20 ft to 160 ft in 5 foot increments. All values are added to an input table in the MathCAD spreadsheet for later use in the analysis of the continuity diaphragms.

It is important to note that QConBridge calculates the maximum moments occurring in the structure per lane loaded. However, analysis and design of bridges require that a critical moment per beam be found. So, distribution factors are calculated and used to adjust the moment per lane into a moment per beam. Spacing, deck thickness, and length requirements are checked to make sure that AASHTO recommended distribution factors can be used.

5.2.5 Thermal Moment

As previously discussed, the thermal effects on a concrete bridge must be taken into account (Imbsen, et al. 1985). The method suggested in the AASHTO LRFD Bridge Design Specifications states that the equation to calculate the axial force in a fully restrained system due to thermal effects is:

$$P = \int_Y E \cdot \alpha \cdot T(Y) \cdot b(Y) dy = \int_Y \sigma(Y) \cdot b(Y) dy \quad (5.9)$$

where:

E = elastic modulus

α = coefficient of thermal expansion

$T(Y)$ = temperature at depth Y

$b(Y)$ = net section width at height Y

$\sigma(Y)$ = longitudinal stress at a fiber located a distance Y from the center of gravity of the cross-section

P = restraining axial force

Likewise, the moment caused by the thermal forces in a fully restrained system is also defined in NCHRP 276 and is as follows:

$$M = \int_Y E \cdot \alpha \cdot T(Y) \cdot b(Y) \cdot Y dy = \int_Y \sigma(Y) \cdot b(Y) \cdot Y dy \quad (5.10)$$

Figure 5.1 illustrates the AASHTO LRFD Zone 3 thermal gradient being applied to the PCBT girder.

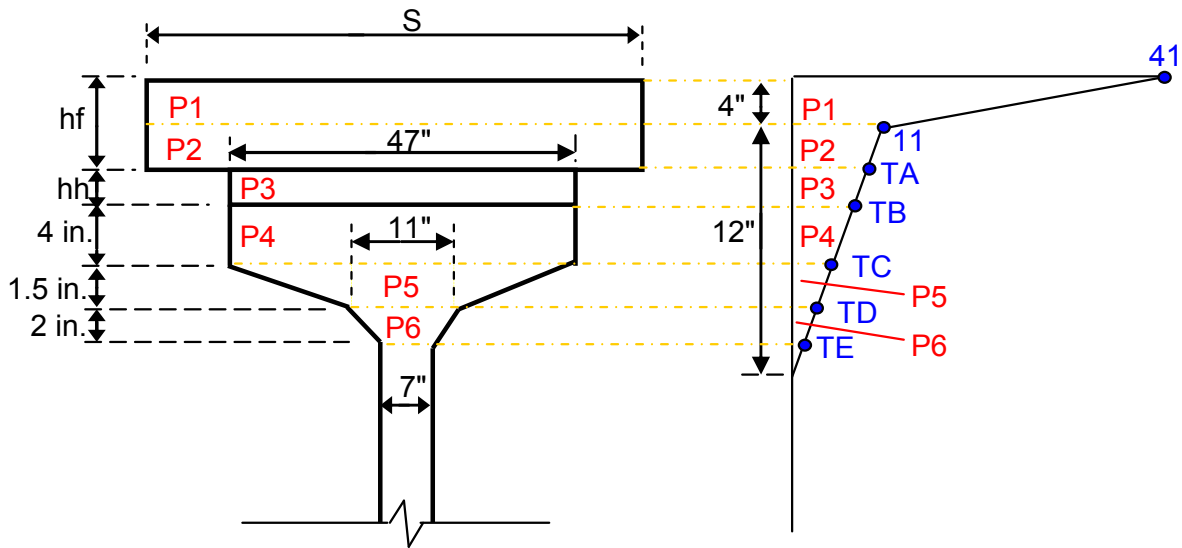


Figure 5.1: Thermal Forces in PCBT Girders

Note that the top and bottom sections of all PCBT girders are the same, so the difference between girder sizes is in web heights. Therefore, the top part of the cross-section shown in Figure 5.1 is valid for all PCBT girder sizes. The negative thermal gradient is not considered because it causes beneficial negative moments over interior supports. See the design example in Appendix C for sample calculations of forces P1 through P6 and for temperatures TA through TE.

Also, notice assumptions made in the model regarding the thickness of the deck and the haunch. Figure 5.1 is based on the assumption that the thickness of the deck is at least 4 in., so the temperature of 11°F is acting in the deck. This is a valid assumption because the VDOT standard specification design aid states that the thickness of the deck should range between 7.5 in. and 8.5 in. (VDOT 2005). In addition, the depth of the deck and haunch together must be at least 8.5 in., so that the temperature gradient reaches 0°F at or before the point labeled “TE” in Figure 5.1. This is a valid assumption because the height of the haunch can be assumed to be at least 1 in. in all cases.

It is important to note that the restraint moment at the interior support is 1.5 times the moment that acts on the end of a beam. See Figure 5.2.

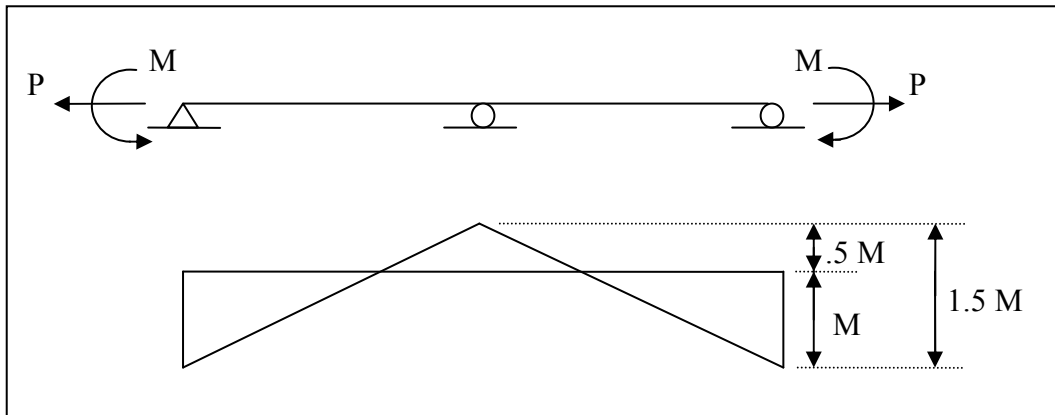


Figure 5.2: Restraint Moment

5.3 Calculations

The PCA Method was used with the improved creep, shrinkage, and prestress loss models, discussed in the previous section, to analyze the time-dependent moments in PCBT girder diaphragms.

5.3.1 Cases Analyzed

For each PCBT girder size, the following cases were analyzed:

- 6 ksi compressive strength, average span length, and narrowest girder spacing
- 6 ksi compressive strength, long span length, and narrowest girder spacing
- 8 ksi compressive strength, average span length, and narrowest girder spacing
- 8 ksi compressive strength, long span length, and narrowest girder spacing
- 6 ksi compressive strength, average span length, and widest girder spacing
- 6 ksi compressive strength, long span length, and widest girder spacing
- 8 ksi compressive strength, average span length, and widest girder spacing
- 8 ksi compressive strength, long span length, and widest girder spacing

These cases were selected because they are considered to be the extreme cases, so they provide bounds for the typical design parameters. The “long span length” was the greatest span length according to the VDOT design aid for a particular girder with a specified compressive strength and girder spacing, and the “average span length” was considered to be about 20 to 25 ft shorter

than the greatest span length. Likewise, the “narrowest girder spacing” was considered to be the smallest girder spacing available on the VDOT design aid for a particular girder size, girder spacing, and compressive strength, while the “widest girder spacing” was the largest girder spacing available.

5.3.2 MathCAD Spreadsheet

The following is a brief description of the calculations that are performed in the MathCAD spreadsheet in Appendix C:

- Input:
 - Beam and deck properties
 - Span length
 - Strand pattern (including number of strands harped)
 - Live loads from QConBridge
- Intermediate Calculations:
 - Calculate transformed cross-sectional properties
 - Check allowable stresses at transfer
 - Calculate creep and shrinkage coefficients
 - From initial time to deck placement
 - From deck placement to end of service
 - Calculate prestress loss
 - From initial time to deck placement
 - From deck placement to end of service
 - Check stresses at deck placement
 - Calculate composite cross-sectional properties
 - Calculate cracking moment of diaphragm

- Time-dependent Calculations:
 - Calculate dead load creep rotation
 - Find the moment to restrain the dead load creep rotation
 - Calculate the end rotation due to prestress
 - Find the moment to restrain prestress rotations
 - Subtract effects of rotation from transfer to deck placement and calculate reduced restraint moment
 - Calculate the diaphragm restraint moment due to loss of prestress
 - Calculate differential shrinkage restraint moment
 - Find the total time-dependent moment in the diaphragm
- Final Calculations:
 - Check stresses at end of service
 - Calculate the thermal restraint moment
 - Calculate the nominal moment capacity of the diaphragm
 - Check if the AASHTO requirements are satisfied
 - Check the flexural strength of the diaphragm

5.4 Results

A comprehensive MathCAD spreadsheet was developed to perform all calculations. See Appendix C for the comprehensive spreadsheet of a two span system. The three-span system is shown in Appendix D. The highlighted fields in the Appendices represent input values that can be adjusted to represent any situation. Results from runs of the MathCAD sheet were recorded in an EXCEL spreadsheet for further analysis. The objective was to determine how many days each PCBT girder must be stored so that positive time-dependent moments will not develop in the continuity diaphragm.

5.4.1 Interpreting Results

Figure 5.3 is a plot of the individual components of the restraint moment in the diaphragm for an average analysis case. These components include the time-dependent, dead load on composite, live load, and thermal restraint moments. The example presented in Figure 5.3 is a PCBT-61 girder with 8 ksi compressive strength concrete, a wide girder spacing (10 ft), and an average span length (60 ft) for the given girder size. As specified by AASHTO, the modified total does not include the contribution of the time-dependent restraint moment if it is negative, but does include it if it is positive. Figure 5.3 illustrates how the restraint moments will change depending on the number of days the girders are stored before they are made continuous and composite. For other cases that were analyzed in this study, the magnitudes of the values in Figure 5.3 are different, but the general patterns are similar.

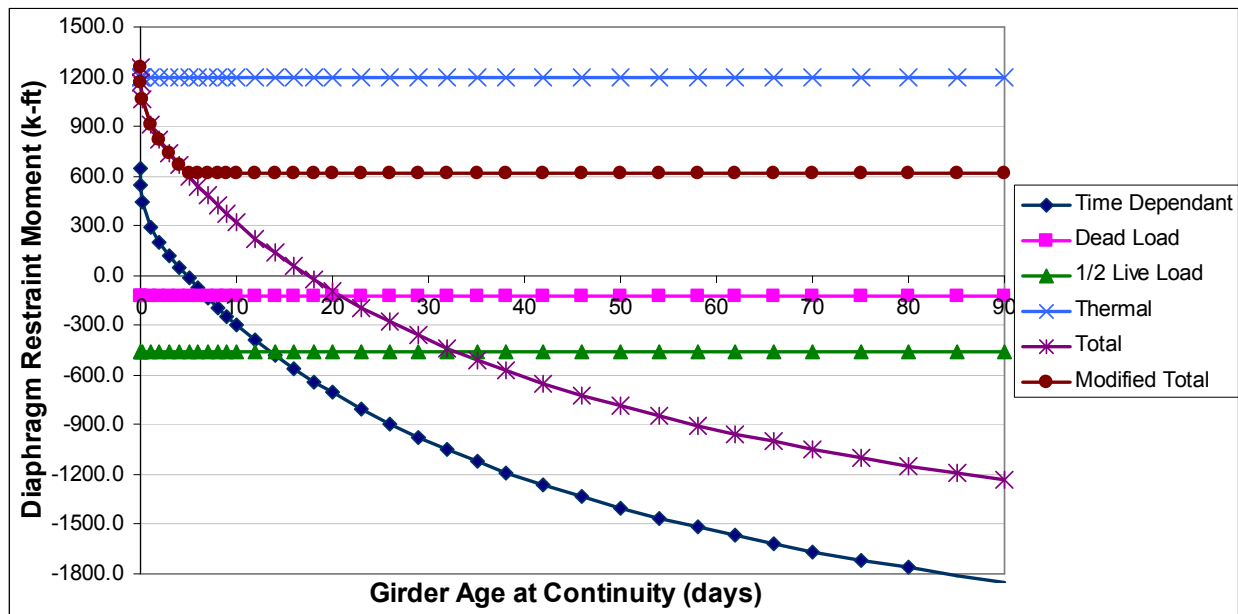


Figure 5.3: Continuity Diaphragm Restraint Moments

Note the magnitude of the positive thermal restraint moment compared to the dead load and live load restraint moment. The positive thermal moment is greater than the sum of the composite dead load and half of the life load. Also notice that that the modified total moment, which does not include the contribution of the time-dependent moment when it is negative, never is negative for this example. This means that this additional criterion involving the modified

total moment will fail, even for an infinite number of storage days. So, the girders must be stored 90 days. When the negative contribution of the time-dependent moment is considered, similar to what is done in this document, the minimum number of storage days for this example is found to be 18 days. This is because the total time-dependent moment will just become negative for this storage duration.

5.4.2 All Results

The previously discussed process of determining the minimum number of storage days was repeated for all of the different cases. They are shown in the following table.

Table 5.1: Experimental Results, PCBT-29 to PCBT 53

| Girder Size (in) | Girder f'c (ksi) | Span Len. (ft) | Deck Space (ft) | Graph Label spacing-f'c-span | Girder Age 2-Span (day) |
|------------------|------------------|----------------|-----------------|------------------------------|-------------------------|
| 29 | 6 | Mid (40) | 6 | big-6-mid | 45 |
| 29 | 6 | Long (45) | 6 | big-6-long | 46 |
| 29 | 8 | Mid (40) | 6 | big-8-mid | 19 |
| 29 | 8 | Long (60) | 6 | big-8-long | 16 |
| 37 | 6 | Mid (40) | 6 | small-6-mid | 52 |
| 37 | 6 | Long (60) | 6 | small-6-long | 30 |
| 37 | 8 | Mid (55) | 6 | small-8-mid | 13 |
| 37 | 8 | Long (80) | 6 | small-8-long | 17 |
| 37 | 6 | Mid (40) | 7.5 | big-6-mid | 48 |
| 37 | 6 | Long (45) | 7.5 | big-6-long | 51 |
| 37 | 8 | Mid (40) | 7.5 | big-8-mid | 26 |
| 37 | 8 | Long (60) | 7.5 | big-8-long | 20 |
| 45 | 6 | Mid (60) | 6 | small-6-mid | 31 |
| 45 | 6 | Long (85) | 6 | small-6-long | 30 |
| 45 | 8 | Mid (75) | 6 | small-8-mid | 7 |
| 45 | 8 | Long (100) | 6 | small-8-long | 20 |
| 45 | 6 | Mid (40) | 9 | big-6-mid | 62 |
| 45 | 6 | Long (45) | 9 | big-6-long | 53 |
| 45 | 8 | Mid (40) | 9 | big-8-mid | 32 |
| 45 | 8 | Long (65) | 9 | big-8-long | 21 |
| 53 | 6 | Mid (80) | 6 | small-6-mid | 24 |
| 53 | 6 | Long (105) | 6 | small-6-long | 40 |
| 53 | 8 | Mid (90) | 6 | small-8-mid | 6 |
| 53 | 8 | Long (115) | 6 | small-8-long | 18 |
| 53 | 6 | Mid (40) | 10 | big-6-mid | 66 |
| 53 | 6 | Long (45) | 10 | big-6-long | 55 |
| 53 | 8 | Mid (50) | 10 | big-8-mid | 25 |
| 53 | 8 | Long (75) | 10 | big-8-long | 20 |

Table 5.2: Experimental Results, PCBT-61 to PCBT 93

| Girder Size (in) | Girder f'c (ksi) | Span Len. (ft) | Deck Space (ft) | Graph Label spacing-f'c-span | Girder Age 2-Span (day) |
|------------------|------------------|----------------|-----------------|------------------------------|-------------------------|
| 61 | 6 | Mid (95) | 6 | small-6-mid | 22 |
| 61 | 6 | Long (120) | 6 | small-6-long | 36 |
| 61 | 8 | Mid (100) | 6 | small-8-mid | 6 |
| 61 | 8 | Long (125) | 6 | small-8-long | 13 |
| 61 | 6 | Mid (40) | 10 | big-6-mid | 67 |
| 61 | 6 | Long (60) | 10 | big-6-long | 43 |
| 61 | 8 | Mid (60) | 10 | big-8-mid | 18 |
| 61 | 8 | Long (85) | 10 | big-8-long | 16 |
| 69 | 6 | Mid (105) | 6 | small-6-mid | 16 |
| 69 | 6 | Long (130) | 6 | small-6-long | 37 |
| 69 | 8 | Mid (110) | 6 | small-8-mid | 4 |
| 69 | 8 | Long (150) | 6 | small-8-long | 5 |
| 69 | 6 | Mid (60) | 10 | big-6-mid | 46 |
| 69 | 6 | Long (85) | 10 | big-6-long | 37 |
| 69 | 8 | Mid (75) | 10 | big-8-mid | 16 |
| 69 | 8 | Long (100) | 10 | big-8-long | 16 |
| 77 | 6 | Mid (110) | 6 | small-6-mid | 15 |
| 77 | 6 | Long (135) | 6 | small-6-long | 29 |
| 77 | 8 | Mid (115) | 6 | small-8-mid | 2 |
| 77 | 8 | Long (140) | 6 | small-8-long | 9 |
| 77 | 6 | Mid (65) | 10 | big-6-mid | 43 |
| 77 | 6 | Long (90) | 10 | big-6-long | 35 |
| 77 | 8 | Mid (90) | 10 | big-8-mid | 14 |
| 77 | 8 | Long (115) | 10 | big-8-long | 18 |
| 85 | 6 | Mid (120) | 6 | small-6-mid | 14 |
| 85 | 6 | Long (145) | 6 | small-6-long | 27 |
| 85 | 8 | Mid (125) | 6 | small-8-mid | 1 |
| 85 | 8 | Long (150) | 6 | small-8-long | 7 |
| 85 | 6 | Mid (85) | 10 | big-6-mid | 34 |
| 85 | 6 | Long (110) | 10 | big-6-long | 38 |
| 85 | 8 | Mid (105) | 10 | big-8-mid | 13 |
| 85 | 8 | Long (130) | 10 | big-8-long | 17 |
| 93 | 6 | Mid (130) | 6 | small-6-mid | 10 |
| 93 | 6 | Long (155) | 6 | small-6-long | 24 |
| 93 | 8 | Mid (130) | 6 | small-8-mid | 1 |
| 93 | 8 | Long (155) | 6 | small-8-long | 6 |
| 93 | 6 | Mid (95) | 10 | big-6-mid | 37 |
| 93 | 6 | Long (120) | 10 | big-6-long | 36 |
| 93 | 8 | Mid (115) | 10 | big-8-mid | 12 |
| 93 | 8 | Long (140) | 10 | big-8-long | 15 |

The highlighted cases in Table 5.1 and Table 5.2 are those that failed the AASHTO requirement, which excludes the contribution of the time-dependent moment if it negative. Therefore, the highlighted cases would need to be stored 90 days since the total moment in the diaphragm will never be negative (because then effects due to negative time-dependent moments must be ignored). There are many of these cases.

5.4.3 General Trends

There are general trends among the results. It is important to recognize and understand these patterns so that continuity diaphragm restraint moments can be better understood.

5.4.3.1 Changes in Length

No comprehensive conclusions can be drawn to compare the change that occurs in the total restraint moment due to changes in the length of the member. In some cases, moving from an average span length to a long span length required a longer storage period for the girders, and in others a shorter storage period resulted. It is difficult to directly determine the effects of adjusting the span length on the total diaphragm restraint moment, because the span length affects all of the individual components of the total restraint moment in different ways. However, the following observations can be noted as span lengths increase for a given number of storage days:

- The thermal moment will not change
- The live load moment will become more negative
- The dead load moment will become more negative
- The time-dependent moment could become either more positive or negative depending on the magnitudes of the changes in the following components:
 - The moment to restrain the dead load creep rotation will become more negative
 - The moment to restrain prestress creep rotations will become more positive
 - The moment to restrain the creep of prestress losses will become more positive
 - The differential shrinkage restraint moment will not change

5.4.3.2 Changes in Compressive Strength

Analysis of the results showed that there was a decrease in the minimum number of storage days when the girder compressive strength was increased from 6 ksi to 8 ksi. The average decrease in the minimum storage days was 65.5%. The largest reduction occurred in the cases consisting of the medium span lengths with the closer girder spacing, which was an average decrease of 80.6% for the cases tested. The smallest reduction occurred in the cases consisting of the long span lengths with the wide girder spacing, which was a decrease of 59.2%.

The decrease in the minimum number of storage days for girders as compressive strength increases is due to several factors. First of all, as the compressive strength increases, there are changes in the transformed area and in the centroid of the transformed area. This will have numerous effects on the calculation of total restraint moment. Also, the ultimate creep and shrinkage will decrease as the concrete strength increases. Therefore, there is a decrease in the minimum number of days that a girder needs to be stored so that the remaining time-dependent effects will not cause positive moments in the diaphragm.

5.4.3.3 Changes in Girder Spacing

The results of the analyzed cases show that there was a 137% average increase in the number of days that the girders needed to be stored so that a positive moment would not develop in the diaphragm when the girder spacing increases from the close to the wide spacing. A larger compressive strength results in a greater degree of change when the girder spacing is adjusted. Also, a more average span length results in greater changes as well. Hence, there is only a moderate (24%) increase in the minimum number of storage days when the girder spacing is changed from close to wide for the cases consisting of the 6 ksi compressive strength with the long span lengths

The girder spacing has several effects on the continuity diaphragm restraint moments. First of all, the dead load moment of the structure in the continuity diaphragm will become more negative as the deck width increases. Likewise, the live load moment in the continuity diaphragm will also become more negative as the deck width increases because the girder distribution factors will increase. Also, differential shrinkage between the deck and the girders

increases because a larger volume of the deck results in a greater shrinkage force in the deck. Most importantly, the thermal gradient that was used in this analysis has a very large component that is applied to the top of the deck. So, increasing the width of the deck substantially increases the positive thermal restraint moment in the continuity diaphragm that needs to be counteracted by the other moments.

5.4.4 Two-Spans vs. Three-Spans

Although it was previously assumed that two-span cases are critical, three-span systems must be further explored because time-dependent factors are interdependent. Appendix D shows a comparison of the calculated terms that change between the two-span and three-span systems. When moving from a two-span case to a three-span case, the composite dead load restraint moment becomes less negative, the live load restraint moment becomes less negative, the thermal restraint moment becomes less positive, the non-composite dead load restraint moment becomes less negative, the prestress restraint moment becomes less positive, and the differential shrinkage moment becomes less negative. Several tests were run on about half of the PCBT girders to compare the two-span and the three span-cases. The results are shown in Table 5.3

The two-span systems are critical for all cases, as shown in Table 5.3. This means that the PCBT girders need to be stored for fewer days before establishing continuity so that a negative diaphragm moment will result. Therefore, it is a valid assumption that the two-span cases are critical and are the only ones that need to be computed.

Table 5.3: Three-Span Systems vs. Two-Span Systems: Minimum Storage Duration

| Girder Size (in) | Girder f'c (ksi) | Span Len. (ft) | Deck Space (ft) | Graph Label space-f'c-span | Girder Age 2-Span (day) | Girder Age 3-Span (day) |
|-------------------------|-------------------------|-----------------------|------------------------|-----------------------------------|--------------------------------|--------------------------------|
| 29 | 6 | Mid (40) | 6 | big-6-mid | 45 | 39 |
| 29 | 6 | Long (45) | 6 | big-6-long | 46 | 40 |
| 29 | 8 | Mid (40) | 6 | big-8-mid | 19 | 16 |
| 29 | 8 | Long (60) | 6 | big-8-long | 16 | 14 |
| 45 | 6 | Mid (60) | 6 | small-6-mid | 31 | 28 |
| 45 | 6 | Long (85) | 6 | small-6-long | 30 | 23 |
| 45 | 8 | Mid (75) | 6 | small-8-mid | 7 | 6 |
| 45 | 8 | Long (100) | 6 | small-8-long | 20 | 12 |
| 45 | 6 | Mid (40) | 9 | big-6-mid | 62 | 55 |
| 45 | 6 | Long (45) | 9 | big-6-long | 53 | 47 |
| 45 | 8 | Mid (40) | 9 | big-8-mid | 32 | 29 |
| 45 | 8 | Long (65) | 9 | big-8-long | 21 | 19 |
| 61 | 6 | Mid (95) | 6 | small-6-mid | 22 | 19 |
| 61 | 6 | Long (120) | 6 | small-6-long | 36 | 23 |
| 61 | 8 | Mid (100) | 6 | small-8-mid | 6 | 4 |
| 61 | 8 | Long (125) | 6 | small-8-long | 13 | 7 |
| 61 | 6 | Mid (40) | 10 | big-6-mid | 67 | 61 |
| 61 | 6 | Long (60) | 10 | big-6-long | 43 | 39 |
| 61 | 8 | Mid (60) | 10 | big-8-mid | 18 | 16 |
| 61 | 8 | Long (85) | 10 | big-8-long | 16 | 4 |
| 77 | 6 | Mid (110) | 6 | small-6-mid | 15 | 12 |
| 77 | 6 | Long (135) | 6 | small-6-long | 29 | 20 |
| 77 | 8 | Mid (115) | 6 | small-8-mid | 2 | 1 |
| 77 | 8 | Long (140) | 6 | small-8-long | 9 | 7 |
| 77 | 6 | Mid (65) | 10 | big-6-mid | 43 | 39 |
| 77 | 6 | Long (90) | 10 | big-6-long | 35 | 31 |
| 77 | 8 | Mid (90) | 10 | big-8-mid | 14 | 12 |
| 77 | 8 | Long (115) | 10 | big-8-long | 18 | 18 |
| 93 | 6 | Mid (130) | 6 | small-6-mid | 10 | 7 |
| 93 | 6 | Long (155) | 6 | small-6-long | 24 | 16 |
| 93 | 8 | Mid (130) | 6 | small-8-mid | 1 | 1 |
| 93 | 8 | Long (155) | 6 | small-8-long | 6 | 4 |
| 93 | 6 | Mid (95) | 10 | big-6-mid | 37 | 33 |
| 93 | 6 | Long (120) | 10 | big-6-long | 36 | 32 |
| 93 | 8 | Mid (115) | 10 | big-8-mid | 12 | 10 |
| 93 | 8 | Long (140) | 10 | big-8-long | 15 | 13 |

5.5 Conclusions

If the designer is willing to perform a somewhat involved analysis, the number of girder storage days can be reduced significantly below 90 days about half of the time. For the other half of the cases that must be stored for 90 days, the total moment in the diaphragm will never

become negative because the contributions of the negative time-dependent moment must be ignored.

If the negative time-dependent restraint moments are considered, the largest minimum number of storage days for girders with a compressive strength of 6 ksi is 67 days and the largest minimum number of storage days for girders with a compressive strength of 8 ksi is 32 days. Note that including the negative time-dependent restraint moments in analysis of girders with a compressive strength of 8 ksi cause a substantial reduction (32 days from 90 days) in the greatest minimum storage duration. In general, narrower girder spacing and higher concrete compressive strength results in shorter required storage duration.

A quick check can be done to see if girders must be stored 90 days. If the sum of the thermal, composite dead load, and half of the live load restraint moments is positive, then the girder must be stored 90 days. This is true because the only restraint moment that varies over time is the time-dependent moment, which must be ignored if it is negative. If the sum of the thermal, composite dead load, and half of the live load restraint moments is negative, then it is very likely that the girder will be able to be stored for less than 90 days. In this case, it would be beneficial to calculate the time-dependent restraint moment and determine the minimum number of storage days that would result in a negative diaphragm restraint moment.

CHAPTER 6: CONCLUSIONS AND RECOMMENDATIONS

6.1 Conclusions and Recommendations

Several conclusions can be drawn from the research presented in this document that will assist in the design of continuity diaphragms for PCBT girders. The topics that are discussed include Testing the PCA Method, Girders Younger than 90 days, and Girders Older than 90 days.

6.1.1 Testing the PCA Method

The stresses throughout the cross-section of a composite bridge system were computed using the PCA Method and then were compared to those found using the Separate Sections Method (or the Trost-Menn Method) to determine accuracy. The PCA Method generally produced conservative estimates of all stresses, and the girder creep coefficient is always a conservative estimation of the creep coefficient that would give results similar to those obtained using the Separate Sections Method. Also, this method is fairly accurate when the girder and the deck creep coefficients are the same, or similar. However, more error is introduced as the creep coefficients become more different from each other, but the method is still overall conservative. Therefore, it has been concluded that the PCA Method adequately predicts the restraint moments that develop in continuity diaphragms due to time-dependent effects.

6.1.2 Girders Older than 90 Days

This section determined how many bent strands need to be extended into continuity diaphragms, in addition to Charles Newhouse's standard detail (see Figure 1.4), to provide sufficient moment capacity for PCBT girders. The applicable AASHTO LRFD article requires, for girders that are older than 90 days at the time continuity is established, that the factored nominal moment of the diaphragm be greater than or equal to 1.2 times the cracking moment. Several girder spacings and span lengths were considered for each girder size.

It was concluded that no additional strands are required for the PCBT-29, PCBT-37, PCBT-45, PCBT-53, and PCBT-61. For the PCBT-69, the design strength was 1.17 times the cracking moment for the worst case analyzed without bent strands, instead of the required 1.2. Therefore, it is highly likely that this detail is adequate without extended strands, but the decision to add strands should be left to the discretion of the designer. The PCBT-77, PCBT-85, and the PCBT-93 require one or two additional bent strands. So, it is recommended that two bent strands be extended into the continuity diaphragm for these three girder sizes.

6.1.3 Girders Younger than 90 Days

The AASHTO LRFD Bridge Design Specifications were used to analyze PCBT girders that are younger than 90 days when continuity is established. AASHTO states that a negative moment must develop in the diaphragm if the girder is stored for less than 90 days before being erected. In addition, the time-dependent moment must be considered if it is positive because it produces a more critical result, but it should be ignored if it is negative. The goal of this aspect of the research was to determine the minimum number of days that PCBT girders need to be stored so that the AASHTO specifications are met.

It was found that if negative time-dependent moments are considered, 67 days is the longest that a PCBT girder needs to be stored for the cases analyzed. However, half of the cases must be stored for 90 days if the negative time-dependent effects are ignored. The factors that seemed to contribute to the necessary 90 day storage time were average span lengths, wide girder spacings, and lower compressive strengths.

If negative time-dependent moments are considered, there are general trends in the data. Analysis of the results showed that there was a decrease in the minimum number of storage days when the girder compressive strength was increased from 6 ksi to 8 ksi and when the girder spacing decreased from the widest spacing to the closest spacing. However, no comprehensive conclusions could be drawn to compare the change that occurs in the total restraint moment due to changes in the length of the member.

Three-span systems were also considered, but the two-span systems were found to be critical for all of the cases in this study. In other words, the PCBT girders need to be stored for fewer days before establishing continuity (so that a negative diaphragm moment will result) if

they are used in three-span systems rather than two-span systems. This is true if negative time-dependent moments are considered or if they are ignored.

6.2 Recommendations for Future Work

The results of this research produce additional questions. First of all, is there a more accurate creep coefficient that can be used in place of the girder creep coefficient when determining stresses in composite systems using the PCA Method? This study showed that although the PCA Method was almost always conservative, the girder creep coefficient was not always close to being accurate. This is especially true if the girder and deck coefficient were not similar. More work is needed to determine if the girder creep coefficient can be simply adjusted for use in the PCA Method to give more accurate results. Also, additional aging coefficients should be considered. This study only considers an aging coefficient of 0.8, which could have a significant impact on the appropriate creep coefficient that should be used in the PCA Method.

Secondly, the behavior of creep and shrinkage are fairly well understood, but there are many different ways to model this behavior. This has been complicated by the many recent advances in the material properties of concrete, which could require older methods of analysis to be further updated. For example, thirty years ago the compressive strength of a typical concrete bridge girder was somewhere between 3000 to 6000 psi, and models existed that calculated the associated time-dependent effects fairly accurately. Since then, a greater understanding of the properties and performance of concrete has been achieved. Concrete mixes now include components, admixtures, and mix proportions considerably different from those in the past. The result is more durable concrete that typically has a compressive strength anywhere from 4000 psi to 10,000 psi. So, it stands to reason that new models should be developed to analyze and design more modern concrete.

In particular, more research is needed to improve the models that analyze prestressed concrete bridge girders made composite with a cast-in-place concrete deck and made continuous over two or more spans. The AASHTO LRFD Bridge Design Specification asserts that the restraint moments that develop in the continuity diaphragm are a function of many factors including time-dependent effects, superimposed permanent load, settlement, live load, and a temperature gradient. The effects that these factors have on restraint moments are still being

explored. Also, additional factors that could possibly contribute to the restraint moments are being considered.

Also, additional design parameters could be varied for PCBT girders that are stored for more than 90 days before erection. For the girders in this study, only the girders' spacings and span lengths were varied for each size girder. So, the diaphragm compressive strength, slab thickness, and haunch height were held constant. The results presented in this study make use of typical design parameters used by VDOT, but varying these parameters could provide more comprehensive results for all possible cases.

Additionally, further research regarding the thermal restraint moment would be beneficial. Although a standard thermal gradient exists for Virginia, experimental testing could improve upon the existing design values. This research illustrated that the thermal restraint moment calculated using the AASHTO thermal gradient was dominant in the design of continuity diaphragm. Therefore, VDOT should consider evaluating a thermal gradient specifically for Virginia to assure that the AASHTO gradient is appropriate. Installing thermocouples into new bridge systems would allow researchers to see how temperature changes through the life of the concrete due to environmental factors. Also, attaching strain gauges to a concrete girder that is part of a bridge would provide insight as to how temperature affects strain due to the surrounding temperatures.

Finally, additional design parameters could also be varied for PCBT girders that are less than 90 days old before they are made composite and continuous. Only different values for the span lengths, girder spacings, and girder compressive strengths were considered for the PCBT girders younger than 90 days. Other design parameters that could be varied to provide a more comprehensive understanding of the results include the age of girder at transfer of prestressing, haunch height, and deck concrete compressive strength. In addition, a sensitivity analysis could be performed on the aging coefficient to determine the magnitude of change that would result from adjusting this parameter.

REFERENCES

- American Association of State Highway and Transportation Officials (AASHTO), (2004). *AASHTO LRFD Bridge Design Specifications - Third Edition with 2005 and 2006 Interims*. Washington, D.C.
- American Concrete Institute (ACI) Manual of Concrete Practice (2002). “Prediction of Creep, Shrinkage, and Temperature Effects in Concrete Structures.” *ACI 209R-92*. Farmington Hills, Michigan.
- American Concrete Institute (ACI) Manual of Concrete Practice (2002). “Report on Factors Affecting Shrinkage and Creep of Hardened Concrete.” *ACI 209R-05*. Farmington Hills, Michigan.
- Bazant, Z.P. (1975). “Theory of Creep and Shrinkage in Concrete Structures: A precis of recent developments.” *Mechanics Today*. American Academy of Mechanics, Vol. 2. Pergamon, New York.
- British Standards Institution, “Steel, Concrete and Composite Bridge, Part I, General Statement.” *British Standard BS 5400*. Crowthorne, Berkshire, England (1978).
- Dimmerling, A., Miller, R. A., Reid, C., Mirmiran, A., Hastak, M., and Baseheart, T. M. (2005). “Connections Between Simply Supported Concrete Beams Made Continuous – Results of NCHRP Project 12-53.” *Transportation Research Record: Journal of the Transportation Research Board*, No. 1928. Transportation Research Board of the National Academies, Washington, D.C.
- Freyermuth, C. L. (1969). “Design of Continuous Highway Bridges with Precast, Prestressed Concrete Girders.” *Journal of the Prestressed Concrete Institute*, Vol. 14, No 2.
- Hognestad, E., Mattock, A. H., Karr, P. H. (1960). “Composite Construction for Continuity.” *Journal of the Prestressed Concrete Institute*, Vol. 5, No 1.
- Imbsen, A., Vandershaf, D.E., Schamber, R. A., and Nutt, R.V. (1985). “Thermal Effects in Concrete Bridge Superstructures.” National Cooperative Highway Research Program Report 276, National Research Council, Washington, D.C.
- MacGregor, J. G., and Wright, J. K. (2005). Reinforced Concrete: Mechanics and Design 4th Edition. Pearson Prentice Hall, Upper Saddle River, New Jersey.
- Mattock, A. H. (1961). “Precast-Prestress Concrete Bridges: 5. Creep and Shrinkage Studies. Development Department Bulletin D46.” *Portland Cement Association, Research and Development Laboratories*, Vol. 3, No 2. Stokie, Illinois.

Mattock, A. H., Kaar, P. H. (1960). "Continuous Precast-Prestressed Concrete Bridges. Development Department Bulletin D43." *Portland Cement Association, Research and Development Laboratories*, Vol. 2, No. 5. Stokie, Illinois.

Menn, C. (1986). Prestressed Concrete Bridges, translated by Gauvreau, P., originally published as Stahlbentonbruken, Springer-Berlag, Wein. Vienna, Austria.

Newhouse, C. D. (2005). "Design and Behavior of Prestressed, Precast Girders Made Continuous – An Analytical and Experimental Study." Ph.D. Dissertation, Virginia Tech.

Nilson, A. H. (1987), Design of Prestressed Concrete – Second Edition, John Wiley and Sons. New York, NY.

Oesterle, R.G., Glikin, J.D., and Larson, S.C. (1989). "Design of Precast Prestressed Girders Made Continuous." National Cooperative Highway Research Program Report 322, National Research Council, Washington, D.C.

Potgieter, I.C., and Gamble, W.L. (1983). "Response of Highway Bridges to Nonlinear Temperature Distributions." *Rep. No. FHWA/IL/UI-201*, University of Illinois at Urbana-Champaign, Urbana-Champaign, IL.

Salmons, J.R. (1974). "End Connections of Pretensioned I-Beam Bridges", Missouri Cooperative Highway Report 73-5C. Missouri State Highway Department, Jefferson City, Missouri.

Virginia Department of Transportation (2006). "Volume V – Part 2: Design Aids – Typical Details." <<http://www.vdot.virginia.gov/business/bridge-v5p2.asp>>

Washington State Department of Transportation (2005). Bridge Engineering Software-QConBridges
<http://www.wsdot.wa.gov/eesc/bridge/software/index.cfm?fuseaction=software_detail&software_id=48>

APPENDIX A: Design of Continuity Diaphragms for Girders Older than 90 Days

These calculations: PCBT-77 with a beam spacing of 8 ft and a span length of 130 ft

Unit definition:

$$\begin{aligned}k &:= 1000\text{lb} & \text{pcf} &:= \frac{\text{lb}}{\text{ft}^3} \\k\text{ft} &:= k \cdot \text{ft} & \mu\epsilon &:= .000001 \\k\text{in} &:= k \cdot \text{in} & \text{psi} &:= \frac{\text{lb}}{\text{in}^2} \\k\text{si} &:= \frac{k}{\text{in}^2} & & \\k\text{lf} &:= \frac{k}{\text{ft}} & & \end{aligned}$$

Variables (PCBT Girder):

$$\begin{aligned}s &:= 8\text{ft} \\l &:= 130\text{ft} \\f_c &:= 4\text{ksi} \\h_d &:= 8\text{in} \\h_h &:= 1\text{in} \\A_s &:= 3.52\text{in}^2 \\I_b &:= 788700\text{in}^4 \\A_b &:= 970.7\text{in}^2 \\h_b &:= 77\text{in} \\y_b &:= 37.67\text{in} \\\text{strands} &:= 1 \\A_{\text{strand}} &:= .153\text{in}^2\end{aligned}$$

Effective width:

$$b := \left(\begin{array}{c} .125 \cdot l \\ 12 \cdot h_d + 7\text{in} \\ s \end{array} \right)$$
$$b_{\text{eff}} := \min(b)$$
$$b_{\text{eff}} = 96\text{in}$$

Gross Area:

$$A_g := A_b + 47\text{in}\cdot h_h + b_{\text{eff}}\cdot h_d$$

$$A_g = 1.786 \times 10^3 \text{ in}^2$$

Gross Centroid:

$$y_g := \frac{A_b \cdot y_b + 47\text{in}\cdot h_h \cdot (h_b + .5\cdot h_h) + b_{\text{eff}}\cdot h_d \cdot (h_b + h_h + .5\cdot h_d)}{A_g}$$

$$y_g = 57.784 \text{ in}$$

Gross Moment of Inertia:

$$I_g := I_b + A_b \cdot (y_g - y_b)^2 + \frac{47\cdot \text{in}\cdot h_h^3}{12} + (47\cdot \text{in}\cdot h_h) \cdot (h_b + .5\cdot h_h - y_g)^2 \dots$$

$$+ \frac{b_{\text{eff}}\cdot h_d^3}{12} + (b_{\text{eff}}\cdot h_d) \cdot (h_b + h_h + .5\cdot h_d - y_g)^2$$

$$I_g = 1.654 \times 10^6 \text{ in}^4$$

Modulus of Rupture:

$$f_r := .24 \cdot \left(\sqrt{\frac{f_c}{\text{ksi}}} \right) \cdot \text{ksi}$$

$$f_r = 0.48 \text{ ksi}$$

Cracking Moment:

$$M_{\text{cr}} := \frac{I_g}{y_g} \cdot f_r$$

$$M_{\text{cr}} = 1.374 \times 10^4 \text{ kin}$$

1.2 times the Cracking Moment:

$$1.2M_{\text{cr}} = 1.649 \times 10^4 \text{ kin}$$

Depth of compression block:

$$a := \frac{A_s \cdot 60 \text{ksi} + A_{\text{strand}} \cdot \text{strands} \cdot \frac{(30 \text{in} - 8.25 \text{in})}{.163} \frac{\text{k}}{\text{in}^3}}{.85 \cdot f_c \cdot b_{\text{eff}}}$$

$$a = 0.71 \text{ in}$$

Effective depth of steel:

$$d_s := h_b + h_h + h_d - 4.63 \text{ in}$$

$$d_s = 81.37 \text{ in}$$

Effective depth of prestress:

$$d_{ps} := h_b + h_h + h_d - 2.25 \text{ in}$$

$$d_{ps} = 83.75 \text{ in}$$

Nominal Flexural Strength:

$$M_n := A_s \cdot 60 \text{ksi} \cdot \left(d_s - \frac{a}{2} \right) + A_{\text{strand}} \cdot \text{strands} \cdot \frac{(30 \text{in} - 8.25 \text{in})}{.163} \frac{\text{k}}{\text{in}^3} \cdot \left(d_{ps} - \frac{a}{2} \right)$$

$$M_n = 1.881 \times 10^4 \text{ kin}$$

Design Strength:

$$.9 \cdot M_n = 1.693 \times 10^4 \text{ kin}$$

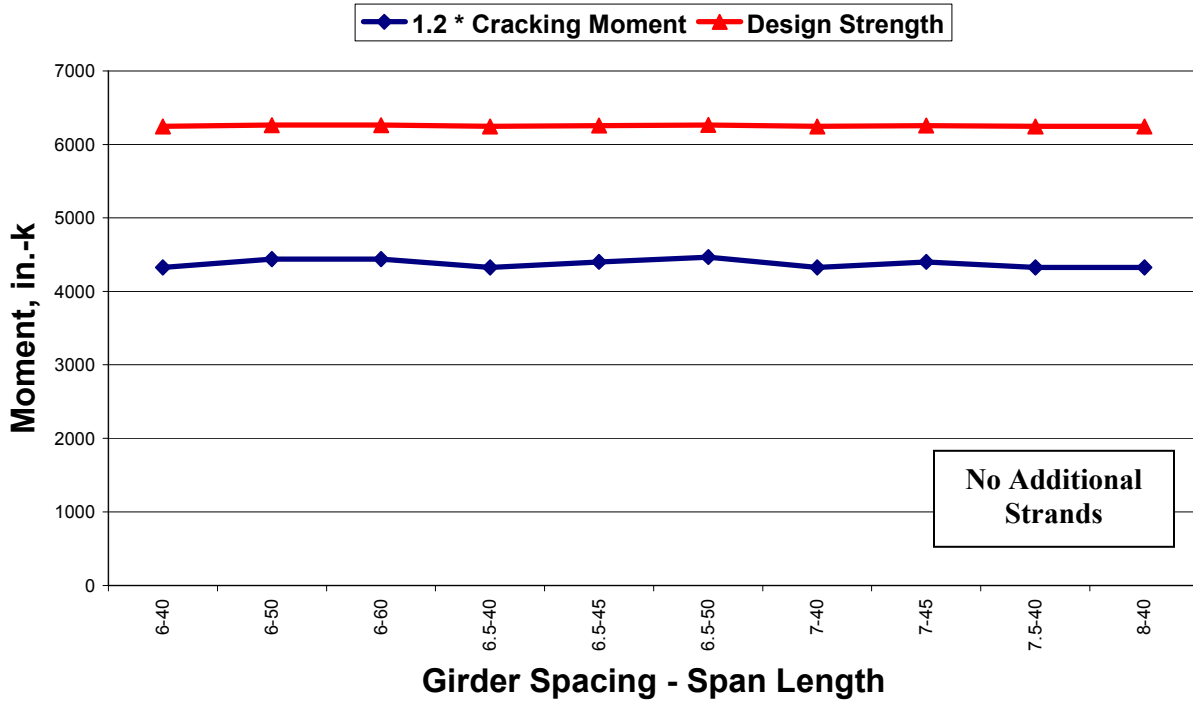
Is diaphragm OK?

$$\text{check} := \begin{cases} \text{check} \leftarrow \text{"NOT OK"} & \text{if } M_{cr} > .9M_n \\ \text{check} \leftarrow \text{"OK"} & \text{if } M_{cr} < .9M_n \end{cases}$$

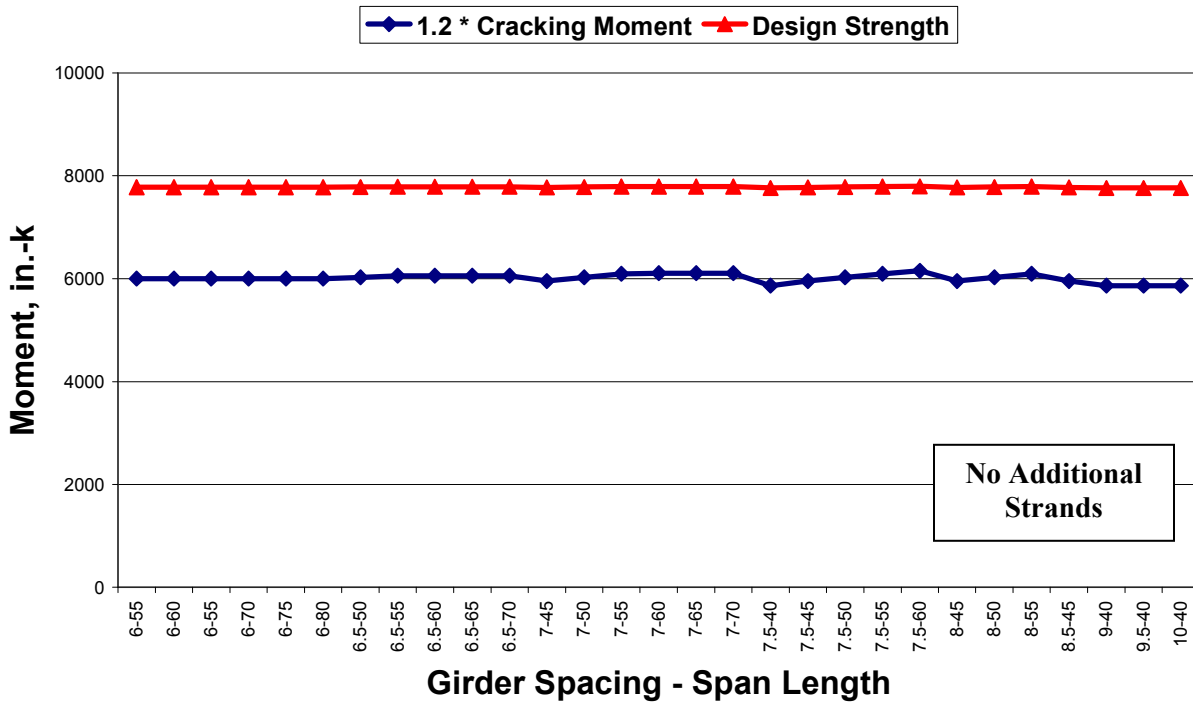
$$\text{check} = \text{"OK"}$$

APPENDIX B: Strands for PCBT Girders Older Than 90 Days

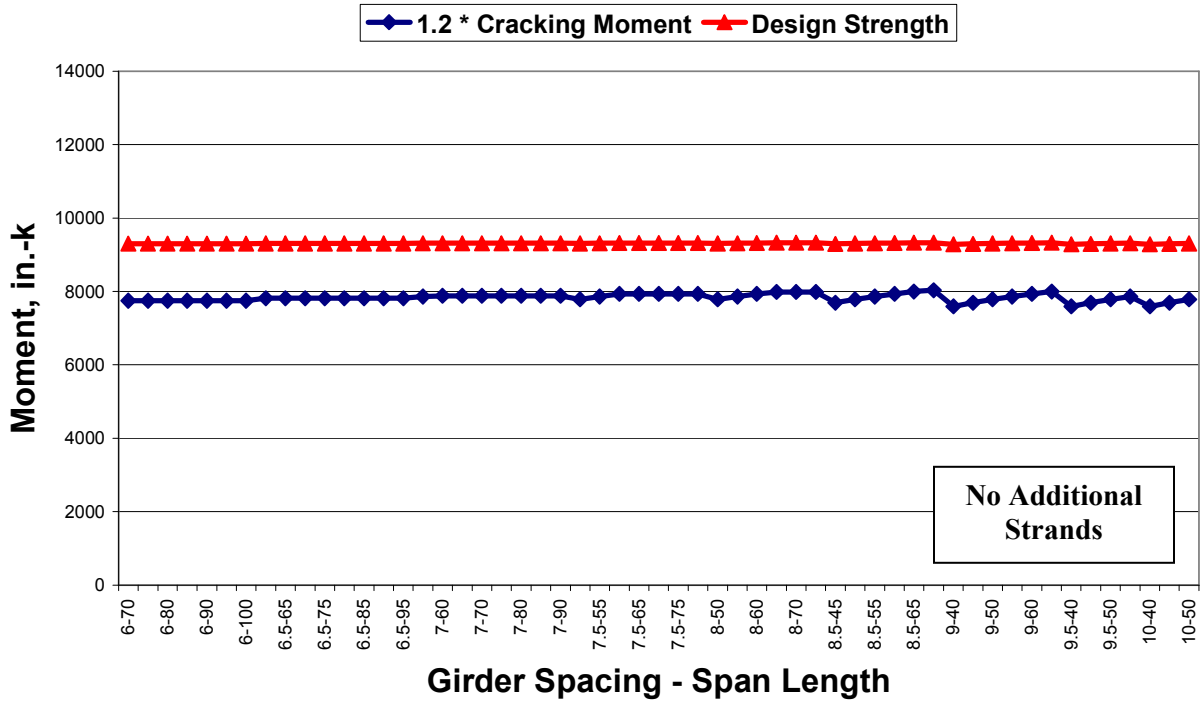
PCBT-29



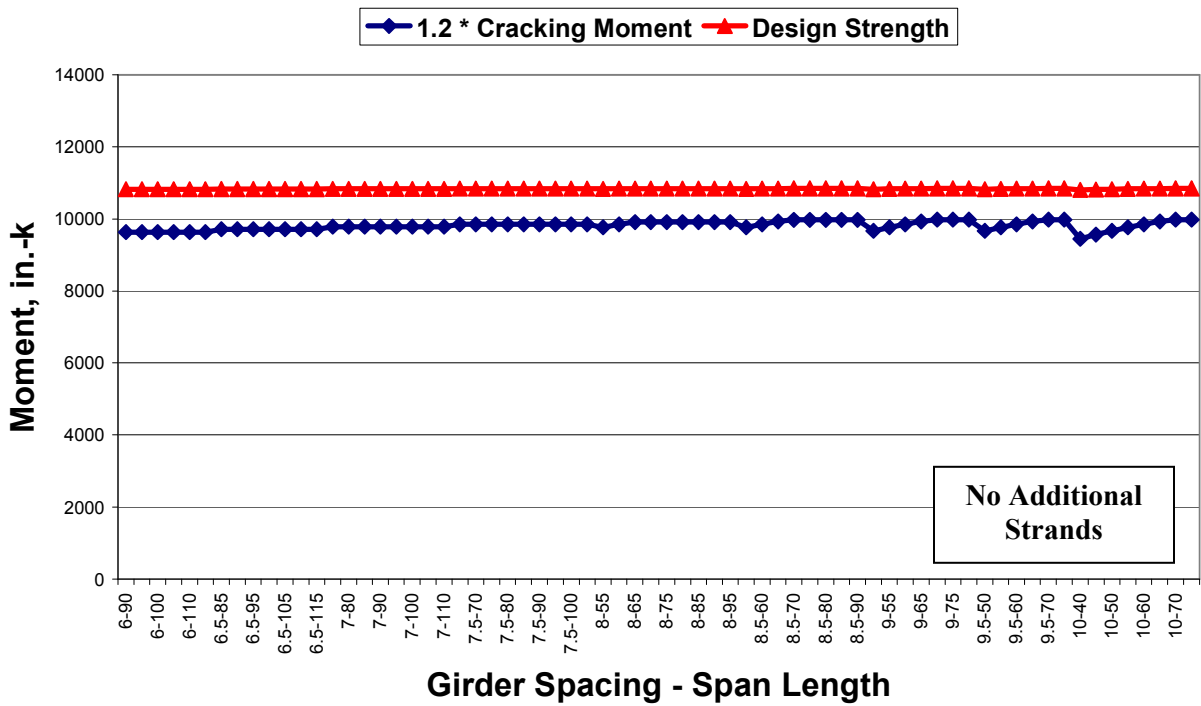
PCBT-37



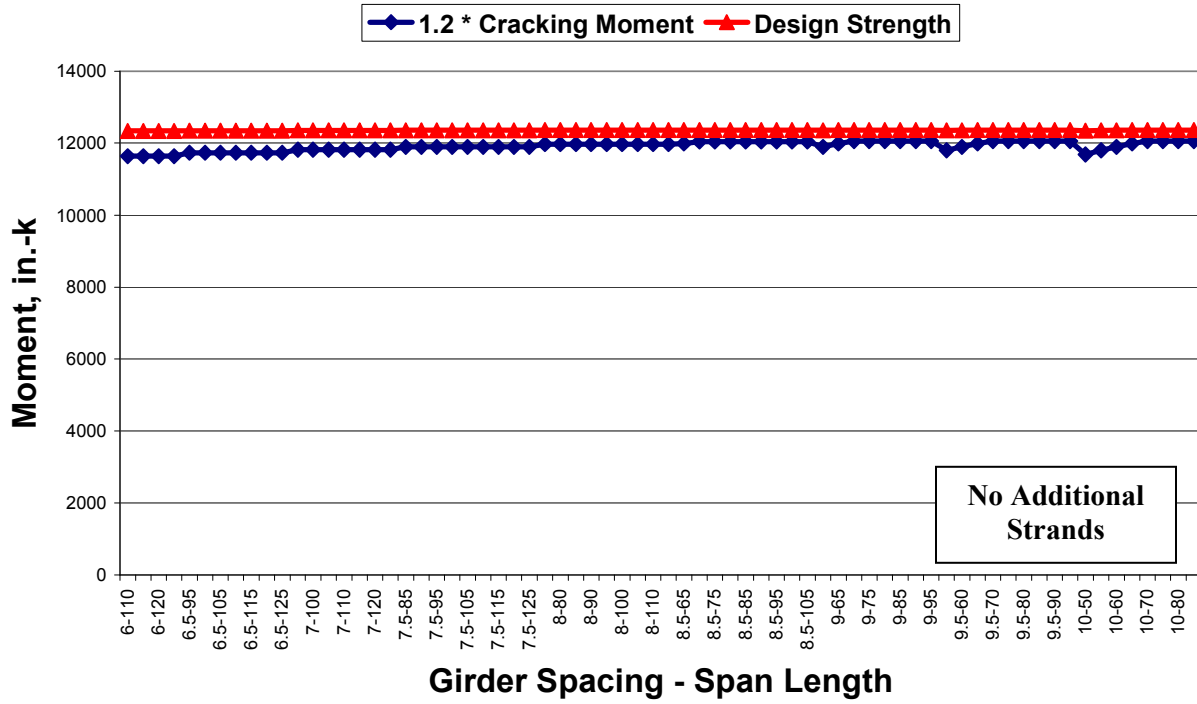
PCBT-45



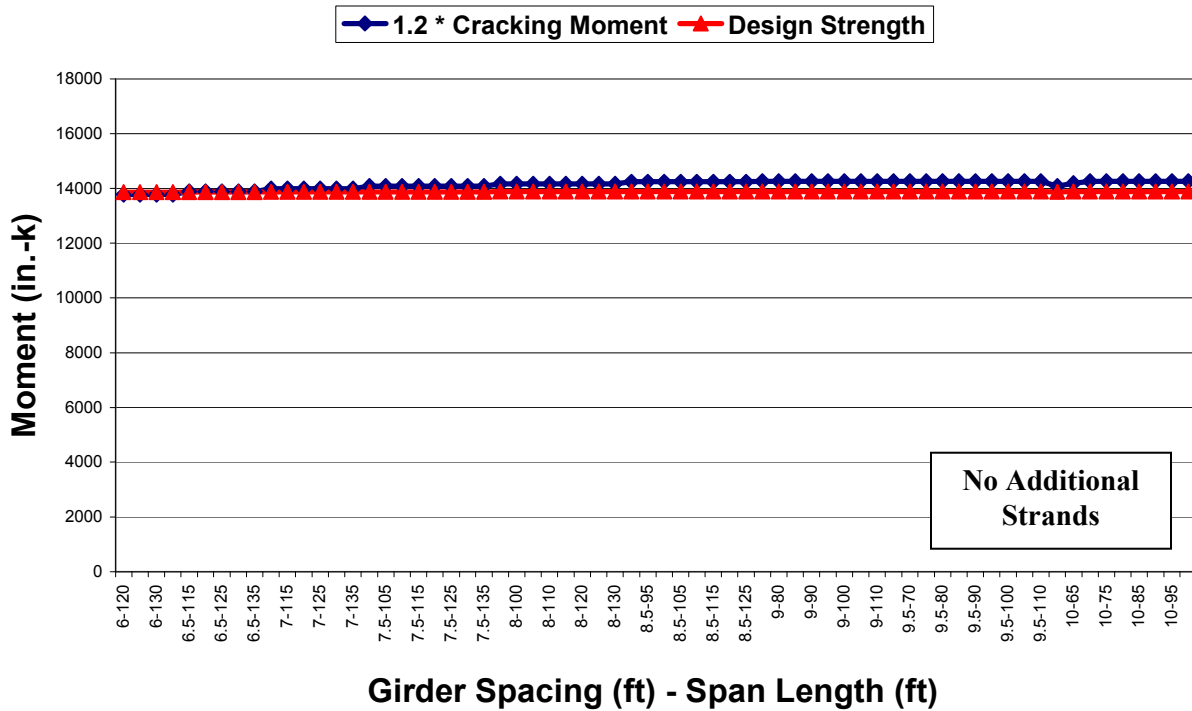
PCBT-53



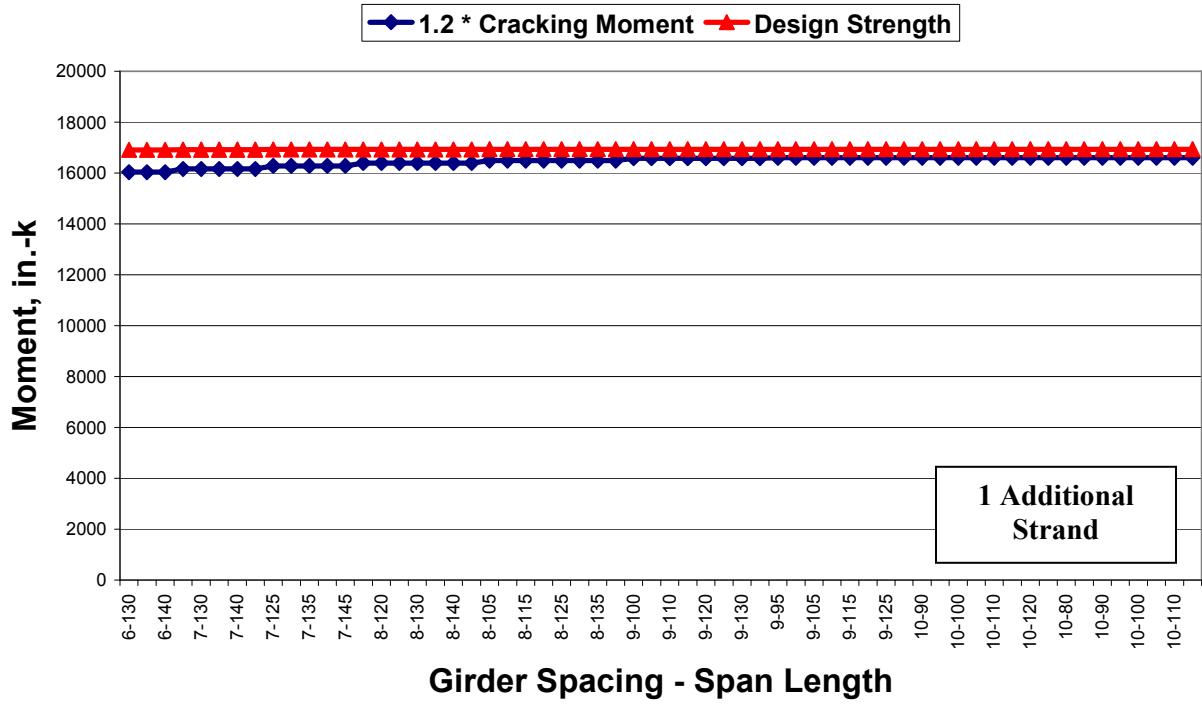
PCBT-61



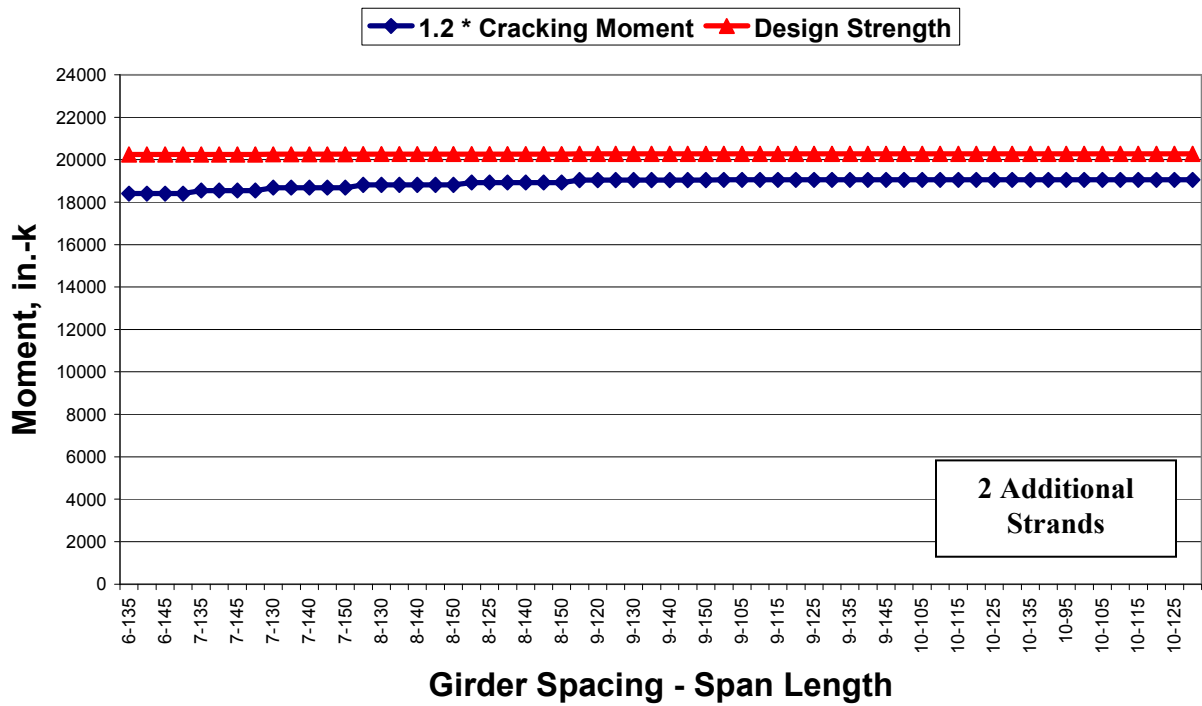
PCBT-69



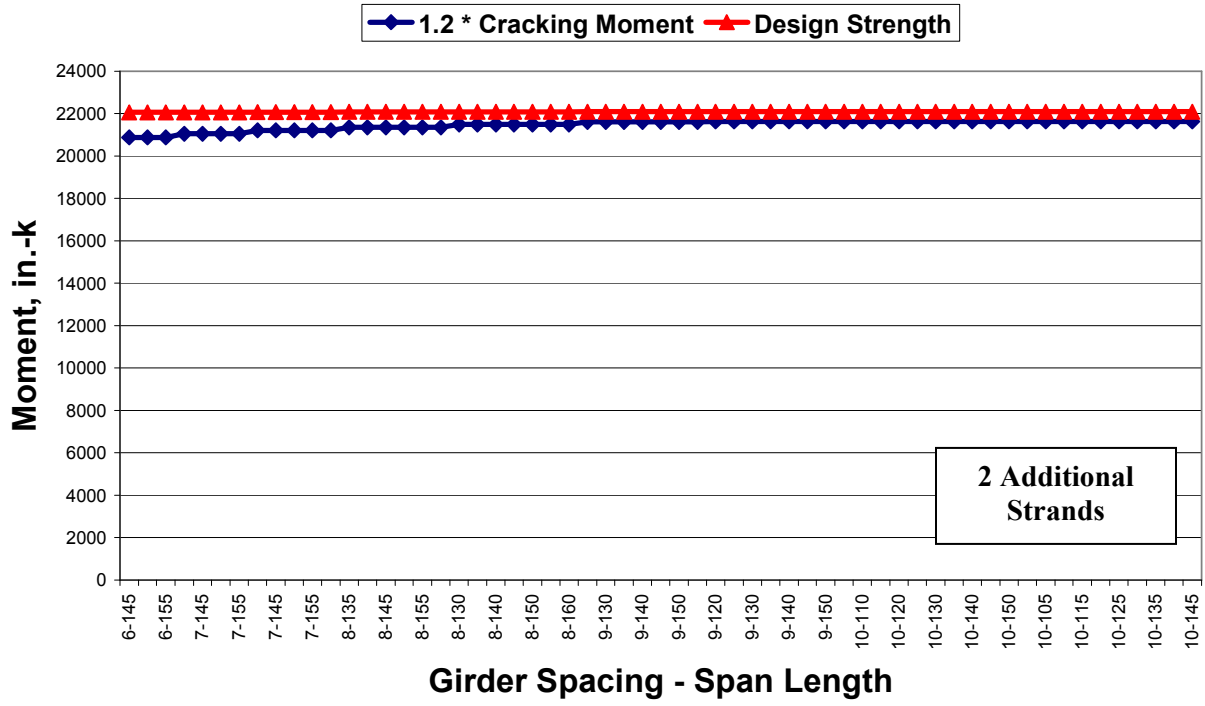
PCBT-77



PCBT-85



PCBT-93



APPENDIX C: 2-Span PCBT Girder Systems Younger than 90 Days

Purpose: Evaluate Continuity Diaphragm Details

sign convention for concrete stresses: "-" for tension, "+" for compression

yellow highlighted regions are input values

UNITS:

$$k := 1000\text{lb}$$

$$\text{kft} := \text{k}\cdot\text{ft}$$

$$\text{kin} := \text{k}\cdot\text{in}$$

$$\text{ksi} := \frac{\text{k}}{\text{in}^2}$$

$$\text{klf} := \frac{\text{k}}{\text{ft}}$$

$$\text{pcf} := \frac{\text{lb}}{\text{ft}^3}$$

$$\mu\epsilon := .000001$$

$$\text{psi} := \frac{\text{lb}}{\text{in}^2}$$

INPUT:

Time Properties

Age of girder at transfer of prestressing- $t_i := 1$ day

Age of girder at deck placement- $t_d := 45$ days

Aging coefficient $\chi := .7$

Girder Properties

Girder concrete- $f_c := 7000\text{psi}$

$$f_{ci} := f_c \cdot 0.8 \quad f_{ci} = 5.6 \times 10^3 \text{ psi}$$

$$w_{\text{gird}} := 150\text{pcf}$$

$$\alpha_{TC} := 6.0 \cdot 10^{-6} \cdot \frac{1}{F} \quad (\text{strain per degree F})$$

Girder height- $h_g := 61\text{in}$

Girder cross-sectional area- $A_g := 858.7\text{in}^2$

Girder moment of inertia- $I_g := 443100\text{in}^4$

Distance from centroid to bottom of girder- $y_{gb} := 29.92\text{in}$

Weight per foot $w_g := w_{\text{gird}} \cdot A_g \quad w_g = 894.479 \frac{\text{lb}}{\text{ft}}$

Span Length- $L_{\text{span}} := 75\text{ft}$

Volume to surface area ratio- $v_s := 3.75\text{in}$

Relative Humidity- $H_{\text{rel}} := 70$ percent

Deck Properties

Girder spacing- $s_g := 10\text{ft}$

Deck depth $h_f := 8.5\text{in}$

Haunch height $h_h := 1.5\text{in}$

Deck concrete $f_{cd} := 4000\text{psi}$

$$w_{\text{deck}} := 150\text{pcf}$$

Strand Pattern Information

For one 0.5 in. strand- $A_{ps1} := 0.153\text{in}^2$
 $E_{ps} := 28000\text{ksi}$
 $f_{pu} := 270\text{ksi}$

Number of 1/2 in. bent prestressing strands in the diaphragm-

$Strands_{bent} := 2$

Strand layout description-

| strand := | allowable strands | total used strands | harped strands | Straight strand distance from bot. |
|-----------|-------------------|--------------------|----------------|------------------------------------|
| | 0 | 1 | 2 | 3 |
| 0 | 14 | 14 | 2 | 2.25 |
| 1 | 14 | 6 | 2 | 4.25 |
| 2 | 12 | 0 | 0 | 6.25 |
| 3 | 6 | 0 | 0 | 8.25 |
| 4 | 2 | 0 | 0 | 10.25 |
| 5 | 2 | 0 | 0 | 12.25 |
| 6 | 2 | 0 | 0 | 14.25 |
| 7 | 2 | 0 | 0 | 16.25 |
| 8 | 2 | 0 | 0 | 18.25 |
| 9 | 2 | 0 | 0 | 20.25 |
| 10 | 2 | 0 | 0 | 22.25 |
| 11 | 2 | 0 | 0 | 24.25 |
| 12 | 2 | 0 | 0 | 26.25 |
| 13 | 2 | 0 | 0 | 28.25 |
| 14 | 2 | 0 | 0 | 30.25 |
| 15 | 2 | 0 | 0 | 32.25 |

INITIAL CALCULATIONS:

Harped Strand Distances:

Calculation of harped strand distances measured from the bottom of the girder -

(it is assumed that the top strand will be harped to 2 in. from the top of the girder, and that all strands will be spaced at 2 in. on center)

$$\text{strand}_{0,4} := \frac{hg}{in} - 2 \quad \text{strand}_{0,4} = 59$$

$$\text{strand}_{1,4} := \frac{hg}{in} - 4 \quad \text{strand}_{1,4} = 57$$

$$\text{strand}_{2,4} := \frac{hg}{in} - 6 \quad \text{strand}_{2,4} = 55$$

$$\text{strand}_{3,4} := \frac{hg}{in} - 8 \quad \text{strand}_{3,4} = 53$$

$$\text{strand}_{4,4} := \frac{hg}{in} - 10 \quad \text{strand}_{4,4} = 51$$

$$\text{strand}_{5,4} := \frac{hg}{in} - 12 \quad \text{strand}_{5,4} = 49$$

$$\text{strand}_{6,4} := \frac{hg}{in} - 14 \quad \text{strand}_{6,4} = 47$$

$$\text{strand}_{7,4} := \frac{hg}{in} - 16 \quad \text{strand}_{7,4} = 45$$

$$\text{strand}_{8,4} := \frac{hg}{in} - 18 \quad \text{strand}_{8,4} = 43$$

$$\text{strand}_{9,4} := \frac{hg}{in} - 20 \quad \text{strand}_{9,4} = 41$$

$$\text{strand}_{10,4} := \frac{hg}{in} - 22 \quad \text{strand}_{10,4} = 39$$

$$\text{strand}_{11,4} := \frac{hg}{in} - 24 \quad \text{strand}_{11,4} = 37$$

$$\text{strand}_{12,4} := \frac{hg}{in} - 26 \quad \text{strand}_{12,4} = 35$$

$$\text{strand}_{13,4} := \frac{hg}{in} - 28 \quad \text{strand}_{13,4} = 33$$

$$\text{strand}_{14,4} := \frac{hg}{in} - 30 \quad \text{strand}_{14,4} = 31$$

$$\text{strand}_{15,4} := \frac{hg}{in} - 32 \quad \text{strand}_{15,4} = 29$$

Table of results -

| | allowable strands | total strands | harped strands | Straight strand distance from bot. | Harped strand distance from bot. |
|------------|-------------------|---------------|----------------|------------------------------------|----------------------------------|
| | 0 | 1 | 2 | 3 | 4 |
| 0 | 14 | 14 | 2 | 2.25 | 59 |
| 1 | 14 | 6 | 2 | 4.25 | 57 |
| 2 | 12 | 0 | 0 | 6.25 | 55 |
| 3 | 6 | 0 | 0 | 8.25 | 53 |
| 4 | 2 | 0 | 0 | 10.25 | 51 |
| 5 | 2 | 0 | 0 | 12.25 | 49 |
| 6 | 2 | 0 | 0 | 14.25 | 47 |
| strand = 7 | 2 | 0 | 0 | 16.25 | 45 |
| 8 | 2 | 0 | 0 | 18.25 | 43 |
| 9 | 2 | 0 | 0 | 20.25 | 41 |
| 10 | 2 | 0 | 0 | 22.25 | 39 |
| 11 | 2 | 0 | 0 | 24.25 | 37 |
| 12 | 2 | 0 | 0 | 26.25 | 35 |
| 13 | 2 | 0 | 0 | 28.25 | 33 |
| 14 | 2 | 0 | 0 | 30.25 | 31 |
| 15 | 2 | 0 | 0 | 32.25 | 29 |

Centroid of Prestress:

Number of strands-

$$\text{Strand} := \sum_{i=0}^{15} \text{strand}_{i,1} \quad \text{Strand} = 20 \quad \text{total strands}$$

$$\text{Strand}_s := \sum_{i=0}^{15} (\text{strand}_{i,1} - \text{strand}_{i,2}) \quad \text{Strand}_s = 16 \quad \text{straight strands}$$

$$\text{Strand}_h := \sum_{i=0}^{15} \text{strand}_{i,2} \quad \text{Strand}_h = 4 \quad \text{harped strands}$$

Center of gravity of strands at various locations -

"e" is eccentricity measured from the bottom of the girder

"x" is distance in inches measured from the end of the beam

For the straight strands -

$$e_s := \frac{\sum_{i=0}^{15} [(\text{strand}_{i,1} - \text{strand}_{i,2}) \cdot \text{strand}_{i,3}]}{\text{Strand}_s} \text{ in} \quad e_s = 2.75 \text{ in}$$

For harped stands at mid span -

$$x := .5 \cdot L$$

$$eh_{ms} := \frac{\left[\sum_{i=0}^{15} (\text{strand}_{i,2} \cdot \text{strand}_{i,3}) \right] \text{in}}{\text{Strand}_h} \quad eh_{ms} = 3.25 \text{ in}$$

$$cgs_{ms} := \frac{es \cdot \text{Strand}_s + eh_{ms} \cdot \text{Strand}_h}{\text{Strand}} \quad cgs_{ms} = 2.85 \text{ in}$$

For harped strands at the ends -

$$x := 0 \text{ in}$$

$$eh_{end} := \frac{\left[\sum_{i=0}^{15} (\text{strand}_{i,2} \cdot \text{strand}_{i,4}) \right] \text{in}}{\text{Strand}_h} \quad eh_{end} = 58 \text{ in}$$

$$cgs_{end} := \frac{es \cdot \text{Strand}_s + eh_{end} \cdot \text{Strand}_h}{\text{Strand}} \quad cgs_{end} = 13.8 \text{ in}$$

For harped strand at the transfer length -

$$x := 25 \text{ in}$$

$$eh_{tl} := eh_{end} - \frac{(eh_{end} - eh_{ms})}{.4 \cdot L} \cdot x \quad eh_{tl} = 54.198 \text{ in}$$

$$cgs_{tl} := \frac{es \cdot \text{Strand}_s + eh_{tl} \cdot \text{Strand}_h}{\text{Strand}} \quad cgs_{tl} = 13.04 \text{ in}$$

For harped stands at 1/2 the distance to the harping point -

$$x := .2 \cdot L$$

$$eh_{.5hp} := eh_{end} - \frac{(eh_{end} - eh_{ms})}{.4 \cdot L} \cdot x \quad eh_{.5hp} = 30.625 \text{ in}$$

$$cgs_{.5hp} := \frac{es \cdot \text{Strand}_s + eh_{.5hp} \cdot \text{Strand}_h}{\text{Strand}} \quad cgs_{.5hp} = 8.325 \text{ in}$$

For harped stands at the harping point -

$$x := .4 \cdot L$$

$$eh_{hp} := eh_{end} - \frac{(eh_{end} - eh_{ms})}{.4 \cdot L} \cdot x \quad eh_{hp} = 3.25 \text{ in}$$

$$cgs_{hp} := \frac{es \cdot \text{Strand}_s + eh_{hp} \cdot \text{Strand}_h}{\text{Strand}} \quad cgs_{hp} = 2.85 \text{ in}$$

Transformed Section Properties:

Initial modulus of elasticity-

$$E_{ci} := 33000 \text{ksi} \cdot \left(0.140 + \frac{f_{ci}}{1000 \text{ksi}}\right)^{1.5} \cdot \sqrt{\frac{f_{ci}}{\text{ksi}}}$$
$$E_{ci} = 4.339 \times 10^3 \text{ksi}$$

Check Eci requirement-

$$\left(0.140 + \frac{f_{ci}}{1000 \text{ksi}}\right) < .155$$
$$\text{check}_{E_{ci}} := \begin{cases} \text{check} \leftarrow \text{"OK"} & \text{if } \left(0.14 + \frac{f_{ci}}{1000000 \text{ksi}}\right) < .155 \\ \text{check} \leftarrow \text{"NOT OK"} & \text{if } 0.14 + \frac{f_{ci}}{1000000 \text{ksi}} \geq .155 \end{cases}$$
$$\text{check}_{E_{ci}} = \text{"OK"}$$

Modular Ratio (initial)-

$$n_i := \frac{E_{ps}}{E_{ci}}$$
$$n_i = 6.454$$

Total area of prestressing steel-

$$A_{ps} := A_{ps1} \cdot \text{Strand}$$
$$A_{ps} = 3.06 \text{in}^2$$

Transformed Area-

$$A_t := A_g + (n_i - 1) \cdot A_{ps}$$
$$A_t = 875.388 \text{in}^2$$

Transformed center of gravity (from bottom at ms) -

$$c_{gt} := \frac{[A_g \cdot y_{gb} + A_{ps} \cdot (n_i - 1) \cdot c_{gs_{ms}}]}{A_t}$$
$$c_{gt} = 29.404 \text{in}$$

Transformed moment of inertia (at ms)-

$$I_t := I_g + A_g \cdot (y_{gb} - c_{gt})^2 + A_{ps} \cdot (n_i - 1) \cdot (c_{gt} - c_{gs_{ms}})^2$$
$$I_t = 4.551 \times 10^5 \text{in}^4$$

Eccentricity of strands at mid-span of transformed section-

$$e_{ms} := c_{gt} - c_{gs_{ms}}$$
$$e_{ms} = 26.554 \text{in}$$

Effective width -

$$b_e := \min\left(s, 12 \cdot h_f + 7 \text{in}, \frac{L}{8}\right)$$
$$b_e = 109 \text{in}$$

Live Load Moments: (for critical case of 2 spans continuous per lane)

Maximum positive and negative moments for a 2 span bridge, using QConBridge Program:

| | span length | positive moment | negative moment |
|------------|-------------|-----------------|-----------------|
| Moments := | 20 | 86.7 | -173.3 |
| | 25 | 111.7 | -223.3 |
| | 30 | 134.4 | -268.7 |
| | 35 | 161.7 | -323.4 |
| | 40 | 194.3 | -388.5 |
| | 45 | 236.7 | -473.4 |
| | 50 | 306.5 | -613 |
| | 55 | 403.7 | -807.4 |
| | 60 | 498.8 | -997.5 |
| | 65 | 592.5 | -1185 |
| | 70 | 683.5 | -1367 |
| | 75 | 767 | -1534 |
| | 80 | 848 | -1696 |
| | 85 | 927.5 | -1855 |
| | 90 | 1003 | -2006 |
| | 95 | 1078 | -2156 |
| | 100 | 1150.5 | -2301 |
| | 105 | 1223 | -2446 |
| | 110 | 1296 | -2592 |
| | 115 | 1366 | -2732 |
| | 120 | 1436 | -2872 |
| | 125 | 1504 | -3008 |
| | 130 | 1574 | -3148 |
| | 135 | 1644.5 | -3289 |
| | 140 | 1716.5 | -3433 |
| 145 | 1787.5 | -3575 | |
| 150 | 1860 | -3720 | |
| 155 | 1933.5 | -3867 | |
| 160 | 2005.5 | -4011 | |

Maximum positive moment -

$$m_{\max} := \begin{cases} \text{for } i \in 0..28 \\ \quad \left| \begin{array}{l} m_{\max} \leftarrow \text{Moments}_{i,1} \text{ if } L = \text{Moments}_{i,0} \text{ ft} \\ \text{break if } L = \text{Moments}_{i,0} \text{ ft} \end{array} \right. \\ m_{\max} \cdot \text{kft} \end{cases} \quad m_{\max} = 767 \text{ kft}$$

Minimum (most negative) moment -

$$m_{\min} := \begin{cases} \text{for } i \in 0..28 \\ \quad \left| \begin{array}{l} m_{\max} \leftarrow \text{Moments}_{i,2} \text{ if } L = \text{Moments}_{i,0} \text{ ft} \\ \text{break if } L = \text{Moments}_{i,0} \text{ ft} \end{array} \right. \\ m_{\max} \cdot \text{kft} \end{cases} \quad m_{\min} = -1.534 \times 10^3 \text{ kft}$$

Additional Dead Load

Noncomposite dead load - $w_{ncdl} := 0.200 \frac{\text{k}}{\text{ft}}$

Composite dead load - $w_{cdl} := 0.270 \frac{\text{k}}{\text{ft}}$

Allowable Stresses:

Initial tension at ends: $\sigma_{ti_e} := -6 \cdot \left(\sqrt{\frac{f_{ci}}{\text{psi}}} \right) \text{psi} \quad \sigma_{ti_e} = -0.449 \text{ ksi}$

Initial tension not at ends: $\sigma_{ti} := -3 \cdot \left(\sqrt{\frac{f_{ci}}{\text{psi}}} \right) \text{psi} \quad \sigma_{ti} = -0.224 \text{ ksi}$

Initial compression: $\sigma_{ci} := .6 \cdot f_{ci} \quad \sigma_{ci} = 3.36 \text{ ksi}$

Service compression under sustained loads: $\sigma_{cs_s} := .45 \cdot f_c \quad \sigma_{cs_s} = 3.15 \text{ ksi}$

Service compression under LL and 1/2 sustained: $\sigma_{cs_{LL}} := .40 \cdot f_c \quad \sigma_{cs_{LL}} = 2.8 \text{ ksi}$

Service compression under total loads: $\sigma_{cs_t} := .6 \cdot f_c \quad \sigma_{cs_t} = 4.2 \text{ ksi}$

Service tension: $\sigma_{ts} := -6 \cdot \sqrt{\frac{f_c}{\text{psi}}} \text{psi} \quad \sigma_{ts} = -0.502 \text{ ksi}$

CALCULATIONS FROM TRANSFER TO DECK PLACEMENT:

Check Stresses at Ends at Transfer: (due to initial prestress)

Jacking Force- $P_{jack} := A_{ps} \cdot 270 \text{ksi} \cdot 0.75$

$$P_{jack} = 619.65 \text{ k}$$

Top fiber stress- $f_{top5} := \frac{P_{jack}}{A_t} - P_{jack} \cdot (c_{gt} - c_{gs_{end}}) \cdot \frac{(hg - c_{gt})}{I_t}$

$$f_{top5} = 0.037 \text{ ksi}$$

Bottom fiber stress - $f_{bot5} := \frac{P_{jack}}{A_t} + P_{jack} \cdot (c_{gt} - c_{gs_{end}}) \cdot \frac{c_{gt}}{I_t}$

$$f_{bot5} = 1.333 \text{ ksi}$$

Check stresses in the top for tension-

$$\text{check}_{top_{eti}} := \begin{cases} \text{check} \leftarrow \text{"OK"} & \text{if } f_{top5} > \sigma_{ti_e} \\ \text{check} \leftarrow \text{"NOT OK"} & \text{if } f_{top5} < \sigma_{ti_e} \end{cases}$$

$$\text{check}_{top_{eti}} = \text{"OK"}$$

Check stresses in the top for compression-

$$\text{check}_{top_{eci}} := \begin{cases} \text{check} \leftarrow \text{"OK"} & \text{if } f_{top5} < \sigma_{ci} \\ \text{check} \leftarrow \text{"NOT OK"} & \text{if } f_{top5} > \sigma_{ci} \end{cases}$$

$$\text{check}_{top_{eci}} = \text{"OK"}$$

Check stresses in the bottom for tension-

$$\text{check}_{bot_{eti}} := \begin{cases} \text{check} \leftarrow \text{"OK"} & \text{if } f_{bot5} > \sigma_{ti} \\ \text{check} \leftarrow \text{"NOT OK"} & \text{if } f_{bot5} < \sigma_{ti} \end{cases}$$

$$\text{check}_{bot_{eti}} = \text{"OK"}$$

Check stresses in the bottom for compression-

$$\text{check}_{bot_{eci}} := \begin{cases} \text{check} \leftarrow \text{"OK"} & \text{if } f_{bot5} < \sigma_{ci} \\ \text{check} \leftarrow \text{"NOT OK"} & \text{if } f_{bot5} > \sigma_{ci} \end{cases}$$

$$\text{check}_{bot_{eci}} = \text{"OK"}$$

Check stresses at mid-span at transfer: (initial prestress and self weight)

Midspan self weight moment- $M_{self} := w_g \cdot \frac{L^2}{8}$
 $M_{self} = 7.547 \times 10^3 \text{ kin}$

Top fiber stress- $f_{top} := \left(\frac{P_{jack}}{A_t} \right) - \left[P_{jack} \cdot e_{ms} \cdot \frac{(hg - cgt)}{I_t} \right] + \left[M_{self} \cdot \frac{(hg - cgt)}{I_t} \right]$
 $f_{top} = 0.089 \text{ ksi}$

Bottom fiber stress - $f_{bot} := \left(\frac{P_{jack}}{A_t} \right) + \left(P_{jack} \cdot e_{ms} \cdot \frac{cgt}{I_t} \right) - \left(M_{self} \cdot \frac{cgt}{I_t} \right)$
 $f_{bot} = 1.283 \text{ ksi}$

Check stresses in the top for tension-

$$\text{checktop}_{ti} := \begin{cases} \text{check} \leftarrow \text{"OK"} & \text{if } f_{top} > \sigma_{ti} \\ \text{check} \leftarrow \text{"NOT OK"} & \text{if } f_{top} < \sigma_{ti} \end{cases}$$

$\text{checktop}_{ti} = \text{"OK"}$

Check stresses in the top for compression-

$$\text{checktop}_{ci} := \begin{cases} \text{check} \leftarrow \text{"OK"} & \text{if } f_{top} < \sigma_{ci} \\ \text{check} \leftarrow \text{"NOT OK"} & \text{if } f_{top} > \sigma_{ci} \end{cases}$$

$\text{checktop}_{ci} = \text{"OK"}$

Check stresses in the bottom for tension-

$$\text{checkbot}_{ti} := \begin{cases} \text{check} \leftarrow \text{"OK"} & \text{if } f_{bot} > \sigma_{ti} \\ \text{check} \leftarrow \text{"NOT OK"} & \text{if } f_{bot} < \sigma_{ti} \end{cases}$$

$\text{checkbot}_{ti} = \text{"OK"}$

Check stresses in the bottom for compression-

$$\text{checkbot}_{ci} := \begin{cases} \text{check} \leftarrow \text{"OK"} & \text{if } f_{bot} < \sigma_{ci} \\ \text{check} \leftarrow \text{"NOT OK"} & \text{if } f_{bot} > \sigma_{ci} \end{cases}$$

$\text{checkbot}_{ci} = \text{"OK"}$

Factors for Time Dependent Effects:

Time development factor-
$$k_{td} := \frac{t_d - t_i}{\left[61 - 4 \cdot \frac{f_{ci}}{ksi} + (t_d - t_i) \right]}$$
$$k_{td} = 0.533$$

Girder Size factor-
$$k_s := 1.45 - .13 \cdot \frac{vs}{in}$$
$$k_s = 0.963$$

Humidity factor for shrinkage-
$$k_{hs} := 2.00 - 0.0143 \cdot H$$
$$k_{hs} = 0.999$$

Concrete strength factor-
$$k_f := \frac{5}{\left(1 + \frac{f_{ci}}{ksi} \right)}$$
$$k_f = 0.758$$

Loading age factor-
$$k_{la_i} := t_1^{-0.118}$$
$$k_{la_i} = 1$$

Humidity factor for creep-
$$k_{hc} := 1.56 - 0.008 \cdot H$$
$$k_{hc} = 1$$

Shrinkage of Girder Concrete: (from transfer to deck placement)

Shrinkage from transfer to deck placement-
$$\epsilon_{bid} := 480 \cdot 10^{-6} \cdot k_{td} \cdot k_s \cdot k_{hs} \cdot k_f$$
$$\epsilon_{bid} = 1.863 \times 10^{-4}$$

Eccentricity of strands with respect to gross section properties-
$$e_{pg} := y_{gb} - c_{gs_{ms}}$$
$$e_{pg} = 27.07 \text{ in}$$

Girder creep at end of service due to loading introduced at transfer-
$$\psi_{bif} := 1.9 \cdot k_{la_i} \cdot k_s \cdot k_{hc} \cdot k_f$$
$$\psi_{bif} = 1.385$$

**Transformed section coefficient
(between initial and deck placement)-**

$$K_{id} := \frac{1}{1 + n_1 \cdot \frac{A_{ps}}{A_g} \cdot \left[1 + \frac{A_g \cdot (e_{pg})^2}{I_g} \right] \cdot (1 + \chi \cdot \psi_{bif})}$$

$$K_{id} = 0.901$$

**Prestress Loss due to shrinkage
from transfer to deck placement-**

$$\Delta f_{pSR} := \epsilon_{bid} \cdot E_{ps} \cdot K_{id}$$

$$\Delta f_{pSR} = 4.7 \text{ ksi}$$

Creep of Girder Concrete: (from transfer to deck placement)

**Girder creep coefficient at time of deck
placement due to loading introduced at transfer-**

$$\psi_{bid} := 1.90 \cdot k_{td} \cdot k_{l_1} \cdot k_s \cdot k_{hc} \cdot k_f$$

$$\psi_{bid} = 0.738$$

**Concrete stress at centroid of strand due to
initial prestress plus self weight of girder-**

$$f_{cgp} := \frac{P_{jack}}{A_t} + P_{jack} \cdot \frac{e_{ms}^2}{I_t} - M_{self} \cdot \frac{e_{ms}}{I_t}$$

$$f_{cgp} = 1.228 \text{ ksi}$$

**Prestress loss due to creep
from transfer to deck placement-**

$$\Delta f_{pCR} := n_1 \cdot f_{cgp} \cdot \psi_{bid} \cdot K_{id}$$

$$\Delta f_{pCR} = 5.269 \text{ ksi}$$

Relaxation of Prestressing Strands: (from transfer to deck placement)

Initial stress in strand after transfer-

$$f_{po} := 0.75 \cdot 270 \text{ ksi} - f_{cgp} \cdot n_1$$

$$f_{po} = 194.578 \text{ ksi}$$

Yield stress-

$$f_{py} := 0.90 \cdot 270 \text{ ksi}$$

$$f_{py} = 243 \text{ ksi}$$

Check requirement -

Note: $f_{po} > .55 \cdot f_{py}$

$$\text{check}_{f_{po}} := \begin{cases} \text{check} \leftarrow \text{"OK"} & \text{if } f_{po} > .55 \cdot f_{py} \\ \text{check} \leftarrow \text{"NOT OK"} & \text{if } f_{po} < .55 \cdot f_{py} \end{cases}$$

$$\text{check}_{f_{po}} = \text{"OK"}$$

Inherent relaxation-

(It is assume that the age of concrete at transfer of prestressing is 1 day)

$$L_i := \left(\frac{f_{po}}{45} \right) \cdot \left(\frac{f_{po}}{f_{py}} - 0.55 \right) \cdot \log \left[\frac{(24 \cdot t_d)}{(24)} \right]$$

$$L_i = 1.792 \text{ ksi}$$

Reduction factor for relaxation losses-

$$\phi_i := 1 - \frac{[3 \cdot (\Delta f_{pSR} + \Delta f_{pCR})]}{f_{po}}$$

$$\phi_i = 0.846$$

Prestress Loss due to relaxation of prestressing strands from transfer to deck placement-

$$\Delta f_{pR1} := \phi_i \cdot L_i \cdot K_{id}$$

$$\Delta f_{pR1} = 1.367 \text{ ksi}$$

Prestress at time of deck placement-

$$f_{pd} := f_{po} - \Delta f_{pSR} - \Delta f_{pCR} - \Delta f_{pR1}$$

$$f_{pd} = 183.242 \text{ ksi}$$

CALCULATIONS FROM DECK PLACEMENT TO END OF SERVICE:

Check stresses at deck placement:

Deck and haunch weight per foot- $w_{dh} := (w_{deck}) \cdot (s \cdot hf + 47 \text{ in} \cdot hh)$

$$w_{dh} = 1.136 \frac{\text{k}}{\text{ft}}$$

Midspan moment due to deck weight- $M_{dh} := w_{dh} \cdot \frac{L^2}{8}$

$$M_{dh} = 9.584 \times 10^3 \text{ kin}$$

Total loss of prestress force- $\Delta PS1 := (\Delta fp_{SR} + \Delta fp_{CR} + \Delta fp_{R1}) \cdot A_{ps}$

$$\Delta PS1 = 34.688 \text{ k}$$

Stress at top- $f_{top2} := f_{top} - \frac{\Delta PS1}{A_g} + \frac{[\Delta PS1 \cdot e_{ms} \cdot (hg - y_{gb})]}{I_g} + M_{dh} \cdot \frac{(hg - c_{gt})}{I_t}$
 $f_{top2} = 0.779 \text{ ksi}$

Stress at bottom- $f_{bot2} := f_{bot} - \frac{\Delta PS1}{A_g} - \frac{(\Delta PS1 \cdot e_{ms} \cdot y_{gb})}{I_g} - M_{dh} \cdot \frac{c_{gt}}{I_t}$
 $f_{bot2} = 0.561 \text{ ksi}$

Check stresses in the top for tension-

$$\text{check}_{top_{td}} := \begin{cases} \text{check} \leftarrow \text{"OK"} & \text{if } f_{top2} > \sigma_{ti} \\ \text{check} \leftarrow \text{"NOT OK"} & \text{if } f_{top2} < \sigma_{ti} \end{cases}$$

$$\text{check}_{top_{td}} = \text{"OK"}$$

Check stresses in the top for compression-

$$\text{check}_{top_{cd}} := \begin{cases} \text{check} \leftarrow \text{"OK"} & \text{if } f_{top2} < \sigma_{ci} \\ \text{check} \leftarrow \text{"NOT OK"} & \text{if } f_{top2} > \sigma_{ci} \end{cases}$$

$$\text{check}_{top_{cd}} = \text{"OK"}$$

Check stresses in the bottom for tension-

$$\text{checkbot}_{td} := \begin{cases} \text{check} \leftarrow \text{"OK"} & \text{if } f_{bot2} > \sigma_{ti} \\ \text{check} \leftarrow \text{"NOT OK"} & \text{if } f_{bot2} < \sigma_{ti} \end{cases}$$

$\text{checkbot}_{td} = \text{"OK"}$

Check stresses in the bottom for compression-

$$\text{checkbot}_{cd} := \begin{cases} \text{check} \leftarrow \text{"OK"} & \text{if } f_{bot2} < \sigma_{ci} \\ \text{check} \leftarrow \text{"NOT OK"} & \text{if } f_{bot2} > \sigma_{ci} \end{cases}$$

$\text{checkbot}_{cd} = \text{"OK"}$

Additional Factors for Time Dependent Effects:

Girder creep coefficient for loads placed at time of deck placement-

$$k_{la_d} := t_d^{-0.118}$$

$k_{la_d} = 0.638$

Deck volume to surface ratio-

$$v_{sd} := \frac{(s \cdot hf)}{(2 \cdot s)}$$

$v_{sd} = 4.25 \text{ in}$

Deck size factor-

$$k_{sd} := 1.45 - 0.13 \cdot \frac{v_{sd}}{\text{in}}$$

$k_{sd} = 0.897$

Deck strength factor-

$$k_{fd} := \frac{5}{\left(1 + \frac{f_{cd}}{\text{ksi}}\right)}$$

$k_{fd} = 1$

Assume all other factors are 1.0

Calculate the Gross Composite Section Properties:

Modulus of Girder Concrete at 28 days- $E_c := 33000 \text{ksi} \cdot \left(0.140 + \frac{f_c}{1000 \text{ksi}}\right)^{1.5} \cdot \sqrt{\frac{f_c}{\text{ksi}}}$
 $E_c = 4.921 \times 10^3 \text{ksi}$

Modulus for Deck Concrete at 28 days- $E_{cd} := 33000 \text{ksi} \cdot \left(0.140 + \frac{f_{cd}}{1000 \text{ksi}}\right)^{1.5} \cdot \sqrt{\frac{f_{cd}}{\text{ksi}}}$
 $E_{cd} = 3.607 \times 10^3 \text{ksi}$

Modular ratio for deck to girder concrete- $n_d := \frac{E_{cd}}{E_c}$
 $n_d = 0.733$

Gross composite area- $A_{gc} := A_g + (hf \cdot be + hh \cdot 47 \text{in}) \cdot n_d$
 $A_{gc} = 1.589 \times 10^3 \text{in}^2$

Centroid (from bottom) of Gross Composite Area- $c_{ggc} := \frac{\left[A_g \cdot y_{gb} + hf \cdot be \cdot \left(hg + hh + \frac{hf}{2} \right) \cdot n_d + hh \cdot 47 \text{in} \cdot \left(hg + \frac{hh}{2} \right) \cdot n_d \right]}{A_{gc}}$
 $c_{ggc} = 46.69 \text{in}$

Moment of Inertia of Gross Composite Area-

$$I_{gc} := I_g + A_g \cdot (y_{gb} - c_{ggc})^2 + \frac{1}{12} \cdot be \cdot hf^3 \cdot n_d + be \cdot hf \cdot n_d \cdot \left(hg + hh + \frac{hf}{2} - c_{ggc} \right)^2 \dots$$

$$+ \left[\frac{1}{12} \cdot 47 \text{in} \cdot hh^3 \cdot n_d + 47 \text{in} \cdot hh \cdot n_d \cdot \left(hg + \frac{hh}{2} - c_{ggc} \right)^2 \right]$$

$$I_{gc} = 9.737 \times 10^5 \text{in}^4$$

Calculate transformed composite cross-sectional properties:

Modular ratio for prestressing strands to girder concrete- $n_s := \frac{E_{ps}}{E_c}$
 $n_s = 5.69$

Transformed composite area- $A_{ct} := A_{gc} + (n_s - 1) \cdot A_{ps}$
 $A_{ct} = 1.604 \times 10^3 \text{in}^2$

Centroid of transformed composite area-

$$cgct := \frac{[Agc \cdot cggc + Aps \cdot (n_s - 1) \cdot cgs_{ms}]}{Act}$$

$$cgct = 46.297 \text{ in}$$

Moment of inertia of transformed composite area-

$$Ict := Igc + Agc \cdot (cggc - cgct)^2 + Aps \cdot (n_s - 1) \cdot (cgct - cgs_{ms})^2$$

$$Ict = 1.001 \times 10^6 \text{ in}^4$$

Shrinkage of girder concrete: (from deck placement to end of service)

Shrinkage from transfer to end of service-

$$\epsilon_{bif} := 480 \cdot 10^{-6} \cdot ks \cdot khs \cdot kf$$

$$\epsilon_{bif} = 3.496 \times 10^{-4}$$

Shrinkage from deck placement to end of service-

$$\epsilon_{bdf} := \epsilon_{bif} - \epsilon_{bid}$$

$$\epsilon_{bdf} = 1.634 \times 10^{-4}$$

Transformed section coefficient (between deck placement and final time)-

$$Kdf := \frac{1}{1 + n_s \cdot \frac{Aps}{Agc} \cdot \left[1 + \frac{Agc \cdot (cggc - cgs_{ms})^2}{Igc} \right] \cdot (1 + \chi \cdot \psi_{bif})}$$

$$Kdf = 0.918$$

Prestress loss due to shrinkage from deck placement to end of service-

$$\Delta fp_{SD} := \epsilon_{bdf} \cdot Eps \cdot Kdf$$

$$\Delta fp_{SD} = 4.2 \text{ ksi}$$

Creep of girder concrete: (from deck placement to end of service)

Prestress loss due to initial prestress and self weight of girder-

$$\Delta fp_{CD1} := n_i \cdot fcgp \cdot (\psi_{bif} - \psi_{bid}) \cdot Kdf$$

$$\Delta fp_{CD1} = 4.709 \text{ ksi}$$

Creep of deck concrete from time of deck placement to end of service-

$$\psi_{ddf} := 1.9 \cdot ksd \cdot khc \cdot kf$$

$$\psi_{ddf} = 1.292$$

Girder creep for loads placed at time of deck placement-

$$\psi_{bdf} := 1.9 \cdot kla_d \cdot ks \cdot khc \cdot kf$$

$$\psi_{bdf} = 0.884$$

Permanent load on composite section (from VDOT design standards)-

$$wcdl = 0.27 \frac{k}{ft}$$

**Moment from permanent composite DL-
(at mid-span)**

$$M_{comp} := w_{cdl} \cdot \frac{L^2}{16}$$

$$M_{comp} = 1.139 \times 10^3 \text{ kin}$$

**Permanent load on non-composite
section (from VDOT Standards)-**

$$w_{ncdl} = 0.2 \frac{k}{ft}$$

**Moment from permanent non-composite DL-
(at mid-span)**

$$M_{ncomp} := w_{ncdl} \cdot \frac{L^2}{8}$$

$$M_{ncomp} = 1.688 \times 10^3 \text{ kin}$$

**Change in stress in concrete at level of strand due
to superimposed loads on composite section-**

$$\Delta f_{ccs} := -M_{comp} \cdot \frac{(c_{gct} - c_{gs_{ms}})}{I_{ct}}$$

$$\Delta f_{ccs} = -0.049 \text{ ksi}$$

**Change in stress in concrete at level
of strand due to deck placement-**

$$\Delta f_{cdp} := -(M_{dh} + M_{ncomp}) \cdot \frac{e_{ms}}{I_t}$$

$$\Delta f_{cdp} = -0.658 \text{ ksi}$$

**Change in stress in concrete at level
of strand due long term losses
between initial and deck placement-**

$$\Delta f_{cl} := -(\Delta f_{pSR} + \Delta f_{pCR} + \Delta f_{pR1}) \cdot \frac{A_{ps}}{A_g} \cdot \left(1 + \frac{A_g \cdot e_{pg}^2}{I_g} \right)$$

$$\Delta f_{cl} = -0.098 \text{ ksi}$$

Prestress loss due to placement of deck-

$$\Delta f_{pCD2} := n_s \cdot (\Delta f_{ccs} + \Delta f_{cdp} + \Delta f_{cl}) \cdot \psi_{bdf} \cdot K_{df}$$

$$\Delta f_{pCD2} = -3.717 \text{ ksi}$$

Total creep of girder concrete-

$$\Delta f_{pCD} := \Delta f_{pCD1} + \Delta f_{pCD2}$$

$$\Delta f_{pCD} = 0.991 \text{ ksi}$$

Relaxation of Prestressing Strands: (from deck placement to end of service)

**Prestress Loss due to relaxation of prestressing
strands from deck placement to end of service-**

$$\Delta f_{pR2} := \Delta f_{pR1}$$

$$\Delta f_{pR2} = 1.367 \text{ ksi}$$

Shrinkage of deck concrete:

Shrinkage of deck from deck placement to end of service-

$$\begin{aligned}\epsilon_{ddf} &:= 480 \cdot 10^{-6} \cdot k_{sd} \cdot k_{hs} \cdot k_{fd} \\ \epsilon_{ddf} &= 4.304 \times 10^{-4}\end{aligned}$$

Force from fully restrained deck-

$$\begin{aligned}P_{sd} &:= \frac{(\epsilon_{ddf} \cdot s \cdot h_f \cdot E_{cd})}{(1 + \chi \cdot \psi_{ddf})} \\ P_{sd} &= 831.369 \text{ k}\end{aligned}$$

Change in stress in concrete at centroid of prestress due to deck shrinkage force-

$$\begin{aligned}\Delta f_{cdf} &:= \frac{P_{sd}}{A_{gc}} - \frac{\left[P_{sd} \cdot \left(h_g + h_h + \frac{h_f}{2} - c_{gct} \right) \cdot (c_{ggc} - c_{gms}) \right]}{I_{gc}} \\ \Delta f_{cdf} &= -0.243 \text{ ksi}\end{aligned}$$

Prestress Gain Due to Shrinkage of Deck in Composite Section-

$$\begin{aligned}\Delta f_{pSS} &:= n_s \cdot \Delta f_{cdf} \cdot K_{df} \cdot (1 + \chi \cdot \psi_{bdf}) \\ \Delta f_{pSS} &= -2.051 \text{ ksi}\end{aligned}$$

Totals:

Total prestress loss from initial to deck cast-

$$\begin{aligned}\Delta f_{pid} &:= \Delta f_{pSR} + \Delta f_{pCR} + \Delta f_{pR1} \\ \Delta f_{pid} &= 11.336 \text{ ksi}\end{aligned}$$

Total prestress loss from deck cast to end of service-

$$\begin{aligned}\Delta f_{pds} &:= \Delta f_{pSD} + \Delta f_{pCD} + \Delta f_{pR2} + \Delta f_{pSS} \\ \Delta f_{pds} &= 4.507 \text{ ksi}\end{aligned}$$

Total prestress loss from initial to end of service-

$$\begin{aligned}\Delta f_{pis} &:= \Delta f_{pid} + \Delta f_{pds} \\ \Delta f_{pis} &= 15.843 \text{ ksi}\end{aligned}$$

Prestress force at end of service -

$$\begin{aligned}P_{eff} &:= \frac{P_{jack}}{A_{ps}} - \Delta f_{pis} \\ P_{eff} &= 186.657 \text{ ksi}\end{aligned}$$

Check Stresses in Girder at End of Service Due to Permanent Loads Only

Note: Distribution factors (DF) are used to convert loads from an analysis per lane to an analysis per beam that can be used for design.

Assumptions so that the AASHTO DF method can be used:

- * Width of the deck is constant
- * At least 4 beams across
- * Beams are parallel with about the same stiffness
- * Roadway part of the overhang is less than or equal to 3 ft
- * Curvature in plan is less than the limit in AASTO section 4.6.1.2
- * Cross-section is consistent with the one in Table 4.6.2.2 - 1 (case K)

Check spacing requirement-

$$\text{checkDF}_s := \begin{cases} \text{check} \leftarrow \text{"OK"} & \text{if } 3.5\text{ft} \leq s \leq 16\text{ft} \\ \text{check} \leftarrow \text{"NOT OK"} & \text{if } \begin{cases} s < 3.5\text{ft} \\ s > 16\text{ft} \end{cases} \end{cases}$$
$$\text{checkDF}_s = \text{"OK"}$$

Check deck thickness requirement-

$$\text{checkDF}_{dt} := \begin{cases} \text{check} \leftarrow \text{"OK"} & \text{if } 4.5\text{in} \leq hf \leq 12\text{in} \\ \text{check} \leftarrow \text{"NOT OK"} & \text{if } \begin{cases} hf < 4.5\text{in} \\ hf > 12\text{in} \end{cases} \end{cases}$$
$$\text{checkDF}_{dt} = \text{"OK"}$$

Check length requirement-

$$\text{checkDF}_l := \begin{cases} \text{check} \leftarrow \text{"OK"} & \text{if } 20\text{ft} \leq L \leq 240\text{ft} \\ \text{check} \leftarrow \text{"NOT OK"} & \text{if } \begin{cases} L < 20\text{ft} \\ L > 240\text{ft} \end{cases} \end{cases}$$
$$\text{checkDF}_l = \text{"OK"}$$

Calculate girder eccentricity to centroid of deck -

$$eg := (hg - ygb) + hh + \frac{hf}{2}$$
$$eg = 36.83 \text{ in}$$

Calculate longitudinal stiffness parameter-

$$k_g := \frac{1}{n_d} \cdot (I_g + eg^2 \cdot Ag)$$
$$k_g = 2193843 \text{ in}^4$$

Check longitudinal stiffness requirement-

$$\text{checkDF}_{\text{kg}} := \begin{cases} \text{check} \leftarrow \text{"OK"} & \text{if } 10000\text{in}^4 \leq \text{kg} \leq 7000000\text{in}^4 \\ \text{check} \leftarrow \text{"NOT OK"} & \text{if } \begin{cases} \text{kg} < 10000\text{in}^4 \\ \text{kg} > 7000000\text{in}^4 \end{cases} \end{cases}$$

$\text{checkDF}_{\text{kg}} = \text{"OK"}$

DF for Moment for 1 lane loaded -

$$\text{DF}_1 := 0.06 + \left(\frac{\text{s}}{14\text{ft}}\right)^.4 \cdot \left(\frac{\text{s}}{\text{L}}\right)^.3 \cdot \left(\frac{\text{kg}}{\text{L} \cdot \text{hf}^3}\right)^.1$$

$\text{DF}_1 = 0.608$

DF for Moment for 2 lane loaded -

$$\text{DF}_2 := 0.075 + \left(\frac{\text{s}}{9.5\text{ft}}\right)^.6 \cdot \left(\frac{\text{s}}{\text{L}}\right)^.2 \cdot \left(\frac{\text{kg}}{\text{L} \cdot \text{hf}^3}\right)^.1$$

$\text{DF}_2 = 0.866$

The controlling DF is the larger of the 2 distribution factors-

$$\text{DF} := \begin{cases} \text{DF} \leftarrow \text{DF}_1 & \text{if } \text{DF}_1 > \text{DF}_2 \\ \text{DF} \leftarrow \text{DF}_2 & \text{if } \text{DF}_1 < \text{DF}_2 \end{cases}$$

$\text{DF} = 0.866$

Live load moments per beam-

$M_{\text{max}} := m_{\text{max}} \cdot \text{DF} \quad M_{\text{max}} = 664 \text{ kft}$

$M_{\text{min}} := m_{\text{min}} \cdot \text{DF} \quad M_{\text{min}} = -1329 \text{ kft}$

Live load moments per beam-

$M_{.5\text{LL}} := M_{\text{min}} \cdot .5 \quad M_{.5\text{LL}} = -664 \text{ kft}$

Calculate Cracking Moment

Calculate Cracking Moment of the Continuity Diaphragm:

Tensile strength of Diaphragm Concrete-

$$f_r := 7.5 \text{psi} \sqrt{\frac{f_{cd}}{\text{psi}}}$$
$$f_r = 474.342 \text{ psi}$$

Cracking Moment-

$$M_{cr} := f_r \cdot \frac{I_{gc}}{c_{gce}}$$
$$M_{cr} = 824.3 \text{ kft}$$

Calculate Time Dependent Moments in Diaphragm

Calculate moment to restrain creep rotation due to dead load:

Dead load restraint moment to restore rotation to zero -

$$M_{DLR} := \frac{(wg + wd h + wncdl) \cdot L^2}{8}$$

$$M_{DLR} = 1.568 \times 10^3 \text{ kft}$$

Creep rotation after continuity -

$$\theta_{cr} := (\psi_{bif} - \psi_{bid}) \cdot \frac{(wg + wd h + wncdl) \cdot L^3}{24 \cdot Eci \cdot It}$$

$$\theta_{cr} = 1.851 \times 10^{-3} \text{ radians}$$

Modify the creep rotation by using:

$$\frac{1}{1 + \chi \psi}$$

Moment to restrain dead load creep rotation -

$$M_{\phi DLR} := \frac{3 \cdot \theta_{cr} \cdot (Eci \cdot It)}{L \cdot [1 + \chi \cdot (\psi_{bif} - \psi_{bid})]}$$

$$M_{\phi DLR} = 698.686 \text{ kft}$$

Calculate moment to restrain rotation due to initial prestress:

Initial end rotation from prestress - (Straight strands only)

$$\theta_{p_s} := \left[\frac{\left(\frac{P_{eff} \cdot A_{ps} \cdot \frac{Strand_s}{Strand}}{2 \cdot Eci \cdot It} \right) \cdot (cggc - es) \cdot (L)}{2 \cdot Eci \cdot It} \right]$$

$$\theta_{p_s} = 0.0046$$

Note: The moment arm is the center of gravity of the gross composite section - not the transformed. So, the effective prestressing force should have the elastic shortening removed.

Initial end rotation from prestress (Harped strands only)-

$$\theta_{p_h} := \left[\frac{\left(\frac{P_{eff} \cdot A_{ps} \cdot \frac{Strand_h}{Strand}}{Eci \cdot It} \right) \cdot \left[.3 \cdot (cggc - eh_{ms}) - .2 \cdot (eh_{end} - cggc) \right] \cdot (L)}{Eci \cdot It} \right]$$

$$\theta_{p_h} = 5.608 \times 10^{-4}$$

Total initial end rotation-

$$\theta_p := \theta_{p_s} + \theta_{p_h}$$

$$\theta_p = 5.137 \times 10^{-3}$$

Restraint moment to restore prestress rotation to zero - $M_{\text{PSR}} := \frac{3 \cdot \theta_p \cdot (E_c \cdot I_t)}{L}$
 $M_{\text{PSR}} = 2.817 \times 10^3 \text{ kft}$

Prestress restraint moment without losses - $M_{\text{PSRi}} := M_{\text{PSR}} \cdot \frac{P_{\text{jack}}}{P_{\text{eff}} \cdot A_{\text{ps}}}$
 $M_{\text{PSRi}} = 3.056 \times 10^3 \text{ kft}$

Losses in prestress restraint moment - $\Delta M_{\text{PSR}} := M_{\text{PSRi}} - M_{\text{PSR}}$
 $\Delta M_{\text{PSR}} = 239.127 \text{ kft}$

Percent of total losses at time of deck placement - $\% \text{losses}_d := \frac{\Delta f_{\text{pid}}}{\Delta f_{\text{pis}}}$
 $\% \text{losses}_d = 0.715$

Prestress restraint moment at time of deck placement - $M_{\text{PSRd}} := M_{\text{PSRi}} - \% \text{losses}_d \cdot \Delta M_{\text{PSR}}$
 $M_{\text{PSRd}} = 2.885 \times 10^3 \text{ kft}$

Modified prestress restraint moment caused by creep rotations at time of deck placement - $M_{\phi \text{PSR}} := M_{\text{PSRd}} \cdot \frac{(\psi_{\text{bif}} - \psi_{\text{bid}})}{1 + \chi \cdot (\psi_{\text{bif}} - \psi_{\text{bid}})}$
 $M_{\phi \text{PSR}} = 1.285 \times 10^3 \text{ kft}$

Remaining prestress restraint moment losses - $M_{\text{PSloss}} := (1 - \% \text{losses}_d) \cdot \Delta M_{\text{PSR}}$
 $M_{\text{PSloss}} = 68.033 \text{ kft}$

Modified remaining prestress restraint moment losses - $M_{\phi \text{PSloss}} := M_{\text{PSloss}} \cdot \frac{1}{1 + \chi \cdot (\psi_{\text{bif}} - \psi_{\text{bid}})}$
 $M_{\phi \text{PSloss}} = 46.816 \text{ kft}$

Calculate moment to restrain rotation due to differential shrinkage:

Differential shrinkage from deck placement to end of service - $\varepsilon_{\text{diffsh}} := \varepsilon_{\text{ddf}} - \varepsilon_{\text{bdf}}$

$$\varepsilon_{\text{diffsh}} = 2.67 \times 10^{-4}$$

Differential shrinkage force - $F_{\text{diffsh}} := \varepsilon_{\text{diffsh}} \cdot (hf \cdot s + hh \cdot 47\text{in}) \cdot E_{\text{cd}}$

(applied at centroid of deck and haunch) $F_{\text{diffsh}} = 1.05 \times 10^3 \text{ k}$

Centroid of differential shrinkage force - $c_{\text{gdiffsh}} := \frac{hf \cdot s \cdot \left(hh + \frac{hf}{2} \right) + hh \cdot 47\text{in} \cdot \left(\frac{hh}{2} \right)}{hf \cdot s + hh \cdot 47\text{in}}$

$$c_{\text{gdiffsh}} = 5.427 \text{ in}$$

Differential shrinkage moment - $M_{\text{diffsh}} := F_{\text{diffsh}} \cdot \left(hg - c_{\text{gdc}} + hh + \frac{c_{\text{gdiffsh}}}{2} \right)$

$$M_{\text{diffsh}} = 1.621 \times 10^3 \text{ kft}$$

Check differential shrinkage restraint moment - $M_{\text{diffrest}} := M_{\text{diffsh}} \cdot 1.5$

$$M_{\text{diffrest}} = 2.431 \times 10^3 \text{ kft}$$

Modified moment for creep relaxation - $M_{\phi\text{DSR}} := \frac{M_{\text{diffrest}}}{1 + \chi \cdot \psi_{\text{bdf}}}$

$$M_{\phi\text{DSR}} = 1.502 \times 10^3 \text{ kft}$$

Calculate final time dependent moments:

$$M_{\text{TD}} := -M_{\phi\text{DLR}} + M_{\phi\text{PSR}} - M_{\phi\text{DSR}} - M_{\phi\text{PSloss}}$$

$$M_{\text{TD}} = -961.852 \text{ kft}$$

Check Stresses in Girder at End of Service Due to Permanent Loads Only

Critical time time dependent moment -

NOTE: In order to develop the most critical stresses, the time dependent moment should only be considered when it is positive.

$$M_{\text{critical_TD}} := \begin{cases} M_{\text{critical_TD}} \leftarrow 0 \text{ kft} & \text{if } M_{\text{TD}} \leq 0 \\ M_{\text{critical_TD}} \leftarrow M_{\text{TD}} & \text{if } M_{\text{TD}} > 0 \end{cases}$$

$$M_{\text{critical_TD}} = 0 \text{ m}^3 \text{ ksi}$$

Calculate stresses at the top at midspan-

$$f_{\text{top3}} := (M_{\text{DLR}}) \cdot \frac{(\text{hg} - \text{cgt})}{I_g} + [M_{\text{comp}} - P_{\text{eff}} \cdot A_{\text{ps}} \cdot (\text{cggc} - \text{cgs}_{\text{ms}}) + M_{\text{critical_TD}}] \cdot \frac{(\text{hg} - \text{cgct})}{I_{\text{ct}}} + \frac{P_{\text{eff}} \cdot A_{\text{ps}}}{A_{\text{gc}}}$$

$$f_{\text{top3}} = 1.35 \text{ ksi}$$

Calculate stresses at the bottom at midspan-

$$f_{\text{bot3}} := (-M_{\text{DLR}}) \cdot \frac{(\text{cgt})}{I_g} + [-M_{\text{comp}} + P_{\text{eff}} \cdot A_{\text{ps}} \cdot (\text{cggc} - \text{cgs}_{\text{ms}}) - M_{\text{critical_TD}}] \cdot \frac{(\text{cgct})}{I_{\text{ct}}} + \frac{P_{\text{eff}} \cdot A_{\text{ps}}}{A_{\text{gc}}}$$

$$f_{\text{bot3}} = 0.216 \text{ ksi}$$

Check stresses in the top for tension-

$$\text{checktop}_{\text{ts}} := \begin{cases} \text{check} \leftarrow \text{"OK"} & \text{if } f_{\text{top3}} > \sigma_{\text{ts}} \\ \text{check} \leftarrow \text{"NOT OK"} & \text{if } f_{\text{top3}} < \sigma_{\text{ts}} \end{cases}$$

$$\text{checktop}_{\text{ts}} = \text{"OK"}$$

Check stresses in the top for compression-

$$\text{checktop}_{\text{cs}} := \begin{cases} \text{check} \leftarrow \text{"OK"} & \text{if } f_{\text{top3}} < \sigma_{\text{cs}} \\ \text{check} \leftarrow \text{"NOT OK"} & \text{if } f_{\text{top3}} > \sigma_{\text{cs}} \end{cases}$$

$$\text{checktop}_{\text{cs}} = \text{"OK"}$$

Check stresses in the bottom for tension-

$$\text{checkbot}_{\text{ts}} := \begin{cases} \text{check} \leftarrow \text{"OK"} & \text{if } f_{\text{bot3}} > \sigma_{\text{ts}} \\ \text{check} \leftarrow \text{"NOT OK"} & \text{if } f_{\text{bot3}} < \sigma_{\text{ts}} \end{cases}$$

$$\text{checkbot}_{\text{ts}} = \text{"OK"}$$

Check stresses in the bottom for compression-

$$\text{checkbot}_{\text{cs}} := \begin{cases} \text{check} \leftarrow \text{"OK"} & \text{if } f_{\text{bot3}} < \sigma_{\text{cs}} \\ \text{check} \leftarrow \text{"NOT OK"} & \text{if } f_{\text{bot3}} > \sigma_{\text{cs}} \end{cases}$$

$$\text{checkbot}_{\text{cs}} = \text{"OK"}$$

Check Stresses at End of Service including Live Loads

Calculate stresses at the top for total loads- $f_{top4} := f_{top3} + M_{max} \cdot \frac{(hg - cgct)}{I_{ct}}$

$$f_{top4} = 1.467 \text{ ksi}$$

Calculate stresses at the bottom for total loads- $f_{bot4} := f_{bot3} - M_{max} \cdot \frac{(cgct)}{I_{ct}}$

$$f_{bot4} = -0.153 \text{ ksi}$$

Calculate stresses at the top for sustained and 1/2 LL- $f_{top6} := \frac{f_{top3}}{2} + M_{max} \cdot \frac{(hg - cgct)}{I_{ct}}$

$$f_{top6} = 0.792 \text{ ksi}$$

Calculate stresses at the bottom for sustained and 1/2 LL- $f_{bot6} := \frac{f_{bot3}}{2} - M_{max} \cdot \frac{(cgct)}{I_{ct}}$

$$f_{bot6} = -0.261 \text{ ksi}$$

Check stresses in the top for tension-

$$\text{checktop}_{ts2} := \begin{cases} \text{check} \leftarrow \text{"OK"} & \text{if } f_{top4} > \sigma_{ts} \\ \text{check} \leftarrow \text{"NOT OK"} & \text{if } f_{top4} < \sigma_{ts} \end{cases}$$

$$\text{checktop}_{ts2} = \text{"OK"}$$

Check stresses in the top for compression (all loads)-

$$\text{checktop}_{cs2} := \begin{cases} \text{check} \leftarrow \text{"OK"} & \text{if } f_{top4} < \sigma_{cs_t} \\ \text{check} \leftarrow \text{"NOT OK"} & \text{if } f_{top4} > \sigma_{cs_t} \end{cases}$$

$$\text{checktop}_{cs2} = \text{"OK"}$$

Check stresses in the top for compression (sustained and 1/2 LL)-

$$\text{checktop}_{cs3} := \begin{cases} \text{check} \leftarrow \text{"OK"} & \text{if } f_{top6} < \sigma_{cs_{LL}} \\ \text{check} \leftarrow \text{"NOT OK"} & \text{if } f_{top6} > \sigma_{cs_{LL}} \end{cases}$$

$$\text{checktop}_{cs3} = \text{"OK"}$$

Check stresses in the bottom for tension-

$$\text{checkbot}_{ts2} := \begin{cases} \text{check} \leftarrow \text{"OK"} & \text{if } f_{bot4} > \sigma_{ts} \\ \text{check} \leftarrow \text{"NOT OK"} & \text{if } f_{bot4} < \sigma_{ts} \end{cases}$$

$$\text{checkbot}_{ts2} = \text{"OK"}$$

Check stresses in the bottom for compression (all loads)-

$$\text{checkbot}_{cs2} := \begin{cases} \text{check} \leftarrow \text{"OK"} & \text{if } f_{bot4} < \sigma_{cs_t} \\ \text{check} \leftarrow \text{"NOT OK"} & \text{if } f_{bot4} > \sigma_{cs_t} \end{cases}$$

$$\text{checkbot}_{cs2} = \text{"OK"}$$

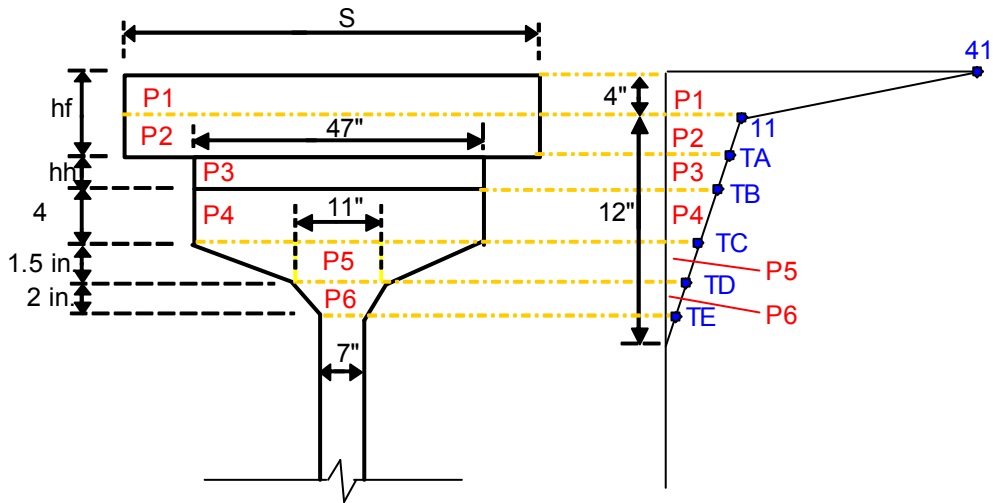
Check stresses in the bottom for compression (sustained and 1/2 LL)-

$$\text{checkbot}_{cs3} := \begin{cases} \text{check} \leftarrow \text{"OK"} & \text{if } f_{bot6} < \sigma_{cs_{LL}} \\ \text{check} \leftarrow \text{"NOT OK"} & \text{if } f_{bot6} > \sigma_{cs_{LL}} \end{cases}$$

$$\text{checkbot}_{cs3} = \text{"OK"}$$

Note: For the loading condition with with the live load, the stresses for the top are checked using Service I and stresses for the bottom are checked using Service III (for the tension check).

Calculate Thermal Restraint Moment



Thermal Forces-

$$P1 := s \cdot 4 \text{ in} \cdot \frac{(41F + 11F)}{2} \cdot \alpha_{TC} \cdot E_{cd} \quad P1 = 270.056 \text{ k}$$

$$TA := 11F - (h_f - 4 \text{ in}) \cdot \frac{11}{12} \cdot \frac{F}{\text{in}} \quad TA = 6.875 F$$

$$P2 := s \cdot (h_f - 4 \text{ in}) \cdot \frac{(11F + TA)}{2} \cdot \alpha_{TC} \cdot E_{cd} \quad P2 = 104.436 \text{ k}$$

$$TB := 11F - (h_f + h_h - 4 \text{ in}) \cdot \frac{11}{12} \cdot \frac{F}{\text{in}} \quad TB = 5.5 F$$

$$P3 := 47 \text{ in} \cdot h_h \cdot \frac{(TA + TB)}{2} \cdot \alpha_{TC} \cdot E_{cd} \quad P3 = 9.439 \text{ k}$$

$$TC := 11F - (h_f + h_h + 4 \text{ in} - 4 \text{ in}) \cdot \frac{11}{12} \cdot \frac{F}{\text{in}} \quad TC = 1.833 F$$

$$P4 := 47 \text{ in} \cdot 4 \text{ in} \cdot \frac{(TB + TC)}{2} \cdot \alpha_{TC} \cdot E_c \quad P4 = 20.353 \text{ k}$$

$$TD := 11F - (h_f + h_h - 4 \text{ in} + 4 \text{ in} + 1.5 \text{ in}) \cdot \frac{11}{12} \cdot \frac{F}{\text{in}} \quad TD = 0.458 F$$

$$P5 := (17.25 \text{ in} \cdot TD + 26.25 \text{ in} \cdot TC) \text{ in} \cdot E_c \cdot \alpha_{TC} \quad P5 = 1.654 \text{ k}$$

$$TE := 0 \quad (\text{assume that TE is very small, so just take the average of TD and TE for P6})$$

$$P6 := \frac{TD}{2} \cdot \frac{(11 \text{ in} + 7 \text{ in})}{2} \text{ in} \cdot 2 \cdot E_c \cdot \alpha_{TC} \quad P6 = 0.122 \text{ k}$$

Thermal Moments (moments summed about transformed composite center of gravity, center of gravities are from top of slab) -

cgct must be measured from the top of the beam: $cgct_{tg} := hg + hh + hf - cgct$

$cgct_{tg} = 24.703 \text{ in}$

$$cg1 := \frac{(11F \cdot 4in) \cdot 2in + \left(\frac{1}{2} \cdot 30F \cdot 4in\right) \cdot \frac{1}{3} \cdot 4in}{(11F \cdot 4in) + \left(\frac{1}{2} \cdot 30F \cdot 4in\right)} \quad cg1 = 1.615 \text{ in}$$

$M1 := P1 \cdot (cgct_{tg} - cg1) \quad M1 = 6.235 \times 10^3 \text{ kin}$

$$cg2 := \frac{\left[TA \cdot (hf - 4in) \cdot \left[4in + \frac{(hf - 4in)}{2} \right] + \frac{(11F - TA)}{2} \cdot (hf - 4in) \cdot \left[4in + \frac{(hf - 4in)}{3} \right] \right]}{TA \cdot (hf - 4in) + \frac{(11F - TA)}{2} \cdot (hf - 4in)} \quad cg2 = 6.077 \text{ in}$$

$M2 := P2 \cdot (cgct_{tg} - cg2) \quad M2 = 1.945 \times 10^3 \text{ kin}$

$$cg3 := \frac{\left[TB \cdot hh \cdot \left(hf + \frac{hh}{2} \right) + \frac{(TA - TB)}{2} \cdot hh \cdot \left(hf + \frac{hh}{3} \right) \right]}{TB \cdot hh + \frac{(TA - TB)}{2} \cdot hh} \quad cg3 = 9.222 \text{ in}$$

$M3 := P3 \cdot (cgct_{tg} - cg3) \quad M3 = 146.127 \text{ kin}$

$$cg4 := \frac{\left[TC \cdot 4 \cdot (hf + hh + 2in) + \frac{(TB - TC)}{2} \cdot 4 \cdot (hf + hh + 1.333in) \right]}{TC \cdot 4 + \frac{(TB - TC)}{2} \cdot 4} \quad cg4 = 11.667 \text{ in}$$

$M4 := P4 \cdot (cgct_{tg} - cg3) \quad M4 = 315.069 \text{ kin}$

$cg5a := \frac{(10.875 \cdot TD + 28.5 \cdot TC)}{17.25 \cdot TD + 26.25 \cdot TC} \text{ in} \quad cg5a = 1.021 \text{ in} \quad (\text{relative from top of taper})$

$M5 := P5 \cdot [cgct_{tg} - (hf + hh + 4in + 1.5in - cg5a)] \quad M5 = 16.914 \text{ kin}$

$M6 := P6 \cdot [cgct_{tg} - (hf + hh + 4in + 1.5in + 1in)] \quad M6 = 0.999 \text{ kin}$

$M_{Thermal} := M1 + M2 + M3 + M4 + M5 + M6 \quad M_{Thermal} = 721.6 \text{ kft}$

Note: Thermal Restraint Moment in a 2-span Continuous System is 1.5 x MThermal

$MR_{Th} := 1.5 \cdot M_{Thermal} \quad MR_{Th} = 1.082 \times 10^3 \text{ kft}$

Calculate Nominal Strength with 4 each No. 6 Hairpins

Area of bent prestressing strands - $A_{bent} := Strands_{bent} \cdot 0.153 \text{in}^2$
 $A_{bent} = 0.306 \text{in}^2$

Stress in strands at general slip - $f_{pu_strand} := \frac{30 - 8.25}{.163} \text{ksi}$
 $f_{pu_strand} = 133.436 \text{ksi}$

NOTE: this assumes a total embedment length of 30 in.

Area of four No. 6 Hairpins (reinforcing steel) - $A_s := 3.52 \text{in}^2$

CG of bars relative to bottom of beam - $c_{ghp} := 4.625 \text{in}$

Yield strength of the hairpins - $f_y := 60 \text{ksi}$

Depth of compression block - $a_{cd} := \frac{(A_s \cdot f_y) + (A_{bent} \cdot f_{pu_strand})}{0.85 \cdot f_{cd} \cdot b_e}$
 $a_{cd} = 0.68 \text{in}$

Moment arm for steel- $d_s := hg + hf + hh - c_{ghp}$
 $d_s = 66.375 \text{in}$

Moment arm for prestress- $d_{ps} := hg + hf + hh - 2.25 \text{in}$
 $d_{ps} = 68.75 \text{in}$

Nominal Moment - $M_n := A_s \cdot f_y \cdot \left(d_s - \frac{a_{cd}}{2} \right) + A_{bent} \cdot f_{pu_strand} \cdot \left(d_{ps} - \frac{a_{cd}}{2} \right)$
 $M_n = 1.395 \times 10^3 \text{kft}$

Check $M_n > 1.2M_{cr}$ - $\Phi M_n := M_n \cdot .9$
 $\Phi M_n = 1.255 \times 10^3 \text{kft}$

$M_{CR} := 1.2 \cdot M_{cr}$

$M_{CR} = 989.188 \text{kft}$

$check\Phi M_n := \begin{cases} check \leftarrow "OK" & \text{if } \Phi M_n > M_{CR} \\ check \leftarrow "NOT OK" & \text{if } \Phi M_n < M_{CR} \end{cases}$

$check\Phi M_n = "OK"$

RESULTS:

Moments for girder older than 90 days:

| | |
|-------------------------------------|---------------------------------------|
| Nominal moment of 4 No. 6 hairpins- | $M_n = 1.395 \times 10^3 \text{ kft}$ |
| Cracking Moment- | $M_{cr} = 824.323 \text{ kft}$ |
| Check $FM_n > 1.2M_{cr}$ - | check $\Phi M_n = \text{"OK"}$ |

Moments for girder younger than 90 days:

| | |
|---|--|
| Superimposed permanent dead load moment at mid-span - (for 2 span continuous system) | $M_{DL} := \frac{-w_{cd} \cdot L^2}{8}$ $M_{DL} = -189.844 \text{ kft}$ |
|---|--|

| | |
|---|-------------------------------|
| Superimposed permanent dead load moment - | $M_{DL} = -189.8 \text{ kft}$ |
|---|-------------------------------|

| | |
|--------------------------------|---------------------------------|
| 50% maximum live load moment - | $M_{.5LL} = -664.3 \text{ kft}$ |
|--------------------------------|---------------------------------|

| | |
|-------------------------------|-------------------------------|
| Total time dependent moment - | $M_{TD} = -961.9 \text{ kft}$ |
|-------------------------------|-------------------------------|

| | |
|----------------------------|--------------------------------|
| Thermal restraint moment - | $MR_{Th} = 1082.4 \text{ kft}$ |
|----------------------------|--------------------------------|

| | |
|------------------------|---|
| Sum of above moments - | $\Sigma M := M_{DL} + M_{.5LL} + M_{TD} + MR_{Th}$ $\Sigma M = -733.6 \text{ kft}$ |
|------------------------|---|

Note: the bottom of the diaphragm is in compression if the ΣM is negative (which is OK), and the bottom of the diaphragm is in tension if ΣM is positive (which is not OK).

$$\text{check}\Sigma M := \begin{cases} \text{check} \leftarrow \text{"NOT OK"} & \text{if } \Sigma M > 0 \\ \text{check} \leftarrow \text{"OK"} & \text{if } \Sigma M < 0 \end{cases}$$

check $\Sigma M = \text{"OK"}$

Modified sum of some above moments -

Note: since the time dependent moment is 0 at the initial time, the time dependent restraint moment will be ignored if it is less than 0 (because the critical time will be the initial time)

$$M_{TD\text{mod}} := \begin{cases} M_{TD\text{mod}} \leftarrow 0 \text{ kft} & \text{if } M_{TD} < 0 \\ M_{TD\text{mod}} \leftarrow M_{TD} & \text{if } M_{TD} > 0 \end{cases}$$

$$M_{TD\text{mod}} = 0 \text{ kft}$$

$$\Sigma M_2 := M_{DL} + M_{.5LL} + M_{TD\text{mod}} + MR_{Th}$$

$$\Sigma M_2 = 228.267 \text{ kft}$$

$$\text{check}\Sigma M_{\text{mod}} := \begin{cases} \text{check} \leftarrow \text{"NOT OK"} & \text{if } \Sigma M_2 > 0 \text{ kft} \\ \text{check} \leftarrow \text{"OK"} & \text{if } \Sigma M_2 < 0 \text{ kft} \end{cases}$$

check $\Sigma M_{\text{mod}} = \text{"NOT OK"}$

Check Strength III Requirement - $\Sigma M_{\text{factored}} := 0.65 \cdot M_{\text{DL}} + 0 \cdot M_{\text{SLL}} + 1.2 \cdot M_{\text{TD}} + 0 \cdot M_{\text{RTh}}$
(use Strength III even though there is no wind load because the live load should not be included because it will reduce the magnitude of the applied moment and not be critical)

$\Sigma M_{\text{factored}} = -1.278 \times 10^3 \text{ kft}$

$\text{check}_{\Sigma M_{\text{factored}}} := \begin{cases} \text{check} \leftarrow \text{"NOT OK"} & \text{if } \Sigma M_{\text{factored}} > \Phi M_n \\ \text{check} \leftarrow \text{"OK"} & \text{if } \Sigma M_{\text{factored}} < \Phi M_n \end{cases}$

$\text{check}_{\Sigma M_{\text{factored}}} = \text{"OK"}$

Check Flexural Strength of Member at Mid-Span:

Stress in Prestressing Steel at Nominal Flexural Resistance (AASHTO 5-33):

Factor for low relaxation strands - $K_{\text{wv}} := 0.28$

Factor for concrete strength -

$$\beta_1 := \begin{cases} \beta \leftarrow .85 & \text{if } f_{cd} \leq 4 \text{ ksi} \\ \beta \leftarrow .85 - (f_{cd} - 4 \text{ ksi}) \cdot \frac{.05}{\text{ksi}} & \text{if } 4 \text{ ksi} \leq f_{cd} \leq 8 \text{ ksi} \\ \beta \leftarrow .65 & \text{if } f_{cd} \geq 8 \text{ ksi} \end{cases}$$

$\beta_1 = 0.85$

Distance from prestress to extreme compression fiber - $dp := hg + hh + hf - cgs_{\text{ms}}$
 $dp = 68.15 \text{ in}$

Depth of the compression section -

$$c := \begin{cases} c \leftarrow \frac{A_{ps} \cdot f_{pu} - .85 \cdot f_{cd} \cdot (hf \cdot be + 47 \text{ in} \cdot hh) \dots}{.85 \cdot f_{cd} \cdot \beta_1 \cdot 47 \text{ in} + K \cdot A_{ps} \cdot \frac{f_{pu}}{dp}} & \text{if } \beta_1 \cdot \frac{A_{ps} \cdot f_{pu} - .85 \cdot f_{cd} \cdot (hf \cdot be + 47 \text{ in} \cdot hh) \dots}{.85 \cdot f_{cd} \cdot \beta_1 \cdot 47 \text{ in} + K \cdot A_{ps} \cdot \frac{f_{pu}}{dp}} > hf + hh \\ c \leftarrow \frac{A_{ps} \cdot f_{pu} - .85 \cdot f_{cd} \cdot (be - 47 \text{ in}) \cdot hf}{.85 \cdot f_{cd} \cdot \beta_1 \cdot 47 \text{ in} + K \cdot A_{ps} \cdot \frac{f_{pu}}{dp}} & \text{if } hf + hh > \beta_1 \cdot \frac{A_{ps} \cdot f_{pu} - .85 \cdot f_{cd} \cdot (be - 47 \text{ in}) \cdot hf}{.85 \cdot f_{cd} \cdot \beta_1 \cdot 47 \text{ in} + K \cdot A_{ps} \cdot \frac{f_{pu}}{dp}} > hf \\ c \leftarrow \frac{A_{ps} \cdot f_{pu}}{.85 \cdot f_{cd} \cdot \beta_1 \cdot be + K \cdot A_{ps} \cdot \frac{f_{pu}}{dp}} & \text{if } \beta_1 \cdot \frac{A_{ps} \cdot f_{pu}}{.85 \cdot f_{cd} \cdot \beta_1 \cdot be + K \cdot A_{ps} \cdot \frac{f_{pu}}{dp}} < hf \end{cases}$$

$c = 2.595 \text{ in}$

Note: "... " in the above equation signifies that there is a continuation of equation

Check to make sure the compression block is not in the web -

$\text{check}_a := \begin{cases} \text{check} \leftarrow \text{"NOT OK"} & \text{if } c \cdot \beta_1 > hf + hh + 4 \text{ in} \\ \text{check} \leftarrow \text{"OK"} & \text{if } c \cdot \beta_1 < hf + hh + 4 \text{ in} \end{cases}$

$\text{check}_a = \text{"OK"}$

Stress in steel -

$$f_{ps} := f_{pu} \cdot \left(1 - K \cdot \frac{c}{d_p} \right)$$

$$f_{ps} = 267.122 \text{ ksi}$$

Check Flexural Resistance:

Depth of compression block -

$$a_{ms} := c \cdot \beta_1$$

$$a_{ms} = 2.206 \text{ in}$$

Nominal moment capacity at mid-span -

$$M_{n_{ms}} := A_{ps} \cdot f_{ps} \cdot \left(d_p - \frac{a_{ms}}{2} \right)$$

$$M_{n_{ms}} = 4567 \text{ kft}$$

Factored nominal moment at mid-span -

$$\phi M_{n_{ms}} := 0.9 \cdot M_{n_{ms}}$$

$$\phi M_{n_{ms}} = 4110.3 \text{ kft}$$

Midspan strength check at service: $M_{critical_{TD}} = 0 \text{ m}^3 \text{ ksi}$

NOTE: This is because the time dependent moment develops over time. There will be no time dependent moment in the continuity diaphragm when the bridge is made composite and continuous. A negative time dependent moment actually helps the strength of the member, so it is assumed that the critical time for that situation is at the initial time. However, a positive time dependent moment will produce a more critical case, so the critical time will be at the end of the service life of the structure.

Calculate Strength I moment -

$$M_{StrengthI} := 1.25 \cdot (M_{DLR} + M_{comp}) + 1.75 \cdot m_{max} + 1.2 \cdot M_{critical_{TD}}$$

$$M_{StrengthI} = 3421.2 \text{ kft}$$

Check that the nominal moment capacity at midspan is greater than the Strength I moment -

$$checkM_{StrengthI} := \begin{cases} \text{check} \leftarrow \text{"OK"} & \text{if } \phi M_{n_{ms}} > M_{StrengthI} \\ \text{check} \leftarrow \text{"NOT OK"} & \text{if } \phi M_{n_{ms}} \leq M_{StrengthI} \end{cases}$$

$$checkM_{StrengthI} = \text{"OK"}$$

SUMMARY:

| | |
|--|--|
| Superimposed permanent dead load moment - | $M_{DL} = -189.8 \text{ kft}$ |
| 50% maximum live load moment - | $M_{.5LL} = -664.3 \text{ kft}$ |
| Total time dependent moment - | $M_{TD} = -961.9 \text{ kft}$ |
| Thermal restraint moment - | $MR_{Th} = 1082.4 \text{ kft}$ |
| Nominal moment at diaphragm - | $\Phi M_n = 1255.5 \text{ kft}$ |
| 1.2 times cracking moment - | $M_{CR} = 989.2 \text{ kft}$ |
| Sum of all moments - | $\Sigma M = -733.6 \text{ kft}$ |
| Sum of moments (Mtd)- | $\Sigma M_2 = 228.3 \text{ kft}$ |
| Sum of factored moments - | $\Sigma M_{\text{factored}} = -1277.6 \text{ kft}$ |
| Nominal moment at mid-span - | $\phi M_{n_{ms}} = 4110.3 \text{ kft}$ |
| Strength I moment at mid-span - | $M_{\text{Strength1}} = 3421.2 \text{ kft}$ |

CHECKS:

Initial modulus of elasticity:

check_{Eci} = "OK"

Initial strand stress:

check_{fpo} = "OK"

Stresses at transfer at mid-span:

check_{top_{ti}} = "OK" check_{top_{ci}} = "OK"

check_{bot_{ti}} = "OK" check_{bot_{ci}} = "OK"

Stresses at transfer at ends:

check_{top_{eti}} = "OK" check_{bot_{eti}} = "OK"

check_{top_{eci}} = "OK" check_{bot_{eci}} = "OK"

Stresses at deck placement:

check_{top_{td}} = "OK" check_{top_{cd}} = "OK"

check_{bot_{td}} = "OK" check_{bot_{cd}} = "OK"

Stresses at service due to permanent loads:

check_{top_{ts}} = "OK" check_{top_{cs}} = "OK"

check_{bot_{ts}} = "OK" check_{bot_{cs}} = "OK"

Stresses at service including live loads:

check_{top_{ts2}} = "OK" check_{top_{cs2}} = "OK"

check_{bot_{ts2}} = "OK" check_{bot_{cs2}} = "OK"

check_{top_{cs3}} = "OK" check_{bot_{cs3}} = "OK"

Distribution factor:

check_{DF_s} = "OK" check_{DF_l} = "OK"

check_{DF_{dt}} = "OK" check_{DF_{kg}} = "OK"

$\Phi M_n > 1.2M_{cr}$:

check ΦM_n = "OK"

Overall sum of moments in diaphragm:

check ΣM = "OK"

Overall sum of moments with sign of M_{td} :

check ΣM_{mod} = "NOT OK"

Overall factored sum of moments in diaphragm:

check $\Sigma M_{factored}$ = "OK"

The compression block is not in the web:

check_a = "OK"

M_n at midspan > Strength I moment -

check $M_{Strength1}$ = "OK"

APPENDIX D: 3-Span PCBT Girder Systems Younger than 90 Days

The MathCAD spreadsheet for 3-span PCBT girder systems is similar to the spreadsheet for 2-span PCBT girder systems that is found in Appendix C. The most positive and negative live load moments obtained from QConBridge for the 3-span system. These modified moments are shown below:

| | span length | positive moment | negative moment |
|------------|----------------|--------------------|--------------------|
| | 20 | 133.3 | -166.6 |
| | 25 | 171.3 | -214.1 |
| | 30 | 209.2 | -261.5 |
| | 35 | 263.2 | -329.0 |
| | 40 | 315.6 | -394.5 |
| | 45 | 381.6 | -477.0 |
| | 50 | 471.3 | -589.1 |
| | 55 | 594.9 | -743.6 |
| | 60 | 734.0 | -917.5 |
| | 65 | 875.2 | -1094 |
| | 70 | 1014 | -1268 |
| | 75 | 1143 | -1429 |
| | 80 | 1270 | -1587 |
| | 85 | 1393 | -1741 |
| Moments := | 90 | 1513 | -1891 |
| | 95 | 1628 | -2035 |
| | 100 | 1744 | -2180 |
| | 105 | 1856 | -2320 |
| | 110 | 1968 | -2460 |
| | 115 | 1078 | -2597 |
| | 120 | 2183 | -2729 |
| | 125 | 2296 | -2870 |
| | 130 | 2407 | -3009 |
| | 135 | 2510 | -3138 |
| | 140 | 2615 | -3269 |
| | 145 | 2726 | -3408 |
| | 150 | 2842 | -3553 |
| | 155 | 2958 | -3698 |
| | 160 | 3068 | -3835 |

All of the other terms in Appendix C are the same for the 3-span system, except for the differences that are noted below:

| Definition of changed term | 2-Span System | 3-Span System |
|---|--|---|
| Mid-span moment due to deck and haunch weight | $M = \frac{w \cdot l^2}{8}$ | $M = \frac{w \cdot l^2}{10}$ |
| Moment from permanent composite dead load at mid-span | $M = w \cdot l^2 \cdot 0.0625$ | $M = w \cdot l^2 \cdot 0.075$ |
| Composite dead load restraint moment | $M = \frac{\theta \cdot 3 \cdot E \cdot I}{l}$ | $M = \frac{\theta \cdot 3 \cdot E \cdot I}{l} \cdot 0.83$ |
| Prestress restraint moment | $M = \frac{\theta \cdot 3 \cdot E \cdot I}{l}$ | $M = \frac{\theta \cdot 3 \cdot E \cdot I}{l} \cdot 0.83$ |
| Differential shrinkage restraint moment | 1.5 * M _{diffsh} | 1.2 * M _{diffsh} |
| Thermal restraint moment | 1.5 * M _{thermal} | 1.2 * M _{thermal} |
| Superimposed permanent dead load moment at mid-span | $M = \frac{w \cdot l^2}{8}$ | $M = \frac{w \cdot l^2}{10}$ |

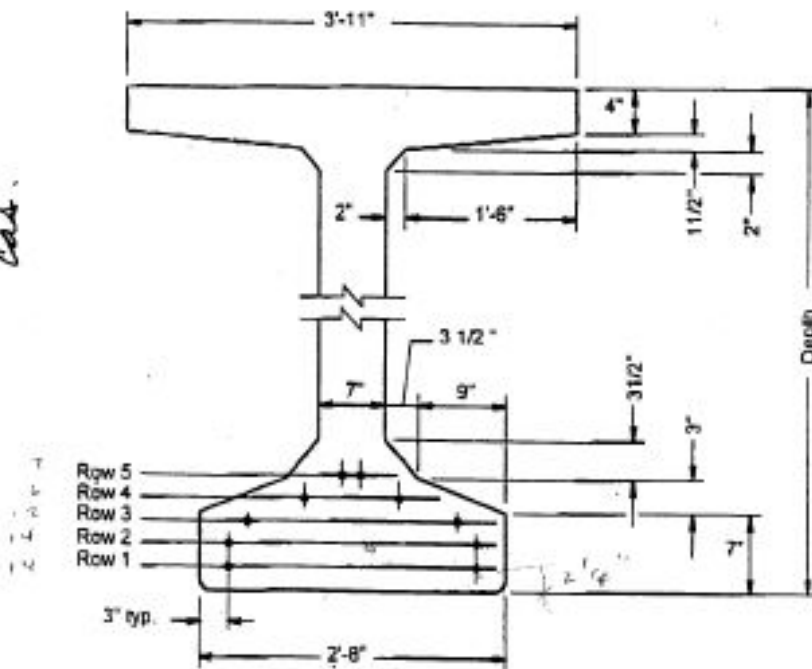
APPENDIX E: PCBT Details and Section Properties

RECEIVED

SEP 12 2001

BAYSHORE CONCRETE PRODUCTS CORP.
CAPE CHARLES, VIRGINIA

cat.



| | | |
|---|-------------|----|
| Maximum number of strands in Row number | 1: | 14 |
| | 2: | 14 |
| | 3: | 12 |
| | 4: | 6 |
| | 5 & higher: | 2 |

| Beam Designation | Depth (in.) | Area (in. ²) | Centroid to Bottom (in.) | Moment of Inertia X 10 ³ (in. ⁴) | Weight (@150 pcf) lbs./lin. ft. |
|------------------|-------------|--------------------------|--------------------------|---|---------------------------------|
| PCBT-29 | 29 | 643.7 | 14.66 | 66.8 | 661 |
| PCBT-37 | 37 | 690.7 | 18.43 | 126.0 | 720 |
| PCBT-45 | 45 | 746.7 | 22.23 | 207.3 | 778 |
| PCBT-53 | 53 | 802.7 | 26.06 | 312.4 | 836 |
| PCBT-61 | 61 | 858.7 | 29.92 | 443.1 | 899 |
| PCBT-69 | 69 | 914.7 | 33.79 | 601.3 | 953 |
| PCBT-77 | 77 | 970.7 | 37.67 | 788.7 | 1011 |
| PCBT-85 | 85 | 1026.7 | 41.57 | 1007.2 | 1070 |
| PCBT-93 | 93 | 1082.7 | 45.48 | 1258.5 | 1128 |

JHM

**PRESTRESSED CONCRETE BEAMS
STANDARD BULB-T DETAILS & SECTION PROPERTIES**

VOL. V - PART 2
DATE: 01AUG2
SHEET 1 of 1

BEAM SPACING = 6'-0"

Number of 1/2" diameter strands

| SPAN LENGTH (ft) | PCBT-28 | | | PCBT-37 | | | PCBT-45 | | | PCBT-63 | | | PCBT-81 | | | PCBT-99 | | | PCBT-117 | | | PCBT-135 | | | PCBT-153 | | | |
|------------------|----------|----------|----------|----------|----------|----------|----------|----------|----------|----------|----------|----------|----------|----------|----------|----------|----------|----------|----------|----------|----------|----------|----------|----------|----------|----------|----------|----|
| | 5000 psi | 7000 psi | 8000 psi | 5000 psi | 7000 psi | 8000 psi | 5000 psi | 7000 psi | 8000 psi | 5000 psi | 7000 psi | 8000 psi | 5000 psi | 7000 psi | 8000 psi | 5000 psi | 7000 psi | 8000 psi | 5000 psi | 7000 psi | 8000 psi | 5000 psi | 7000 psi | 8000 psi | 5000 psi | 7000 psi | 8000 psi | |
| 40 | 12 | 12 | 12 | 12 | 12 | 14 | 14 | 14 | 14 | 16 | 16 | 16 | 16 | 18 | 18 | 20 | 20 | 20 | 20 | 22 | 22 | 22 | 20 | 20 | 20 | 22 | 22 | 22 |
| 45 | 14 | 14 | 14 | 14 | 14 | 16 | 16 | 16 | 16 | 18 | 18 | 18 | 18 | 20 | 20 | 22 | 22 | 22 | 22 | 24 | 24 | 24 | 20 | 20 | 20 | 22 | 22 | 22 |
| 50 | 16 | 16 | 16 | 14 | 14 | 16 | 16 | 16 | 16 | 18 | 18 | 18 | 18 | 20 | 20 | 22 | 22 | 22 | 22 | 24 | 24 | 24 | 20 | 20 | 20 | 22 | 22 | 22 |
| 55 | 20 | 20 | 20 | 16 | 16 | 18 | 18 | 18 | 18 | 20 | 20 | 20 | 20 | 22 | 22 | 24 | 24 | 24 | 24 | 26 | 26 | 26 | 20 | 20 | 20 | 22 | 22 | 22 |
| 60 | 24 | 18 | 18 | 18 | 18 | 20 | 20 | 20 | 20 | 22 | 22 | 22 | 22 | 24 | 24 | 26 | 26 | 26 | 26 | 28 | 28 | 28 | 20 | 20 | 20 | 22 | 22 | 22 |
| 65 | | 20 | 20 | 18 | 18 | 20 | 20 | 20 | 20 | 22 | 22 | 22 | 22 | 24 | 24 | 26 | 26 | 26 | 26 | 28 | 28 | 28 | 20 | 20 | 20 | 22 | 22 | 22 |
| 70 | | 24 | 24 | 20 | 20 | 22 | 22 | 22 | 22 | 24 | 24 | 24 | 24 | 26 | 26 | 28 | 28 | 28 | 28 | 30 | 30 | 30 | 20 | 20 | 20 | 22 | 22 | 22 |
| 75 | | | | 22 | 22 | 24 | 24 | 24 | 24 | 26 | 26 | 26 | 26 | 28 | 28 | 30 | 30 | 30 | 30 | 32 | 32 | 32 | 20 | 20 | 20 | 22 | 22 | 22 |
| 80 | | | | 24 | 24 | 26 | 26 | 26 | 26 | 28 | 28 | 28 | 28 | 30 | 30 | 32 | 32 | 32 | 32 | 34 | 34 | 34 | 20 | 20 | 20 | 22 | 22 | 22 |
| 85 | | | | 28 | 28 | 30 | 30 | 30 | 30 | 32 | 32 | 32 | 32 | 34 | 34 | 36 | 36 | 36 | 36 | 38 | 38 | 38 | 20 | 20 | 20 | 22 | 22 | 22 |
| 90 | | | | 34 | 34 | 36 | 36 | 36 | 36 | 38 | 38 | 38 | 38 | 40 | 40 | 42 | 42 | 42 | 42 | 44 | 44 | 44 | 20 | 20 | 20 | 22 | 22 | 22 |
| 95 | | | | | | 38 | 38 | 38 | 38 | 40 | 40 | 40 | 40 | 42 | 42 | 44 | 44 | 44 | 44 | 46 | 46 | 46 | 20 | 20 | 20 | 22 | 22 | 22 |
| 100 | | | | | | | | | | 44 | 44 | 44 | 44 | 46 | 46 | 48 | 48 | 48 | 48 | 50 | 50 | 50 | 20 | 20 | 20 | 22 | 22 | 22 |
| 105 | | | | | | | | | | | | | | 48 | 48 | 50 | 50 | 50 | 50 | 52 | 52 | 52 | 20 | 20 | 20 | 22 | 22 | 22 |
| 110 | | | | | | | | | | | | | | | | | | | | 54 | 54 | 54 | 20 | 20 | 20 | 22 | 22 | 22 |
| 115 | | | | | | | | | | | | | | | | | | | | | | | 20 | 20 | 20 | 22 | 22 | 22 |
| 120 | | | | | | | | | | | | | | | | | | | | | | | 20 | 20 | 20 | 22 | 22 | 22 |
| 125 | | | | | | | | | | | | | | | | | | | | | | | 20 | 20 | 20 | 22 | 22 | 22 |
| 130 | | | | | | | | | | | | | | | | | | | | | | | 20 | 20 | 20 | 22 | 22 | 22 |
| 135 | | | | | | | | | | | | | | | | | | | | | | | 20 | 20 | 20 | 22 | 22 | 22 |
| 140 | | | | | | | | | | | | | | | | | | | | | | | 20 | 20 | 20 | 22 | 22 | 22 |
| 145 | | | | | | | | | | | | | | | | | | | | | | | 20 | 20 | 20 | 22 | 22 | 22 |
| 150 | | | | | | | | | | | | | | | | | | | | | | | 20 | 20 | 20 | 22 | 22 | 22 |
| 155 | | | | | | | | | | | | | | | | | | | | | | | 20 | 20 | 20 | 22 | 22 | 22 |
| 160 | | | | | | | | | | | | | | | | | | | | | | | 20 | 20 | 20 | 22 | 22 | 22 |

- Notes to designer:
1. Strands: Seven-wire Grade 270 low-relaxation strands, 2" grid (spacing), droop points at 0.4L and 0.6L.
 2. Slab thickness: 7 1/2" incl. 1/2" w.s.
 3. Dead Loads: Non-Composite = 0.20 kips/ft. each weight of beam and slab.
Composite = 0.27 kips/ft.
 4. Live Load: HS20-44.
 5. Allowable tension = 6/f_y.
 6. Strand designs shown with asterisks(*) exceed max. number of draped strands(14) or max. total uplift force(40kips) for strand restraining devices. Additional investigation by designer is required.

BULB-T PRELIMINARY DESIGN TABLES
BEAM SPACING = 6'-0"

VOL V - PART 2
DATE: 01JUL12
SHEET 1 of 9
FILE NO:

BEAM SPACING = 9'-8"

Number of 1/2" diameter strands

| SPAN LENGTH (ft.) | PCBT-29 | | | PCBT-37 | | | PCBT-45 | | | PCBT-53 | | | PCBT-61 | | | PCBT-69 | | | PCBT-77 | | | PCBT-85 | | | PCBT-93 | | | | | | |
|-------------------|---------------------------------------|----------|----------|---------------------------------------|----------|----------|---------------------------------------|----------|----------|---------------------------------------|----------|----------|---------------------------------------|----------|----------|---------------------------------------|----------|----------|---------------------------------------|----------|----------|---------------------------------------|----------|----------|---------------------------------------|----------|----------|---------------------------------------|-----|-----|-----|
| | 8000 psi f _c = 5000 psi | 7000 psi | 6000 psi | 8000 psi f _c = 5000 psi | 7000 psi | 6000 psi | 8000 psi f _c = 5000 psi | 7000 psi | 6000 psi | 8000 psi f _c = 5000 psi | 7000 psi | 6000 psi | 8000 psi f _c = 5000 psi | 7000 psi | 6000 psi | 8000 psi f _c = 5000 psi | 7000 psi | 6000 psi | 8000 psi f _c = 5000 psi | 7000 psi | 6000 psi | 8000 psi f _c = 5000 psi | 7000 psi | 6000 psi | 8000 psi f _c = 5000 psi | 7000 psi | 6000 psi | 8000 psi f _c = 5000 psi | | | |
| 40 | | | | 14 | | | 18 | 18 | 20 | 18 | 18 | 20 | 22 | 22 | 20 | 20 | 22 | 22 | 20 | 20 | 22 | 22 | 24 | 24 | 26 | 24 | 24 | 26 | 28 | | |
| 45 | | | | | 14 | 16 | 16 | 16 | 16 | 18 | 18 | 18 | 18 | 18 | 20 | 20 | 20 | 20 | 22 | 22 | 20 | 20 | 22 | 22 | 24 | 24 | 26 | 24 | 24 | 26 | |
| 50 | | | | | | 16 | 16 | 16 | 16 | 16 | 16 | 18 | 18 | 18 | 20 | 20 | 20 | 20 | 22 | 22 | 20 | 20 | 22 | 22 | 24 | 24 | 26 | 24 | 24 | 26 | |
| 55 | | | | | | | 16 | 16 | 16 | 16 | 16 | 16 | 18 | 18 | 18 | 20 | 20 | 20 | 20 | 22 | 22 | 20 | 20 | 22 | 22 | 24 | 24 | 26 | 24 | 24 | 26 |
| 60 | | | | | | | 16 | 16 | 16 | 16 | 16 | 16 | 18 | 18 | 18 | 20 | 20 | 20 | 20 | 22 | 22 | 20 | 20 | 22 | 22 | 24 | 24 | 26 | 24 | 24 | 26 |
| 65 | | | | | | | 16 | 16 | 16 | 16 | 16 | 16 | 18 | 18 | 18 | 20 | 20 | 20 | 20 | 22 | 22 | 20 | 20 | 22 | 22 | 24 | 24 | 26 | 24 | 24 | 26 |
| 70 | | | | | | | 18 | 18 | 18 | 18 | 18 | 18 | 20 | 20 | 20 | 20 | 20 | 20 | 22 | 22 | 20 | 20 | 22 | 22 | 24 | 24 | 26 | 24 | 24 | 26 | 28 |
| 75 | | | | | | | 18 | 18 | 18 | 18 | 18 | 18 | 20 | 20 | 20 | 20 | 20 | 20 | 22 | 22 | 20 | 20 | 22 | 22 | 24 | 24 | 26 | 24 | 24 | 26 | 28 |
| 80 | | | | | | | 22 | 22 | 22 | 22 | 22 | 22 | 24 | 24 | 24 | 24 | 24 | 24 | 26 | 26 | 24 | 24 | 26 | 26 | 28 | 28 | 30 | 30 | 30 | 30 | 30 |
| 85 | | | | | | | 24 | 24 | 24 | 24 | 24 | 24 | 26 | 26 | 26 | 26 | 26 | 26 | 28 | 28 | 26 | 26 | 28 | 28 | 30 | 30 | 30 | 30 | 30 | 30 | 30 |
| 90 | | | | | | | 26 | 26 | 26 | 26 | 26 | 26 | 28 | 28 | 28 | 28 | 28 | 28 | 30 | 30 | 28 | 28 | 30 | 30 | 30 | 30 | 30 | 30 | 30 | 30 | 30 |
| 95 | | | | | | | 32 | 32 | 32 | 32 | 32 | 32 | 34 | 34 | 34 | 34 | 34 | 36 | 36 | 34 | 34 | 36 | 36 | 38 | 38 | 38 | 38 | 38 | 38 | 38 | 38 |
| 100 | | | | | | | 36 | 36 | 36 | 36 | 36 | 36 | 38 | 38 | 38 | 38 | 38 | 40 | 40 | 38 | 38 | 40 | 40 | 42 | 42 | 42 | 42 | 42 | 42 | 42 | 42 |
| 105 | | | | | | | 40 | 40 | 40 | 40 | 40 | 40 | 42 | 42 | 42 | 42 | 42 | 44 | 44 | 42 | 42 | 44 | 44 | 46 | 46 | 46 | 46 | 46 | 46 | 46 | 46 |
| 110 | | | | | | | 44 | 44 | 44 | 44 | 44 | 44 | 46 | 46 | 46 | 46 | 46 | 48 | 48 | 46 | 46 | 48 | 48 | 50 | 50 | 50 | 50 | 50 | 50 | 50 | 50 |
| 115 | | | | | | | 48 | 48 | 48 | 48 | 48 | 48 | 50 | 50 | 50 | 50 | 50 | 52 | 52 | 50 | 50 | 52 | 52 | 54 | 54 | 54 | 54 | 54 | 54 | 54 | 54 |
| 120 | | | | | | | 54 | 54 | 54 | 54 | 54 | 54 | 56 | 56 | 56 | 56 | 56 | 58 | 58 | 56 | 56 | 58 | 58 | 60 | 60 | 60 | 60 | 60 | 60 | 60 | 60 |
| 125 | | | | | | | 60 | 60 | 60 | 60 | 60 | 60 | 62 | 62 | 62 | 62 | 62 | 64 | 64 | 62 | 62 | 64 | 64 | 66 | 66 | 66 | 66 | 66 | 66 | 66 | 66 |
| 130 | | | | | | | 66 | 66 | 66 | 66 | 66 | 66 | 68 | 68 | 68 | 68 | 68 | 70 | 70 | 68 | 68 | 70 | 70 | 72 | 72 | 72 | 72 | 72 | 72 | 72 | 72 |
| 135 | | | | | | | 72 | 72 | 72 | 72 | 72 | 72 | 74 | 74 | 74 | 74 | 74 | 76 | 76 | 74 | 74 | 76 | 76 | 78 | 78 | 78 | 78 | 78 | 78 | 78 | 78 |
| 140 | | | | | | | 78 | 78 | 78 | 78 | 78 | 78 | 80 | 80 | 80 | 80 | 80 | 82 | 82 | 80 | 80 | 82 | 82 | 84 | 84 | 84 | 84 | 84 | 84 | 84 | 84 |
| 145 | | | | | | | 84 | 84 | 84 | 84 | 84 | 84 | 86 | 86 | 86 | 86 | 86 | 88 | 88 | 86 | 86 | 88 | 88 | 90 | 90 | 90 | 90 | 90 | 90 | 90 | 90 |
| 150 | | | | | | | 90 | 90 | 90 | 90 | 90 | 90 | 92 | 92 | 92 | 92 | 92 | 94 | 94 | 92 | 92 | 94 | 94 | 96 | 96 | 96 | 96 | 96 | 96 | 96 | 96 |
| 155 | | | | | | | 96 | 96 | 96 | 96 | 96 | 96 | 98 | 98 | 98 | 98 | 98 | 100 | 100 | 98 | 98 | 100 | 100 | 102 | 102 | 102 | 102 | 102 | 102 | 102 | 102 |
| 160 | | | | | | | 102 | 102 | 102 | 102 | 102 | 102 | 104 | 104 | 104 | 104 | 104 | 106 | 106 | 104 | 104 | 106 | 106 | 108 | 108 | 108 | 108 | 108 | 108 | 108 | 108 |

Notes to designer:

1. Strands: Seven-wire Grade 270 low-relaxation strands, 2" grid (spacing), drap points at 0.4L and 0.6L.
2. Slab thickness: 8 1/2" incl. 1/2" w.s.
3. Dead Load: Non-Composite = 0.27 kps/ft. excl. weight of beam and slab.
Composite = 0.31 kps/ft.
4. Live Load: HS20-44.
5. Allowable Tension = 6√f_c.
6. Strand designs shown with asterisks(*) exceed max. number of draped strands(14) or max. total uplift force(40kps) for strand retaining devices. Additional investigation by designer is required.

BULB-T PRELIMINARY DESIGN TABLES
BEAM SPACING = 9'-6"

VOL V - PART 2
DATE: 01JUL12
SHEET 8 OF 9
FILE NO

BEAM SPACING = 10'-0"

Number of 1/2" diameter strands

| SPAN LENGTH (ft.) | PCBT-26 | | | PCBT-37 | | | PCBT-45 | | | PCBT-53 | | | PCBT-61 | | | PCBT-69 | | | PCBT-77 | | | PCBT-85 | | | PCBT-93 | | |
|-------------------|---------------------------|----------|----------|---------------------------|----------|----------|----------|---------------------------|----------|----------|----------|---------------------------|----------|----------|----------|---------------------------|----------|----------|----------|---------------------------|----------|----------|----------|---------------------------|----------|----------|----------|
| | f _c = 5000 psi | 7000 psi | 8000 psi | f _c = 5000 psi | 6000 psi | 7000 psi | 8000 psi | f _c = 5000 psi | 6000 psi | 7000 psi | 8000 psi | f _c = 5000 psi | 6000 psi | 7000 psi | 8000 psi | f _c = 5000 psi | 6000 psi | 7000 psi | 8000 psi | f _c = 5000 psi | 6000 psi | 7000 psi | 8000 psi | f _c = 5000 psi | 6000 psi | 7000 psi | 8000 psi |
| 40 | | | | | | | 14 | | | | | | | | | | | | | | | | | | | | |
| 45 | | | | | | | | 16 | 16 | 16 | 16 | 18 | 18 | 18 | 18 | 20 | 20 | 22 | 22 | 24 | 24 | 24 | 24 | 26 | 26 | 26 | 26 |
| 50 | | | | | | | | 16 | 16 | 16 | 16 | 18 | 18 | 18 | 18 | 20 | 20 | 22 | 22 | 24 | 24 | 24 | 24 | 26 | 26 | 26 | 26 |
| 55 | | | | | | | | 16 | 16 | 16 | 16 | 18 | 18 | 18 | 18 | 20 | 20 | 22 | 22 | 24 | 24 | 24 | 24 | 26 | 26 | 26 | 26 |
| 60 | | | | | | | | 16 | 16 | 16 | 16 | 18 | 18 | 18 | 18 | 20 | 20 | 22 | 22 | 24 | 24 | 24 | 24 | 26 | 26 | 26 | 26 |
| 65 | | | | | | | | | | | | 20 | 20 | 20 | 20 | 22 | 22 | 24 | 24 | 24 | 24 | 24 | 24 | 26 | 26 | 26 | 26 |
| 70 | | | | | | | | | | | | 22 | 22 | 22 | 22 | 24 | 24 | 24 | 24 | 24 | 24 | 24 | 24 | 26 | 26 | 26 | 26 |
| 75 | | | | | | | | | | | | 24 | 24 | 24 | 24 | 26 | 26 | 26 | 26 | 26 | 26 | 26 | 26 | 26 | 26 | 26 | 26 |
| 80 | | | | | | | | | | | | 28 | 28 | 28 | 28 | 30 | 30 | 30 | 30 | 30 | 30 | 30 | 30 | 30 | 30 | 30 | 30 |
| 85 | | | | | | | | | | | | | | | | | | | | | | | | | | | |
| 90 | | | | | | | | | | | | | | | | | | | | | | | | | | | |
| 95 | | | | | | | | | | | | | | | | | | | | | | | | | | | |
| 100 | | | | | | | | | | | | | | | | | | | | | | | | | | | |
| 105 | | | | | | | | | | | | | | | | | | | | | | | | | | | |
| 110 | | | | | | | | | | | | | | | | | | | | | | | | | | | |
| 115 | | | | | | | | | | | | | | | | | | | | | | | | | | | |
| 120 | | | | | | | | | | | | | | | | | | | | | | | | | | | |
| 125 | | | | | | | | | | | | | | | | | | | | | | | | | | | |
| 130 | | | | | | | | | | | | | | | | | | | | | | | | | | | |
| 135 | | | | | | | | | | | | | | | | | | | | | | | | | | | |
| 140 | | | | | | | | | | | | | | | | | | | | | | | | | | | |
| 145 | | | | | | | | | | | | | | | | | | | | | | | | | | | |
| 150 | | | | | | | | | | | | | | | | | | | | | | | | | | | |
| 155 | | | | | | | | | | | | | | | | | | | | | | | | | | | |
| 160 | | | | | | | | | | | | | | | | | | | | | | | | | | | |

Notes to designer:

1. Strands: Seven-wire Grade 270 low-relaxation strands, 2" grid (spacing), drap points at 0.4L and 0.6L.
2. Slab thickness: 8 1/2" incl. 1/2" w.s.
3. Dead Loads: Non-Composite = 0.28 kips/ft. excl. weight of beam and slab. Composite = 0.32 kips/ft.
4. Live Load: HS20-44.
5. Allowable Tension = 6V_s.
6. Strand designs shown with asterisks(*) exceed max. number of draped strands(14) or max. total uplift force(40kips) for strand restraining devices. Additional investigation by designer is required.

BULB-T PRELIMINARY DESIGN TABLES
BEAM SPACING = 10'-0"

VOL. V - PART 2
DATE: 01JUL12
SHEET 9 of 9
FILE NO.